Mechanisms of bacterial interaction in phototrophic consortia

Von der Fakultät für Lebenswissenschaften

der Technischen Universität Carolo-Wilhelmina zu Braunschweig

zur Erlangung des Grades

einer Doktorin der Naturwissenschaften

(Dr. rer. nat.)

genehmigte

D i s s e r t a t i o n

von Petra Marion Henke
aus Braunschweig

1. Referent: Professor Dr. Jörg Overmann
2. Referent: Professor Dr. Dieter Jahn
Eingereicht am: 12.08.2015
Mündliche Prüfung (Disputation) am: 11.01.2016

Druckjahr 2016

Vorveröffentlichungen der Dissertation

Teilergebnisse aus dieser Arbeit wurden mit Genehmigung der Fakultät für Lebenswissenschaften, vertreten durch den Mentor der Arbeit, in folgenden Beiträgen vorab veröffentlicht:

Tagungsbeiträge

Henke, P., Wanner, G., Rohde, M., Huang, S. & Overmann, J.: Insights into the molecular basis of cell-cell interactions in phototrophic consortia. Vereinigung für Allgemeine und Angewandte Mikrobiologie Jahrestagung 2014, Dresden (2014).

Henke, P., Müller, J. F., Wanner, G., McGlynn, S., Orphan, V. & Overmann, J.: Tight symbiotic interactions in the pelagic sulfur cycle - the case of phototrophic consortia. European Molecular Biology Organization - Microbial Sulfur Metabolism. Helsingör, Dänemark (2015).

Henke, P., Müller, J. F., Wanner, G., McGlynn, S., Orphan, V. & Overmann, J.: Phototrophic consortia: a model for symbiotic interaction between two prokaryotes. 15th international Symposium on Phototrophic Prokaryotes, Tübingen (2015).

Posterbeiträge

Henke, P. & Overmann, J.: Four putative symbiosis genes of *Chlorobium chlorochromatii*. (Poster) Vereinigung für Allgemeine und Angewandte Mikrobiologie Jahrestagung 2011, Karlsruhe (2011).

Henke, P., McGlynn, S., Orphan, V., Wanner, G., Rohde, M. & Overmann, J..: Molecular basis of symbiosis investigated in "*Chlorochromatium aggregatumii*". (Poster) Vereinigung für Allgemeine und Angewandte Mikrobiologie Jahrestagung 2012, Tübingen (2012).

Henke, P., Rohde, M. & Overmann, J.: Interaction of symbiotic bacteria in phototrophic consortia. (Poster) Vereinigung für Allgemeine und Angewandte Mikrobiologie Jahrestagung 2013, Bremen (2013)

Dedicated to my parents and my beloved, late sister Kerstin Jane Niehus, née Henke.

Table of contents

Chapter 1

Summary

Terrestrial, freshwater and marine communities host an immense variety of microbial symbiosis. Bacterial interactions play an important role in nature, demonstrated e.g. by the *Rhizobium*-legume symbiosis, in which bacteria provide combined nitrogen and the plant host dicarboxylic acids. This symbiosis has been estimated to reduce 120 million tons of atmospheric nitrogen to ammonia each year. A highly structured association of microorganisms, so-called consortia, appear to represent the most developed type of bacterial interaction between non-related prokaryotes. A valuable model system for studying symbiosis is the phototrophic consortium "*Chlorochromatium aggregatum*", which can be maintained in a laboratory culture.

"*C. aggregatum*" consists of the green sulfur bacteria, *Chlorobium chlorochromatii*, which surround a central, *Betaproteobacterium* in a highly structured arrangement. *Chl. chlorochromatii*, also termed epibiont, can be maintained as a pure culture in the laboratory, enabling comparative studies between the symbiotic and the free-living epibiont. Recent genomic, transcriptomic and physiological studies of the two partners in the consortia provided insights into the molecular basis of the stable association between the two bacteria. In addition, a signal exchange between the epibionts and the central bacterium has been postulated.

This thesis summarizes laboratory experiments which had the objective to further elucidate the molecular and physiological mechanisms of the bacterial interactions in the consortium "*Chlorochromatium aggregatum*".

The expression of three symbiotic proteins in the epibiont and the subsequent transfer to the central bacterium could be shown. Four previously described putative symbiotic proteins which are unique to *Chl. chlorochromatii* in comparison to 11 genomes of free-living relatives, were chosen for localization experiments within the consortium, as the protein sequences contain virulence factors. In this thesis, polyclonal antibodies targeting the protein products of Cag_0614, Cag_0616 and Cag_1919 were successfully established. Western blot analysis of Cag_1919 and dot blot analysis of Cag_0614 and Cag_0616 showed that the proteins were expressed in the consortium and in a pure culture of *Chl. chlorochromatii.* The immunofluorescence signal of the protein product of Cag_1919 was localized between the epibionts and the central bacterium. Immunogold labelling with cryosectioned consortia narrowed the localization to the membrane region of the central bacterium. The immunofluorescence signals of the protein products of Cag_0614 and Cag_0616 were

localized within the central bacterium. Immunogold labelling localized the protein product of Cag_0614 in the cytoplasm and the membrane region of the central bacterium, whereas Cag_0616 was solely localized in the membrane region of the central bacterium. Therefore, proteins containing virulence factors are involved in the symbiotic relationship between two different bacteria.

Metabolic coupling between the two partner bacteria in the consortium was investigated by tracking the flux of labelled carbon and nitrogen through the two partner organisms using nanoSIMS analysis. Measurements showed a simultaneous incorporation of labelled carbon into the epibiont and the central bacterium, indicating the transfer of newly synthesized small organic matter instead of macromolecules. Depending on the nitrogen availability of the epibiont cell, the flux of carbon changed. Each epibiont transferred 1.15 % of its incorporated ^{13}C to the central bacterium when the consortia were incubated with ammonium. The transfer increased to 30 % when the cells were grown under a nitrogen gas phase without ammonium. NanoSIMS measurements of the consortia incubated with $^{15}N_2$ did not show an incorporation of ^{15}N into the cells of the consortium. Consortia are therefore not likely to grow solely on nitrogen gas; even though the association with a green sulfur bacterium, capable of fixing atmospheric nitrogen, was considered as a competitive advantage for the central bacterium.

The effect of zaragozic acid on consortia aggregates was tested, due to a report which suggested the involvement of zaragozic acid in disrupting lipid microdomains. The function of lipid microdomains has been attributed in major parts to the recruitment and concentration of molecules involved in cellular signaling. As the number of single epibionts and the number of disaggregated consortia in the cultivation with zaragozic acid increased, the possible disruption of lipid microdomains in the membrane of the epibiont and its implications for intercellular signaling in the consortium was considered in a theoretical model.

This work studied several aspects of interactions between nonrelated prokaryotes, generating new insights into a model for bacterial symbiosis.

Chapter 2

Introduction

2.1 Symbiosis – a short overview

The original definition of symbiosis is the "living together" of two organisms of different species (De Bary, 1879). Today the term is mostly applied to any type of persistent biological interaction, i.e. mutualism, commensalistic or parasitic (Douglas, 2010). Symbiosis occurs in all domains of life, with partnerships involving microorganisms mostly described for associations between prokaryotes and eukaryotes. A prominent example is the root nodule symbiosis of rhizobia with legumes in which the bacteria provide combined nitrogen and the plant dicarboxylic acids. *Cyanobacteria* and *Alphaproteobacteria* which developed into chloroplasts and mitochondria (Schwartz & Margulis, 1982) are well established examples of endosymbiosis. Symbioses between archaea and eukaryotes have also been described, including methanogens of arthropods and archaeal symbionts of sponges (Moissl-Eichinger & Huber, 2011). Another interesting example is the relationship between certain algae or cyanobacteria with fungi resulting in the formation of lichens (Ahmadjian, 1963; Lamb, 1959). Terrestrial, freshwater and marine communities host an immense variety of microbial symbiosis (Moran, 2006).

2.2 Significance of symbiotic prokaryotes

Prokaryotic symbiosis is wide spread and often involves non-bacterial partners. Age estimations of some of these symbioses range between 250 and 20 million years (Baumann *et al.,* 1998; Dubilier *et al.,* 1995) and phylogenetic analyses of eukaryotic hosts and their prokaryotic symbionts have provided evidence for a close coevolution (Bandi *et al.,* 1995; Baumann *et al.,* 1998; Sauer *et al.,* 2000). However, symbiotic associations are also difficult to maintain in the laboratory, due to technical limitations (Overmann, 2006).

A well-studied exception is the *Rhizobium*-legume symbiosis, mainly due to their importance in agriculture, as it is estimated that the symbiosis reduces 120 million tons of atmospheric nitrogen to ammonia each year (Freiberg *et al.,* 1997). Interestingly, the strategies and genetic characteristics used by the nitrogen-fixing bacterial symbionts of legume plants are similar to those used by phytopathogenic bacteria to invade and chronically infect the plant host (Soto *et al.,* 2006).

The bacterial symbiont *Regiella insecticola,* on the other hand, has a major effect on its aphids host resistance against fungal pathogens (Scarborough *et al.,* 2005), while other

symbiotic bacteria are known to affect immunity by influencing the intestinal immune system (Macdonald & Monteleone, 2005).

As another example, sulfate-reducing bacteria have adapted to form consortia with archaea; these symbiotic associations anaerobically oxidize methane (Boetius *et al.,* 2000; Hinrichs *et al.,* 1999). Other forms of symbiosis involves the loss of genetic information, an extreme example being *Nanoarcheaum equitans*, an obligate symbiont which has the smallest sequenced microbial genome (490 kb) to date (Waters *et al.,* 2003).

Two different bacteria can be found in the symbiosis of phototrophic consortia. Green sulfur bacteria surround a central *Betaproteobacterium.* The biomass of phototrophic consortia can amount to two-thirds of the total bacterial biomass in the chemocline of lakes (Gasol *et al.,* 1995). In addition, the green sulfur bacteria associated in consortia, dominant the natural community of green sulfur bacteria in the chemocline (Glaeser & Overmann, 2003a). This indicates that the metabolic interactions of the bacteria in phototrophic consortia could be influencing the biogeochemical cycling of sulfur and carbon in their natural habitat (Overmann & Schubert, 2002).

However the known number of bacteria and archaea, which form symbiotic interaction with other prokaryotes, is quite small compared to symbiosis which involves a eukaryotic partner. Therefore they occur either rarely in nature or have so far been overlooked (Overmann & Schubert, 2002).

2.3 Phototrophic consortia

Phototrophic consortia represent one of the most highly developed interspecies associations between prokaryotes, in which different types of prokaryotes maintain a permanent cell-to-cell contact (Schink & Stams, 2006). In general phototrophic consortia consist of one central motile proteobacterium surrounded by up to 69 green sulfur bacteria, so called epibionts (Fröstl & Overmann, 2000; Overmann & Schubert, 2002; Overmann, 2006).

Since the first description of "*Chlorochromatium aggregatum*" by Lauterborn (Lauterborn, 1906), eight morphologically different types of phototrophic consortia containing a motile central bacterium have been found (Fig. 1). The distinguishing features are the colour (green or brown), the cellular morphology and number of epibionts and the overall shape of the consortia (Overmann, 2006).

The most frequently observed morphology type is barrel-shaped and motile (Overmann, 2006), like "*Chlorochromatium aggregatum*" (green epibionts) (Lauterborn, 1906; Overmann *et al.,* 1998) and "*Pelochromatium roseum*" (brown epibionts) (Tuschak *et al.,* 1999) (Fig. 1 A). Both carry 12-20 epibionts, while the more globular-shaped "*Chlorochromatium*

magnum" consists of ≥ 40 green epibionts (Fröstl & Overmann, 2000) (Fig. 1 C). "*Pelochromatium latum*" is similar in size but with brown epibionts and a more globular shape (Glaeser & Overmann, 2004). The consortium "*Pelochromatium roseo-viride"* (Fig. 1 C) is the only known phototrophic consortium which harbours two layers of epibionts. The inner layer consists of brown epibionts and the outer of green epibionts (Gorlenko & Kuznetsov, 1972). The green epibionts of "*Chlorochromatium lunatum*" and the brown epibionts of "*Pelochromatium selenoides*" have a distinct crescent cell shape (Abella *et al.,* 1998) (Fig. 1 D), while the consortium type "*Chlorochromatium glebulum"* in itself has a bent form (Fröstl & Overmann, 2000) (Fig. B). The green epibionts of this consortium contain gas vacuols.

The phototrophic consortia also contain two non-flagellated, non-motile, morphotypes, "*Chloroplana vacuolata*" and "*Cylindrogloea bactifera*", which differ from the other consortia in their immotility and different cell arrangements. "*Chloroplana vacuolata*" (Fig. 1 F) consists of green sulfur bacteria chains alternating with longer colourless bacteria forming a flat sheath; both cell types contain gas vacuols (Dubinina & Kuznetsov, 1976).

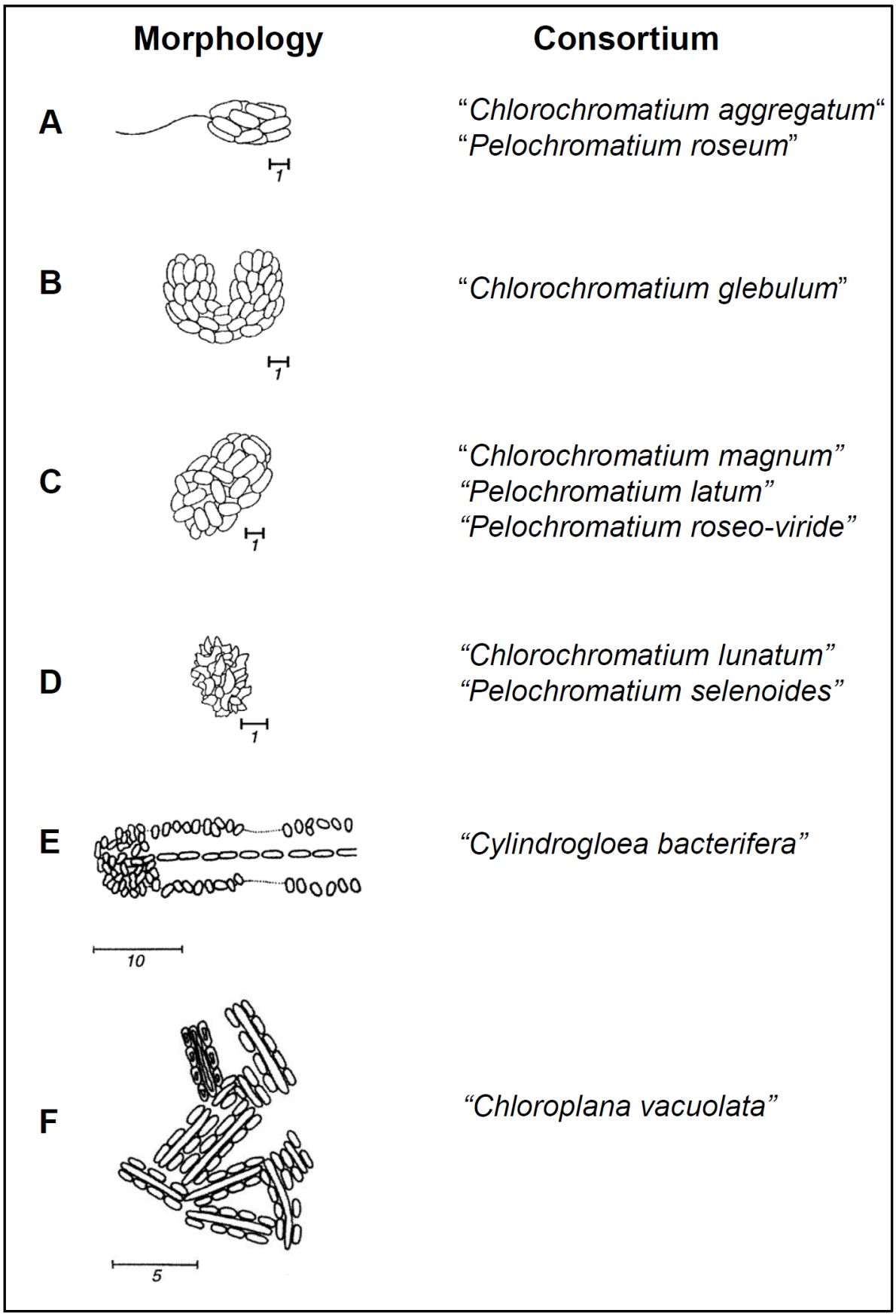

Figure 1: Morphology of phototrophic consortia modified according to Overmann and Schubert 2002.

"*Cylindrogloea bactifera*" consists of a central chain of colourless bacteria which is surrounded by green sulfur bacteria with thick capsules (Perfiliev 1914; Skuja 1956) (Fig. 1 E). Phototrophic consortia can be found in freshwater lakes around the world and colonize water layers with low light intensities and low sulfide concentrations (Overmann *et al.,* 1998; Glaeser & Overmann, 2004). Brown-coloured epibionts in comparison to their green counterparts absorb a greater portion of the blue-green or green wavelength spectrum (Overmann *et al.,* 1998). This part of the light spectrum reaches deeper water layers, therefore favouring brown coloured consortia in greater water depths.

Green sulfur bacteria may occur up to 88% as epibionts in phototrophic consortia rather than as free-living epibionts, indicating a selective advantage over an independent lifestyle (Glaeser & Overmann, 2003a). In phototrophic consortia, the epibionts have gained motility, but two different types of non-motile consortia also exist. It therefore stands to reason that motility is not the only advantage gained by green sulfur bacteria in phototrophic consortia.

As described above all phototrophic consortia consist of two different bacteria, leading to a binary name, which is without standing in nomenclature (Trüper & Pfennig, 1971) and written with quotation marks.

2.4 "*Chlorochromatium aggregatum*"

As the only available laboratory culture "C *aggregatum*" is the best-characterized phototrophic consortium to date. An enrichment culture was obtained from Lake Dagow, Germany (Fröstl & Overmann, 1998) and in succeeding work the epibionts were purified with deep agar dilution series. The epibiont *Chlorobium chlorochromatii*, a green sulfur bacterium, surrounds the central bacterium, "*Candidatus* Symbiobacter mobilis*"* (Fig. 2).

Hair-like filaments cover the entire surface of the epibionts, connecting the epibionts and the epibionts with the central bacterium alike. Shearing forces may disconnect a central bacterium from the consortium, but a major part of the epibionts stay connected. It is very likely that the filaments form an interconnecting network enclosing the central bacterium in an elastic cage. The outer membrane of the central bacterium forms periplasmic tubules (PT) which are in linear contact with the epibionts (Fig. 3 A). PTs are best observed at the poles of the central cell where they can reach up to 200 nm (Wanner *et al.,* 2008).

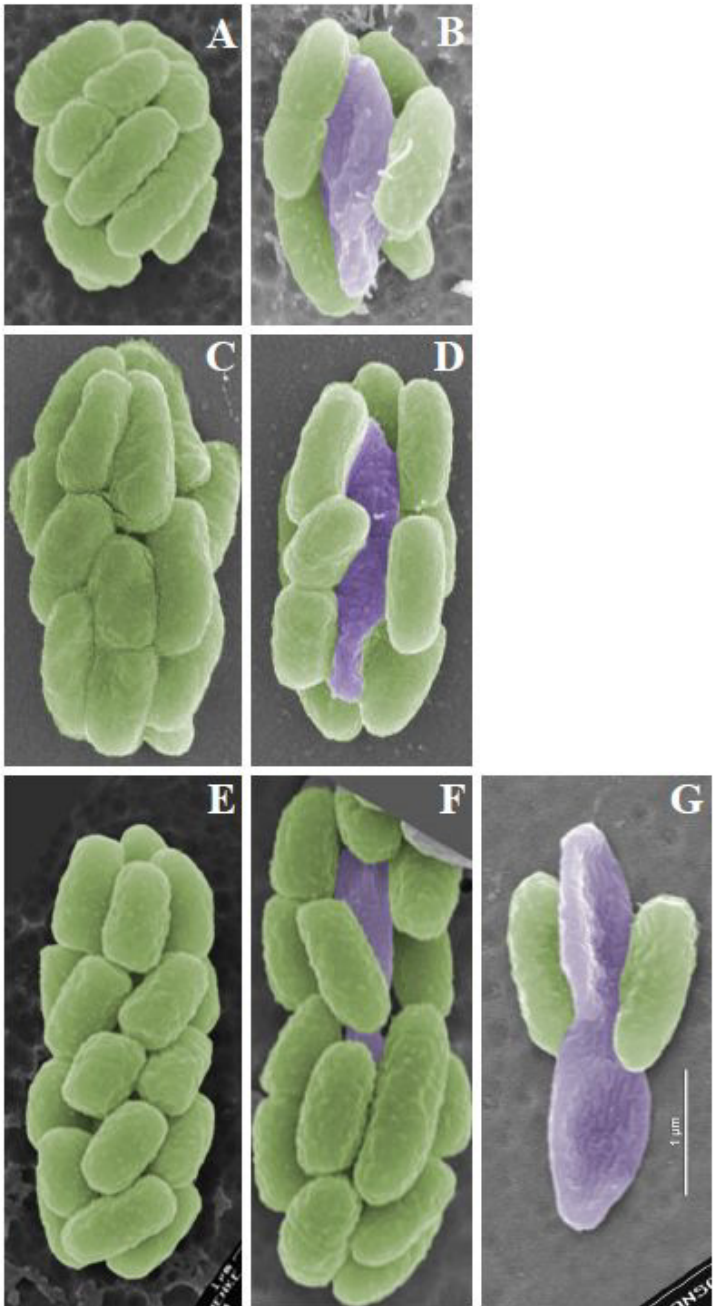

Figure 2: Scanning electron micrographs "C. aggregatum". Epibionts are shown in false colour green, central bacteria in purple (A-G). (A) Consortium in an early stage of cell division, also seen in (B) with a partially uncovered central bacterium. (C and D) Consortia with elongated epibiont cells (C) and elongated central bacterium (D). (E, F and G) Consortia during cell division into two daughter consortia. (F) Consortium with partially and (G) entirely uncovered central bacterium (Liu *et al.,* 2013).

2.4.1 The epibiont *Chlorobium chlorochromatii*

The epibiont *Chl. chlorochromatii* is the symbiotic green sulfur bacterium in "*C. aggregatum*". The cells are 2.7 (±0.6) µm long and 0.5 (±0.1) µm wide, non-motile rods with a Gram-negative cell structure. They grow photolithoautotrophic only under strictly anoxic conditions with hydrogen sulfide as electron donor. The epibiont, as the growth of the pure culture of *Chl. chlorochromatii* clearly shows, is not obligately symbiotic, but neither *Chl. chlorochromatii* nor any other epibiont of known phototrophic consortia have been detected in a free-living state in natural bacterial communities. Epibionts contain chlorosomes, antenna structures containing light harvesting pigments, which in the epibiont were determined as bacteriochlorophyll *c* and carotenoids (mainly γ-carotene and its derivates) (Vogl *et al.,* 2006).

Bioinformatic analysis of the genome showed the capability to fix CO_2 by the reverse tricarboxylic acid cycle and N_2 with the complete set of *nif* genes.

2.4.2 The central bacterium "*Candidatus* Symbiobacter mobilis"

The central bacterium is rod shaped with tapered ends and belongs to the *Comamonadaceae* within the *Betaproteobacteria* (Kanzler, Birgit E.M. *et al.,* 2005; Pfannes *et al.,* 2007). Compared to the 8 free-living members of its family the genome has lost 32% of its core genome. Bioinformatic analysis showed a substantial gene loss during evolution, especially for genes involved in metabolism. In contrast the genes involved in signal transduction, cell envelope biogenesis and cell motility are overrepresented (Liu *et al.,* 2013). Cell motility is gained through a single polar flagellum (Fig. 3 B) (Wanner *et al.,* 2008), which enables the consortium to exhibit scotophobotaxis (fear of the dark) and a positive chemotaxis towards sulfide, thiosulfate, 2-oxoglutarate and citrate (Fröstl & Overmann, 1998).

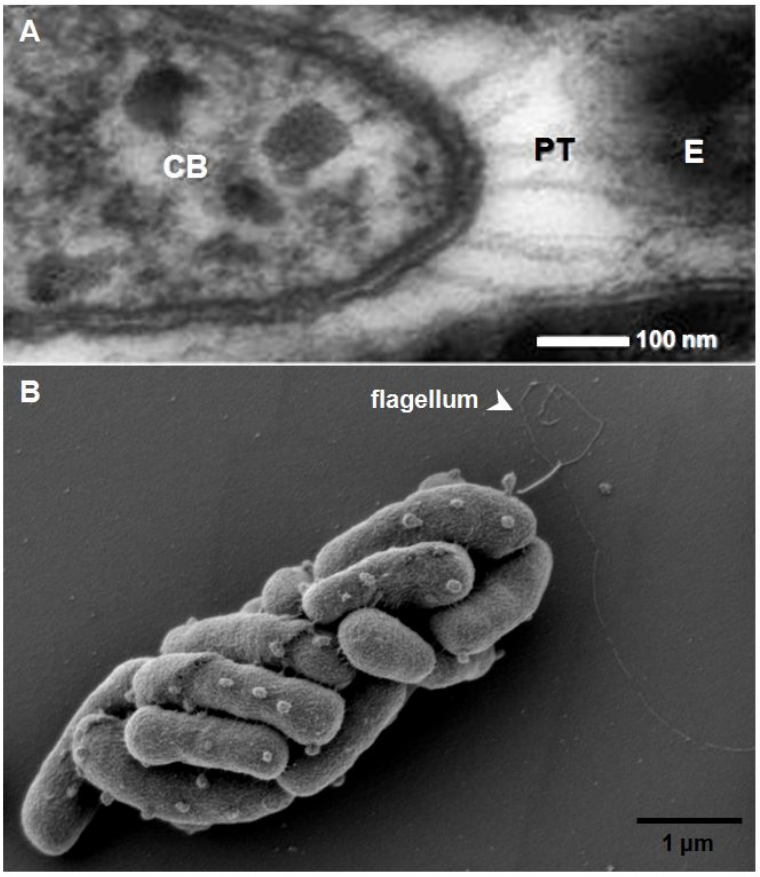

Figure 3: "*Chlorochromatium aggregatum***".** (A) TEM of ultrathin section of the central bacterium, depicting periplasmic tubules. CB = central bacterium, E = epibiont (Wanner *et al.,* 2008). (B) Scanning electron image of "*C. aggregatum*" with flagellum.

The central bacterium has probably gained the sensors for phototaxis through horizontal gene transfer from a member of the *Gammaproteobacteria*. Similar clusters were found in both, the same gene order and sequence in several purple bacteria (Liu *et al.,* 2013) which occur in the same lakes as the consortia (Govindjee *et al.,* 2009) and are often positively chemotactic to sulfide (Gest, 1995; Thar & Kühl, 2001). Although the central bacterium possesses chemotaxis capabilities, its metabolic capabilities are limited. The genome does not show any pathways for autotrophic CO_2 fixation and only limited pathways for energy production.

2.5 "*C. aggregatum*" as a model system for symbiosis

In theory the cells of the consortium could randomly attach when they encounter each other. However, studies based on 16S rRNA gene sequences have shown that phototrophic consortia with the same morphology sharing the same habitat contain only one single type of epibiont (Glaeser & Overmann, 2004). In addition, most consortia of one type contain the same number of epibionts (Overmann *et al.,* 1998), suggesting that the epibionts have adapted to a life in association. These epibionts simultaneously double with the central bacterium to form

two intact daughter consortia, after the elongated consortium divides by a transverse constriction through the aggregate (Wanner *et al.,* 2008). Cell division is therefore clearly highly synchronized, raising the question if interspecies signal transfer occurs.

In periods of darkness both partners of the consortia are inactive. This effect has also been observed in consortia of chemocline water samples with [U-^{14}C] 2-oxoglutarate as substrate (Glaeser & Overmann, 2003a). ^{14}C 2-oxoglutarate was only incorporated if light and sulfide was supplied. Thus the symbiotic partner's metabolism may be synchronized to one another, as the epibionts and the central bacterium of "*C. aggregatum*" divide simultaneously coordinately to form two complete new consortia (Overmann & Schubert, 2002).

The partners of the consortium also exhibit features indicating adaptation to their symbiotic lifestyle. In the associated state, chlorosomes are absent in the epibionts at the site of attachment to the central bacterium (Wanner *et al.,* 2008), whereas in free-living epibionts, as well as in all other known species of green sulfur bacteria, chlorosomes are distributed evenly along the inner face of the cytoplasmic membrane.

The genome of the central bacterium strongly implicates bacteriophytochromes as sensors for phototaxis (Liu *et al.,* 2013). The consortium shows a scotophobic response towards lights and chemotaxis towards sulfide. Both light and sulfide can be used in anoxygenic photosynthesis conducted by the epibiont. A prominent ultrastructure located in the cytoplasm of the central bacterium is the zipper-like crystalline structure (Wanner *et al.,* 2008) resembling the chemotaxis receptor Tsr of *E. coli* (Lefman et al., 2004; Weis et al., 2003; Zhang et al., 2004; Zhang et al., 2007). Overproduction of Tsr in *E. coli* leads to internal membrane networks which resemble a structure described as membrane whirls (Wanner *et al.,* 2008) in the central bacterium (Lefman *et al.,* 2004). The central bacterium is not only the motor for this response, but also possesses the system responsible for orientation towards compounds necessary for metabolic pathways of the epibiont. Directed motility is an advantage gained by the epibiont, compared to the free-living green sulfur bacteria. This selective advantage seems to contribute towards the high percentage (88 %) epibionts account for, compared to all green sulfur bacteria present in the natural habitat (Glaeser & Overmann, 2003a).

The partners also form connections between themselves. Besides the periplasmic tubules formed by the central bacterium, hair-like filaments were discovered on the surface of the epibionts, interconnecting the epibiont with one another and their central bacterium. The consortium represents a unique opportunity to study the interaction between two different

bacteria as (i) the consortium shows structural signs of interaction; (ii) signal exchange has been postulated and (iii) both partners show adaptations to a symbiotic lifestyle.

2.5.1 The molecular basis of the symbiotic interaction in "*C. aggregatum*"

To gain a better understanding as to which molecular factors contribute to the cell-cell interaction in "*C. aggregatum*", different studies comparing the genome, transcriptome and proteome of the two partners in the consortia have been conducted.

As all cultivation attempts to cultivate the central bacterium have failed and the genome of the central bacterium has undergone massive gene loss, it has been concluded that the central bacterium is no longer capable of independent growth. Genes involved in signal transduction, cell envelope biogenesis and cell motility are overrepresented, showing an adaptation of the genome to its symbiotic lifestyle (Liu *et al.,* 2013).

To identify open reading frames (ORFs) that are unique to *Chl. chlorochromatii,* 11 genomes of free-living relatives were compared to the genome of the epibiont by *in silico* substractive hybridization analysis. A total of 186 ORFs could be identified which included ABC transporters, proteins involved in the cell membrane, cell wall and capsule formation and four proteins with virulence factors (Wenter *et al.,* 2010). Previous work has already identified four constitutively transcribed putative symbiosis genes (Cag_0616, Cag_ 0614, Cag_1919, Cag_1920) (Vogl *et al.,* 2008). Cag_0614 and Cag_0616 represent the largest open reading frames in the prokaryotic world known up to date (110,418 bp and 61,938 bp) and Cag_1919 was reported to contain a repeat-in-toxin (RTX) domain which are often found in Gram-negative pathogenic bacteria. RTX domains are the hallmark of RTX toxins that contain glycine- and aspartate-rich nonapeptide repeats with the consensus sequence GGxGxD (Baumann *et al.,* 1993). RTX toxins are translocated in one step across the inner and outer membrane by the type I secretion system, a widespread transport system in Gram-negative bacteria (Delepelaire, 2004; Holland *et al.,* 2005). Cag_1920 codes for a putative haemolysin. Cag_0614 and Cag_0616 contain, like β-helical exoproteins, a β-helical character which has been hypothesized to provide the energy for translocation of proteins with autotransporter functions (Thanassi *et al.,* 2005). Thus the genome of the epibiont contains putative symbiotic proteins with the theoretical means to cross the membrane of the epibiont.

The proteome of the epibiont in free-living state was compared to that in the symbiotic state by 2-D differential gel electrophoresis. A P-II protein (Cag_1245, Wenter *et al.,* 2010) was identified in the proteome of the symbiotic epibiont. P-II proteins are involved in the regulation of the nitrogen metabolism (Forchhammer, 2008; Leigh & Dodsworth, 2007), as

Cag_1245 was shown to be up-regulated in the symbiotic epibiont (Wenter *et al.,* 2010), a more detailed study of the nitrogen metabolism would be of great interest.

2.5.2 RTX proteins

RTX proteins are a steadily growing group of proteins produced by Gram-negative bacteria and exhibit two common features: (1) The characteristic glycine- and aspartate-rich sequences, typically nonapeptides with the consensus sequence G-G-X-G-(N/D)-D-x-(L/I/F)-X. They are located in the carboxy-terminal end of the protein (2006; Linhartová *et al.,* 2010) and vary in number within the members of the RTX family (Satchell, 2007). These consensus regions always function as sites for calcium ions binding and are responsible for the protein family name (repeats-in-toxin) (Welch, 2001). (2) The unique mode of secretion of RTX proteins across the bacterial envelope via the type I secretion system (T1SS). Following the protein export binding of calcium ions to the nonapeptide repeats appears to promote folding which imposes adoption of a functional conformation (Felmlee & Welch, 1988; Ludwig *et al.,* 1988; Rose *et al.,* 1995). Consecutive nanopeptide RTX repeats generate a characteristic parallel β-roll structure, in which each repeat forms a half-site of the β-roll structure. The GGxG part of the consensus sequence forms the tight turn in the β-roll, followed by a β-strand and calcium ions are embedded within the strand (Baumann *et al.,* 1993).

The proteins of the RTX family exhibit a wide range of activities and molecular masses from 40 to > 600 kDa (Linhartová *et al.,* 2010). The RTX pore-forming toxins involved in bacterial pathogenesis are one of the well-known members of the RTX family. For example, the well-characterized HlyA hemolysin of *Escherichia coli* binds to mammalian cell membranes and lyses cells by pore-formation (Issartel *et al.,* 1991). To this date only pore-forming toxins which target eukaryotic host cells are known. Other subfamilies include secreted proteases, lipases, bacteriocins, and S-layer (surface-layer) proteins (Linhartová *et al.,* 2010). Proteases belong to the microbial zinc metalloproteases (Hooper, 1994; Miyoshi & Shinoda, 2000) which are also secreted by a variety of pathogens. RTX bacteriocins inhibit the growth of other bacterial strains and have been found in Gram-negative plant endosymbionts and pathogens (Oresnik *et al.,* 1999; Simpson *et al.,* 2000; Venter *et al.,* 2001).

Extracellular RTX lipases have been considered as tools for the biotechnological and food industry (Jaeger *et al.,* 1994). Other RTX proteins have been identified among S-layer proteins which cover the entire outer surface of a broad spectrum of bacteria and archaea (Sleytr & Beveridge, 1999). A key function of the S-layer seems to be the protection of bacteria in the complex environments of bacterial biofilms (Linhartová *et al.,* 2010).

In addition to the more classically recognized RTX proteins genome sequencing revealed the existence of very large members of RTX classified proteins, the sizes ranging from 200 to 900 kDa. For the time being, there are two major subfamilies: the large repetitive RTX adhesins, which function in biofilm development (biofilm associated proteins (BAP)) and cellular adherence, and the MARTX (multifunctional-autoprocessing RTX) toxins, which target eukaryotic cells during pathogenesis (Satchell, 2011).

RTX proteins have therefore important roles in the colonization of various habitats and hosts by Gram-negative bacteria. They contribute to biofilm formation in the environment and to intoxication during infection. It has also been stated that the growing database of bacterial and biochemical activities of RTX proteins still remains to be characterized (Linhartová *et al.,* 2010). The epibiont in "*C. aggregatum*" encodes the RTX domain protein Cag_1919, which in turn generates has several function possibilities. These different functions could be involved in the biofilm formation of the consortia on the inside of the glass flask during cultivation and on the other hand Cag_1919 could be involved in a so far undiscovered function of bacteria-bacteria interaction.

2.5.3 Metabolic coupling between the two partners

Several physological experiments have been conducted to investigate a possible metabolic coupling between the two partners of a consortium. According to genome analysis autotrophy can only be performed by the epibiont (Liu *et al.,* 2013). Thus fixation of HCO_3^-, which was used in ^{14}C- and ^{13}C-labeling experiments, could have only been performed by the epibiont but not by the central bacterium. The incorporation of $H^{14}CO_3^-$ into the partner organisms of "*C. aggregatum*" (Suppl. Fig. S 6), increased simultaneously in both partners (Müller, 2013). In contrast, consortia cultures incubated in the dark did not incorporate labelled carbon into their cells. It was concluded that carbon had to be fixed by the epibiont and subsequently transferred to the central bacterium (Müller, 2013).

Consortia were also incubated with $H^{13}CO_3^-$ to study the labelling pattern of amino acids in the two partners. The nearly identical ^{13}C-labelling patterns of the amino acids in the epibiont and the central bacterium suggested that amino acids are one of the possible transferred substrates in the cells of consortia. Amino acids in the form of dissolved combined amino acids (BCAAs) and dissolved free BCAAs were indeed detected in the supernatant of pure epibiont culture. The epibiont also possesses two transporters capable of amino acid transport, an ABC-type oligopeptide transporter and an ABC-type branched chain amino acid transporter, which are highly transcribed in the symbiotic epibiont incubated in the light (Müller, 2013). Additionally, the results of an experiment in which epibionts were treated

with the extracellular cross-linkers DTSSP and BS_3 conducted by Wenter *et al.*, indicated that an ABC-type branched chain amino acid transporter is localized at the cell surface or in the periplasm (Wenter *et al.,* 2010).

Transcriptome analysis of the two partners in the consortium revealed that the gene showing the second highest mRNA transcription of the central bacterial genome is the porin forming gene *ompC*. This gene is transcribed 46.3 times higher in the light compared to the experiment conducted in the dark (Müller, 2013). OmpC forms a wide pore (Benz & Hancock, 1981) which allows passive diffusion of a broad range of small molecular weight hydrophilic materials (Nikaido, 1979), leading to the conclusion that the pore is involved in the uptake of excreted substrates from the epibiont (Müller, 2013). Furthermore, the central bacterium possesses all genes required for synthesizing the 20 proteinogenic amino acids (except *serA*), and is therefore likely also synthesizing amino acids. An ABC-type branched-chain amino acid transport system and two ABC-type oligopeptide transport systems are located in the genome of the central bacterium (Liu *et al.,* 2013).

Several genes involved in nitrogen metabolism, including various Nif proteins and the nitrogen regulatory protein P-II, were found to be differentially regulated when the symbiotic and the free-living epibionts were compared (Wenter *et al.,* 2010). Combined with the significantly increased expression of the nitrogenase genes *nifH, NifE, nifB* in the symbiotic epibiont cells, it was suggested that the epibiont might be experiencing nitrogen limitation in the symbiotic state, which could have been caused by an increased synthesis and transfer of amino acids (Wenter *et al.,* 2010).

Therefore the possible transfer of carbon and nitrogen between the epibiont and the central bacterium should be considered in greater detail.

2.5.4 Organic substrates of the central bacterium and the epibiont

In addition to amino acids other possible transferred substrates between the partners of the consortium have also been taken into consideration. The candidates 2-oxoglutarate, which is also excreted by green sulfur bacteria (Sirevåg & Ormerod, 1970), and carbohydrates have been identified (Müller, 2013). Green sulfur bacteria are able to synthesize glycogen as non-membrane-bound granules, when carbon substrates and light energy are present in excess, but inorganic nutrients like ammonium and phosphate are limited (Sirevåg & Ormerod, 1970). Furthermore, the epibont excretes large amounts of sugars, mainly glucose, into the growth media (Pfannes, 2007). Therefore, it was concluded that carbohydrates could be transported by the highly transcribed permease (Cag_1339) in the epibiont and taken up by four proteins responsible for sugar transport in the central bacterium (Müller, 2013).

2-oxoglutarate stimulates the growth of not only *"C. aggregatum"* (Fröstl & Overmann, 1998) but has also been shown to be incorporated *in situ* by *Pelochromatium roseum* (Glaeser & Overmann, 2003b). As the central bacterium genome encodes a suitable 2-oxoglutarate TRAP-type dicarboxylate transporter (Liu *et al.,* 2013) and the epibiont does not use this compound (Vogl *et al.,* 2006), 2-oxoglutarate is taken up by the central bacterium. Interestingly, 2-oxoglutarate uptake appears to be controlled by the physiological state of the epibionts (Glaeser & Overmann, 2003b). Since growth of the *Chl. chlorochromatii* is stimulated by photoassimilation of acetate (Vogl *et al.,* 2006) and the central bacterium should be able to extend its glycolytic pathway beyond pyruvate to acetate (Liu *et al.,* 2013), there is already a strong evidence of metabolic coupling.

The central bacterium also incorporates external carbon sources, but transcriptome analysis revealed that although the central bacterium should be active in the dark, its activity is highly reduced compared with its activity in the light, where the epibiont is able to perform photosynthesis (Müller, 2013). Thus it was suggested that the symbiotic partner's metabolism may be synchronized to one another (Müller, 2013), as the epibionts and the central bacterium of "*C. aggregatum*" divide together to form two complete consortia (Overmann & Schubert, 2002).

2.6 Aims of this study

The phototrophic consortium "*C. aggregatum*" is an important model system for the investigation of bacterial interactions, as it is one of the few interspecies interactions that can be studied in the laboratory (Overmann, 2006).

Previous research on this association revealed first insights into the molecular basis and metabolic coupling of the symbiosis. This research already included the identification of four constitutively transcribed putative symbiosis genes (Cag_1919, Cag_1920, Cag_0614 and Cag_0616) (Wenter *et al.,* 2010; Vogl *et al.,* 2008). As these proteins contain virulence factors and the ORFs Cag_0614 and Cag_0616 represent the largest open reading frames in the prokaryotic world known to date, one goal of this thesis was to localize the proteins in the consortium and therefore to investigate their putative involvement in the symbiosis in more detail. Since Cag_1919 was reported to contain a repeat-in-toxin (RTX) domain, which are often found in Gram-negative pathogenic bacteria, the involvement of this motif in the symbiotic consortium was of special interest.

Since preceding investigations had shown the transfer of carbon from the epibiont to the central bacterium, a second goal was to investigate the metabolic coupling between the two bacteria in the phototrophic consortium. Thus the flow of carbon should be tracked on its path through the consortium with nanoSIMS analysis. In addition the exchange of nitrogen between the two symbiotic partners should be traced, as genes involved in the nitrogen metabolism of the symbiotic epibiont are differentially regulated compared to the free-living epibiont. Therefore labelled nitrogen substrates should also be tracked with nanoSIMS analysis.

2.7 References

(2006). *The Comprehensive Sourcebook of Bacterial Protein Toxins:* Elsevier.

Abella, C., **Cristina, X.**, **Martinez, A.**, **Pibernat, I. & Vila, X. (1998).** Two new motile phototrophic consortia: "*Chlorochromatium lunatum*" and "*Pelochromatium selenoides*". *Archives of Microbiology* **169**, 452–459.

Ahmadjian, V. (1963). The fungi of lichens. *Scientific American* **208**, 122–132.

Bandi, C., **Sironi, M.**, **Damiani, G.**, **Magrassi, L.**, **Nalepa, C. A.**, **Laudani, U. & Sacchi, L. (1995).** The establishment of intracellular symbiosis in an ancestor of cockroaches and termites. *Proceedings. Biological sciences / The Royal Society* **259**, 293–299.

Baumann, P., **Baumann, L.**, **Clark, M. A. & Thao, M. L. (1998).** *Buchnera aphidicola*: the endosymbiont of aphids. *ASM News* **64**, 203–209.

Baumann, U., **Wu, S.**, **Flaherty, K. M. & McKay, D. B. (1993).** Three-dimensional structure of the alkaline protease of Pseudomonas aeruginosa: a two-domain protein with a calcium binding parallel beta roll motif. *EMBO J.* **12**, 3357–3364.

Benz, R. & Hancock, R. E. (1981). Properties of the large ion-permeable pores formed from protein F of *Pseudomonas aeruginosa* in lipid bilayer membranes. *Biochimica et biophysica acta* **646**, 298–308.

Boetius, A., **Ravenschlag, K.**, **Schubert, C. J.**, **Rickert, D.**, **Widdel, F.**, **Gieseke, A.**, **Amann, R.**, **Jørgensen, B. B.**, **Witte, U. & Pfannkuche, O. (2000).** A marine microbial consortium apparently mediating anaerobic oxidation of methane. *Nature* **407**, 623–626.

De Bary, H. A. (1879). Die Erscheinung der Symbiose. Vortrag auf der Versammlung der Naturforscher und Aerzte zu Cassel. *Strassburg:Tübner*, 21–22.

Delepelaire, P. (2004). Type I secretion in gram-negative bacteria. *Biochim. Biophys. Acta* **1694**, 149–161.

Douglas, A. E. (2010). *The symbiotic habit*. Princeton (New Jersey): Princeton University Press.

Dubilier, N., **Giere, O.**, **Distel, D. L. & Cavanaugh, C. M. (1995).** Characterization of chemoautotrophic bacterial symbionts in a gutless marine worm Oligochaeta, Annelida) by phylogenetic 16S rRNA sequence analysis and in situ hybridization. *Applied and environmental microbiology* **61**, 2346–2350.

Dubinina, G. A. & Kuznetsov, S. I. (1976). The Ecological and Morphological Characteristics of Microorganisms in Lesnaya Lamba (Karelia). *Int. Revue ges. Hydrobiol. Hydrogr.* **61**, 1–19.

Felmlee, T. & Welch, R. A. (1988). Alterations of amino acid repeats in the *Escherichia coli* hemolysin affect cytolytic activity and secretion. *Proceedings of the National Academy of Sciences of the United States of America* **85**, 5269–5273.

Forchhammer, K. (2008). P(II) signal transducers: novel functional and structural insights. *Trends in Microbiology* **16**, 65–72.

Freiberg, C., **Fellay, R.**, **Bairoch, A.**, **Broughton, W. J.**, **Rosenthal, A. & Perret, X. (1997).** Molecular basis of symbiosis between *Rhizobium* and legumes. *Nature* **387**, 394–401.

Fröstl, J. M. & Overmann, J. (1998). Physiology and tactic response of the phototrophic consortium " Chlorochromatium aggregatum ". *Archives of Microbiology* **169**, 129–135.

Fröstl, J. M. & Overmann, J. (2000). Phylogenetic affiliation of the bacteria that constitute phototrophic consortia. *Archives of Microbiology* **174**, 50–58.

Gasol, J. M., **Jurgens, K.**, **Massana, R.**, **Calderon-Paz, J. I. & Pedros-Alio, C. (1995).** Mass development of *Daphnia pulex* in a sulfide-rich pond (Lake Ciso). *Archiv fuer Hydrobiologie*, 279–296.

Gest, H. (1995). Phototaxis and other sensory phenomena in purple photosynthetic bacteria. *FEMS Microbiology Reviews* **16**, 287–294.

Glaeser, J. & Overmann, J. (2003a). Characterization and in situ carbon metabolism of phototrophic consortia. *Applied and environmental microbiology* **69**, 3739–3750.

Glaeser, J. & Overmann, J. (2003b). The significance of organic carbon compounds for in situ metabolism and chemotaxis of phototrophic consortia. *Environ. Microbiol.* **5**, 1053–1063.

Glaeser, J. & Overmann, J. (2004). Biogeography, evolution, and diversity of epibionts in phototrophic consortia. *Appl. Environ. Microbiol.* **70**, 4821–4830.

Gorlenko, V. M. & Kuznetsov, S. I. (1972). Vertical distribution of phototrophic consortia in the Kononèr Lake of the Mari ASSR. *Microbiol.* **40**, 651–652.

Govindjee, H., Daldal, F., Thurnauer, M. C. & Beatty, J. T., eds. (2009). *The Purple Phototrophic Bacteria*. Dordrecht: Springer Netherlands.

Hinrichs, K. U., **Hayes, J. M.**, **Sylva, S. P.**, **Brewer, P. G. & DeLong, E. F. (1999).** Methane-consuming archaebacteria in marine sediments. *Nature* **398**, 802–805.

Holland, I. B., **Schmitt, L. & Young, J. (2005).** Type 1 protein secretion in bacteria, the ABC-transporter dependent pathway (review). *Mol. Membr. Biol.* **22**, 29–39.

Hooper, N. M. (1994). Families of zinc metalloproteases. *FEBS letters* **354**, 1–6.

Issartel, J. P., **Koronakis, V. & Hughes, C. (1991).** Activation of *Escherichia coli* prohaemolysin to the mature toxin by acyl carrier protein-dependent fatty acylation. *Nature* **351**, 759–761.

Jaeger, K. E., **Ransac, S.**, **Dijkstra, B. W.**, **Colson, C.**, **van Heuvel, M. & Misset, O. (1994).** Bacterial lipases. *FEMS Microbiology Reviews* **15**, 29–63.

Kanzler, Birgit E.M., Pfannes, K. R., **Vogl, K. & Overmann, J. (2005).** Molecular characterization of the nonphotosynthetic partner bacterium in the consortium "*Chlorochromatium aggregatum*". *Appl. Environ. Microbiol.* **71**, 7434–7441.

Lamb, I. N. (1959). Lichens. *Scientific American*, 144–156.

Lauterborn, R. (1906). Zur Kenntnis der sapropelischen Flora. *Allgemeine Botanische Zeitschrift*, 196–197.

Lefman, J., **Zhang, P.**, **Hirai, T.**, **Weis, R. M.**, **Juliani, J.**, **Bliss, D.**, **Kessel, M.**, **Bos, E.**, **Peters, P. J. & Subramaniam, S. (2004).** Three-dimensional electron microscopic imaging of membrane invaginations in Escherichia coli overproducing the chemotaxis receptor Tsr. *Journal of Bacteriology* **186**, 5052–5061.

Leigh, J. A. & Dodsworth, J. A. (2007). Nitrogen regulation in bacteria and archaea. *Annual review of microbiology* **61**, 349–377.

Linhartová, I., **Bumba, L.**, **Mašín, J.**, **Basler, M.**, **Osička, R.**, **Kamanová, J.**, **Procházková, K.**, **Adkins, I. & Hejnová-Holubová, J. & other authors (2010).** RTX proteins: a highly diverse family secreted by a common mechanism. *FEMS Microbiology Reviews* **34**, 1076–1112.

Liu, Z., **Müller, J.**, **Li, T.**, **Alvey, R. M.**, **Vogl, K.**, **Frigaard, N.-U.**, **Rockwell, N. C.**, **Boyd, E. S. & Tomsho, L. P. & other authors (2013).** Genomic analysis reveals key aspects of

prokaryotic symbiosis in the phototrophic consortium "*Chlorochromatium aggregatum*". *Genome Biol* **14**, R127.

Ludwig, A., **Jarchau, T.**, **Benz, R. & Goebel, W. (1988).** The repeat domain of Escherichia coli haemolysin (HlyA) is responsible for its Ca2+-dependent binding to erythrocytes. *Molecular & general genetics : MGG* **214**, 553–561.

Macdonald, T. T. & Monteleone, G. (2005). Immunity, inflammation, and allergy in the gut. *Science (New York, N.Y.)* **307**, 1920–1925.

Miyoshi, S. & Shinoda, S. (2000). Microbial metalloproteases and pathogenesis. *Microbes and infection / Institut Pasteur* **2**, 91–98.

Moissl-Eichinger, C. & Huber, H. (2011). Archaeal symbionts and parasites. *Curr. Opin. Microbiol.* **14**, 364–370.

Moran, N. A. (2006). Symbiosis. *Current biology : CB* **16**, R866-71.

Müller, J. (2013). Interspecies interaction and diversity of green sulfur bacteria. Ph.D thesis, München: LMU, Department of Biology.

Nikaido, H. (1979). Permeability of the outer membrane of bacteria. *Angewandte Chemie (International ed. in English)* **18**, 337–350.

Oresnik, I. J., **Twelker, S. & Hynes, M. F. (1999).** Cloning and characterization of a *Rhizobium leguminosarum* gene encoding a bacteriocin with similarities to RTX toxins. *Applied and environmental microbiology* **65**, 2833–2840.

Overmann, J., Tuschak, C., Sass, H. & Frostl, J. (1998). The ecological niche of the consortium "*Pelochromatium roseum*". *Arch. Microbiol.* **169**, 120–128.

Overmann, J. (2006). Symbiosis between non-related bacteria in phototrophic consortia. *Progress in molecular and subcellular biology* **41**, 21–37.

Overmann, J. & Schubert, K. (2002). Phototrophic consortia: model systems for symbiotic interrelations between prokaryotes. *Arch. Microbiol.* **177**, 201–208.

Pfannes, K. R. (2007). *Characterization of the symbiotic bacterial partners in phototrophic consortia. PhD Thesis*.

Pfannes, K. R., **Vogl, K. & Overmann, J. (2007).** Heterotrophic symbionts of phototrophic consortia: members of a novel diverse cluster of Betaproteobacteria characterized by a tandem rrn operon structure. *Environ. Microbiol.* **9**, 2782–2794.

Rose, T., **Sebo, P.**, **Bellalou, J. & Ladant, D. (1995).** Interaction of calcium with Bordetella pertussis adenylate cyclase toxin. Characterization of multiple calcium-binding sites and calcium-induced conformational changes. *The Journal of biological chemistry* **270**, 26370–26376.

Satchell, K. J. (2011). Structure and function of MARTX toxins and other large repetitive RTX proteins. *Annual review of microbiology* **65**, 71–90.

Satchell, K. J. (2007). MARTX, multifunctional autoprocessing repeats-in-toxin toxins. *Infection and immunity* **75**, 5079–5084.

Sauer, C., **Stackebrandt, E.**, **Gadau, J.**, **Hölldobler, B. & Gross, R. (2000).** Systematic relationships and cospeciation of bacterial endosymbionts and their carpenter ant host species: proposal of the new taxon Candidatus Blochmannia gen. nov. *International journal of systematic and evolutionary microbiology* **50 Pt 5**, 1877–1886.

Scarborough, C. L., **Ferrari, J. &** Godfray, H C J **(2005).** Aphid protected from pathogen by endosymbiont. *Science (New York, N.Y.)* **310**, 1781.

Schink, B. & Stams, A. J. M. (2006). Syntrophism among Prokaryotes. In *The Prokaryotes*, pp. 309–335. Edited by M. Dworkin, S. Falkow, E. Rosenberg, K.-H. Schleifer & E. Stackebrandt. New York, NY: Springer New York.

Schwartz, W. & Margulis, L. (1982). Symbiosis in Cell Evolution. Life and its Environment on the Early Earth. *Z Allg Mikrobiol* **22**, 427.

Simpson, A. J., **Reinach, F. C.**, **Arruda, P.**, **Abreu, F. A.**, **Acencio, M.**, **Alvarenga, R.**, **Alves, L. M.**, **Araya, J. E. & Baia, G. S. & other authors (2000).** The genome sequence of the plant pathogen *Xylella fastidiosa*. The *Xylella fastidiosa* Consortium of the Organization for Nucleotide Sequencing and Analysis. *Nature* **406**, 151–159.

Sirevåg, R. & Ormerod, J. G. (1970). Carbon dioxide fixation in green sulphur bacteria. *The Biochemical journal* **120**, 399–408.

Sleytr, U. B. & Beveridge, T. J. (1999). Bacterial S-layers. *Trends in Microbiology* **7**, 253–260.

Soto, M. J., **Sanjuán, J. & Olivares, J. (2006).** Rhizobia and plant-pathogenic bacteria: common infection weapons. *Microbiology (Reading, England)* **152**, 3167–3174.

Thanassi, D. G., **Stathopoulos, C.**, **Karkal, A. & Li, H. (2005).** Protein secretion in the absence of ATP: the autotransporter, two-partner secretion and chaperone/usher pathways of Gram-negative bacteria (Review). *Mol Membr Biol* **22**, 63–72.

Thar, R. & Kühl, M. (2001). Motility of *Marichromatium gracile* in response to light, oxygen, and sulfide. *Applied and environmental microbiology* **67**, 5410–5419.

Trüper, H. G. & Pfennig, N. (1971). Family of Phototrophic Green Sulfur Bacteria: Chlorobiaceae Copeland, the Correct Family Name; Rejection of Chlorobacterium Lauterborn; and the Taxonomic Situation of the Consortium-Forming Species: Request for an Opinion. *International Journal of Systematic Bacteriology* **21**, 8–10.

Tuschak, C., **Glaeser, J. & Overmann, J. (1999).** Specific detection of green sulfur bacteria by in situ hybridization with a fluorescently labeled oligonucleotide probe. *Archives of Microbiology* **171**, 265–272.

Venter, A. P., **Twelker, S.**, **Oresnik, I. J. & Hynes, M. F. (2001).** Analysis of the genetic region encoding a novel rhizobiocin from *Rhizobium leguminosarum* bv. viciae strain 306. *Canadian journal of microbiology* **47**, 495–502.

Vogl, K., **Glaeser, J.**, **Pfannes, K. R.**, **Wanner, G. & Overmann, J. (2006).** *Chlorobium chlorochromatii* sp. nov., a symbiotic green sulfur bacterium isolated from the phototrophic consortium "Chlorochromatium aggregatum". *Archives of Microbiology* **185**, 363–372.

Vogl, K., **Wenter, R.**, **Dressen, M.**, **Schlickenrieder, M.**, **Plöscher, M.**, **Eichacker, L. & Overmann, J. (2008).** Identification and analysis of four candidate symbiosis genes from '*Chlorochromatium aggregatum*', a highly developed bacterial symbiosis. *Environ. Microbiol.* **10**, 2842–2856.

Wanner, G., **Vogl, K. & Overmann, J. (2008).** Ultrastructural characterization of the prokaryotic symbiosis in "*Chlorochromatium aggregatum*". *J. Bacteriol.* **190**, 3721–3730.

Waters, E., **Hohn, M. J.**, **Ahel, I.**, **Graham, D. E.**, **Adams, M. D.**, **Barnstead, M.**, **Beeson, K. Y.**, **Bibbs, L. & Bolanos, R. & other authors (2003).** The genome of *Nanoarchaeum equitans*: insights into early archaeal evolution and derived parasitism. *Proceedings of the National Academy of Sciences of the United States of America* **100**, 12984–12988.

Weis, R. M., **Hirai, T.**, **Chalah, A.**, **Kessel, M.**, **Peters, P. J. & Subramaniam, S. (2003).** Electron microscopic analysis of membrane assemblies formed by the bacterial chemotaxis receptor Tsr. *Journal of Bacteriology* **185**, 3636–3643.

Welch, R. A. (2001). RTX toxin structure and function: a story of numerous anomalies and few analogies in toxin biology. *Current topics in microbiology and immunology* **257**, 85–111.

Wenter, R., **Hütz, K.**, **Dibbern, D.**, **Li, T.**, **Reisinger, V.**, **Plöscher, M.**, **Eichacker, L.**, **Eddie, B. & Hanson, T. & other authors (2010).** Expression-based identification of genetic determinants of the bacterial symbiosis "*Chlorochromatium aggregatum*". *Environmental Microbiology*.

Zhang, P., **Bos, E.**, **Heymann, J.**, **Gnaegi, H.**, **Kessel, M.**, **Peters, P. J. & Subramaniam, S. (2004).** Direct visualization of receptor arrays in frozen-hydrated sections and plunge-frozen specimens of E. coli engineered to overproduce the chemotaxis receptor Tsr. *Journal of microscopy* **216**, 76–83.

Zhang, P., **Khursigara, C. M.**, **Hartnell, L. M. & Subramaniam, S. (2007).** Direct visualization of *Escherichia coli* chemotaxis receptor arrays using cryo-electron microscopy. *Proceedings of the National Academy of Sciences of the United States of America* **104**, 3777–3781.

Chapter 3

Experimental procedures

3.1 Materials

3.1.1 *Eschericha coli* strains

Table 1: Description of *E. coli* strains.

***E. coli* strain**	**Genotype or description**	**Resistance**	**Reference**
M15 [pREP4]	*Nal*^{S}, *Str*^{S}, *Rif*^{S}, *Thi*$^-$, *Lac*$^-$, *Ara*$^+$, *Gal*$^+$, *Mtl*$^-$, *F*$^-$, *RecA*$^+$, *Uvr*$^+$, *Lon*$^+$ [(Kan^R, *lacI*]	Kanamycin (from plasmid)	Villarejo and Zabin 1974[1] From Roche/QIAGEN
SG13009	*Nal*^{S}, *Str*^{S}, *Rif*^{S}, *Thi*$^-$, *Lac*$^-$, *Ara*$^+$, *Gal*$^+$, *Mtl*$^-$, *F*$^-$, *RecA*$^+$, *Uvr*$^+$, *Lon*$^+$ [(Kan^R, *lacI*]	Kanamycin (from plasmid)	Gottesman et al. 1981[2] From QIAGEN
XL-1 Blue	*recA1 endA1 gyrA96 thi-1 hsdR17, supE44 relA1 lac* [F' *pro AB lacI*^{q}, *ZΔM15* Tn*10* (Tet^r)]	Tetracyclin	Agilent Technologies, CA, USA

3.1.2 Antibiotics

Table 2: Antibiotic concentrations.

Antibiotic	**Stock conc. (mg/ml)**	**Final conc. (µg/ml)**
Ampicillin (Amp)	100	100
Kanamycin (Kan)	25	25
Tetracyclin (Tet)	50	50
Tetracyclin for protein expression	75	75

[1] Villarejo & Zabin (1974)

[2] Gottesman *et al.* (1981)

3.1.3 Media

Table 3: Media used in this study.

Medium	**Contents per 1l**
Lysogeny Broth (LB)	10g Bacto-tryptone 5g Yeast extract 10g Sodium chloride pH 7
Terrific Broth (TB)	12 g Tryptone 24 g Yeast extract 4 ml Glycerol 0.17 M KH_2PO_4 0.72 M K_2HPO_4
NZCYM	10 g Casein hydrolysate enzymatic 5 g Yeast extract 5 g Sodium chloride 1 g Casamino acids 2 g $MgSO_4 \cdot 7H_2O$ pH 7
Yeast extract tryptone (2x YT)	16 g Tryptone 10 g Yeast extract 4 g Sodium chloride pH 7
K3	1.8 mM KH_2PO_4 0.93 mM NH_4Cl 0.25 mM $MgCl_2 \cdot 6\ H_20$ 0.34 mM $CaCl_2 \cdot 2\ H_20$ 17.86 mM $NaHCO_3$ 0.5 mM $Na_2S \cdot 9\ H_2O$ 1 ml 7 Vitamine solution 1 ml SL10 0.5 ml SL12
K4	1.8 mM KH_2PO_4 0.93 mM NH_4Cl 0.25 mM $MgCl_2 \cdot 6\ H_20$ 0.34 mM $CaCl_2 \cdot 2\ H_20$ 10 mM $NaHCO_3$ 10 mM HEPES 0.5 mM $Na_2S \cdot 9\ H_2O$ 1 ml 7 Vitamine solution 1 ml SL10 0.5 ml SL12

Table 4: Media supplements used in this study.

Media components	**Contents per 1l**
7 Vitamine solution	0.08 g 4-Aminobenzoesäure 0.02 g D(+)-Biotin 0.2 g Nikotinsäure 0.1 g Ca^{2+}-D(+)-Pantothenat 0.3 g Pyridoxinhydrochlorid 0.2 g Thiaminhydrochlorid 0.01 g Cyanocobalamin
SL10 (Widdel et al. 1983)	1.5 g Fe(II)Cl_2·4 H_2O 0.19 g $CoCl_2$·6 H_2O 0.1 g $MnCl_2$·2 H_2O 0.07 g $ZnCl_2$ 0.1 g $MgCl_2$·4 H_2O 0.024 g $NiCl_2$·6 H_2O 0.036 g Na_2MoO_4·2 H_2O 0.006 g H_3BO_3 0.002 g $CuCl_2$·2 H_2O
SL12 (Tschech and Pfennig, 1984)	3 g EDTA-Na_2 1.1 g FeSO4·H_2O 0.19 g $CoCl_2$·6 H_2O 0.05 g $MnCl_2$·2 H_2O 0.042 g $ZnCl_2$ 0.024 g $NiCl_2$·6 H_2O 0.018 g Na_2MoO_4·2 H_2O 0.3 g H_3BO_3 0.002 g $CuCl_2$·2 H_2O

3.1.4 Buffers

Table 5: Buffers used in this study.

Buffers	Contents
General	
Phosphate-buffered saline (PBS)	137 mM NaCl 2.7 mM KCl, 10 mM Na_2HPO_4 1.8 mM KH_2PO_4 pH 7.4
TAE buffer (Tris, Acetic acid, EDTA)	40 mM Tris 40 mM acetic acid 1 mM EDTA
Transformation buffer (TSB)	100 ml LB 5 ml 1M $MgSO_4$ 5 ml DMSO 10g PEG filter sterilize
Cell fractionation	
Membrane buffer *E. coli* (MBE)	50 mM Tris-HCl pH 7.5 5 mM $MgCl_2$ 10 % (v/v) glycerol
Cytoplasm buffer consortia (CBC)	10 mM Tris-HCl pH 7 7.5 mM EDTA 0.2 mM dithiothreitol (DTT)
Membrane buffer consortia (MBC)	50 mM Tris-HCl pH 8 2 % (w/v) Triton X-100 10 mM $MgCl_2$ 100 mM NaCl 10% (v/v) glycerol
SDS PAGE	
10x SDS running buffer	25 mM Tris base 192 mM glycine 0.1% (w/v) SDS
Fixation Buffer	10 % glacial acetic acid 40 % Ethanol
Coomassie staining Buffer	Combine 1:1 (v/v) before use: 0.2 % Brilliant Blue R in 90 % ethanol with 20 % glacial acetic acid
Destaining Buffer	10 % glacial acetic acid 20 % ethanol

Gels	**Contents for two gels**
Resolving gel (12%)	2.09 ml H_2O 3.75 ml 0.5M Tris-HCl pH 6.8 50 µl 20% (w/v) SDS 4 ml 30% (w/v) Acrylamide 100 µl 10% (w/v) APS 10 µl TEMED
Resolving gel (10%)	1.09 ml H_2O 3.75 ml 0.5M Tris-HCl pH 6.8 50 µl 20% (w/v) SDS 5 ml 30% (w/v) Acrylamide 100 µl 10% (w/v) APS 10 µl TEMED
Stacking gel	2.5 ml H_2O 1.25 ml 0.5M Tris-HCl pH 6.8 25 µl 20% (w/v) SDS 1 ml 30% (w/v) Acrylamide 50 µl 10% (w/v) APS 5 µl TEMED
Western Blot	
Transfer buffer	25 mM Tris base 192 Mm Glycine 20% (v/v) Methanol
PBS Tween (PBST)	1 x PBS 1 % Tween 20
Recombinant protein expression	
Lysis buffer	50 mM NaH2PO4 300 mM NaCl 10 mM imidazole
8 M Urea IB buffer	100 mM NaH_2PO_4 10 mM Tris-HCl 8 M Urea pH 7.2
Recombinant protein expression – Miniprep purification	
Buffer B (Binding buffer)	7 M Urea 100 mM NaH2PO4 100 mM Tris-HCl pH 8 filter sterilize
Buffer C (Wash buffer)	8 M Urea 100 mM NaH2PO4 100 mM Tris-HCl pH 6.3 filter sterilize

Buffer E (Elution buffer)	8 M Urea 100 mM NaH2PO4 100 mM Tris-HCl pH 4.5 filter sterilize
Recombinant protein expression – Äkta purification	
Binding Buffer	20 mM $NaPO_4$ 0.5 M NaCl 20 mM Imidazol 8 M Urea pH 7.4 filtrate
Elution Buffer	20 mM $NaPO_4$ 0.5 M NaCl 500 mM Imidazol 8 M Urea pH 7.4 filtrate
Dialysis	
Buffer I	6 M Urea 20 mM Hepes pH 7.9 300 mM KCl 5 mM MgCl2 10 % Glycerol 1 mM DTT
Buffer II	20 mM Hepes pH 7.9 300 mM KCl 5 mM MgCl2 10 % Glycerol 1 mM DTT
Antibody preparation - Äkta	
Sample buffer	1 M Tris-HCl pH 9 filter sterilize
Binding buffer	20 mM citric acid pH 7 filter sterilize
Elution Buffer	100 mM citric acid pH 3.8 filter sterilize
Microscopy	
Mounting Media	20 mM Tris pH 8 0.5 % N-propylgallate 90 % (v/v) glycerol

3.1.5 Plasmids

Table 6: Plasmids used in this study.

Plasmid	Genotype or description	Resistance	Reference
pREP4	Repressor plasmid with constitutively expressed *lac I*	Kanamycin	Qiagen, Venlo, Netherlands
pQE vectors	Low-copy plasmid; T5 transcription-translation system Two *lac* operator sequences	Ampicillin	Stüber et al 1990[3]
pQE60	C-terminal 6x His-tag sequence	Ampicillin	Qiagen, Venlo, Netherlands
pQE30Xa	N-terminal 6x His-tag sequence; Factor Xa protease recognition site	Ampicillin	Qiagen, Venlo, Netherlands
pQE1919	Expression of the protein product of Cag_1919	Ampicillin	This work
pQE1920	Expression of a fragment of the protein product of Cag_1920	Ampicillin	This work
pQE0614a	Expression of a fragment of the protein product of Cag_0614	Ampicillin	This work
pQE0614b	Expression of a fragment of the protein product of Cag_0614	Ampicillin	This work
pQE0616a	Expression of a fragment of the protein product of Cag_0616	Ampicillin	This work
pQE0616b	Expression of a fragment of the protein product of Cag_0616	Ampicillin	This work

3.1.6 Oligonucleotides

Table 7: Oligonucleotides used in this project.

Oligonucleotide	Sequence (5'-3')	Application
pQE60RTXfor	GCGCCCATGGCTGATTTTATTAGG	Cloning of the plasmid pQE1919
pQE60RTXrev	GCGCGGATCCTTACAAGAAGAGC	Cloning of the plasmid pQE1919
0616-pQE80-1_for	GCGCGGATCCGAGCTAACTATTG	Cloning of the plasmid pQE0616a
0616-pQE80-1_rev	GCGCCTGCAGTGATAAACTACTATTG	Cloning of the plasmid pQE0616a

[3] Stueber *et al.* (1990)

0616-pQE80-2_for	GCGCGGATCCGAGGAATTAGAACGG	Cloning of the plasmid pQE0616b
0616-pQE80-2_rev	GCGCCTGCAGAAGCCCTTGCGAA	Cloning of the plasmid pQE0616b
0614-pQE80-1_for	GCGCGGATCCATGGCTGAATATGC	Cloning of the plasmid pQE0614b
0614-pQE80-1_rev	GCGCCTGCAGTGCATCGTTAATGC	Cloning of the plasmid pQE0614b
0614-pQE80-2_for	GCGCGGATCCTACAAGTCGGG	Cloning of the plasmid pQE0614a
0614-pQE80-2_rev	GCGCCTGCAGTCCGAAGCGTAC	Cloning of the plasmid pQE0614a
1920-pQE80_for	GCGCGGATCCGGCTGGCGAAGGCTAC	Cloning of the plasmid pQE1920
1920-pQE80_rev	GCGCCTGCAGTGGCACATTCCATAC	Cloning of the plasmid pQE1920

3.2 Bacterial cultures and growth conditions

3.2.1 "*Chlorochromatium. aggregatum*" and *Chlorobium chlorochromatii*

Enrichments of the consortium "*Chlorochromatium. aggregatum*" were grown in 10 l glass flasks containing anoxic sulfide-reduced K3 medium (Kanzler *et al.,* 2005) and incubated at room temperature under continuous illumination of 25 mmol quanta m^{-2} s^{-1} incident light intensity of tungsten light bulbs. Under these conditions a dense biofilm of consortia forms on the inner surface of the culture vessel, which can be harvested separately from the accompanying bacteria (Pfannes *et al.,* 2007). The pure culture of the epibiont *Chlorobium chlorochromatii* CaD was grown under the same conditions in 50 ml bottles containing SL10 medium with the addition of acetate (3 mM).

3.2.2 *Eschericha coli* strains

Escherichia coli M15 (Qiagen, Venlo, Netherlands) was used for cloning procedures and amplification of the plasmids, while *E. coli* XL-1 Blue (Agilent Technologies, CA, USA) (Tab. 1) was used for the expression of recombinant proteins.

3.3 Primer design for recombinant protein expression

The ORFs Cag_0614, Cag_0616, Cag_1919 and Cag_1920 of the epibiont were extracted from the NCBI database and utilized to design primer sequences. To ensure a unique sequence within the consortia, the amino acid sequences were compared through a Blast (basic local alignment tool) search (Altschul *et al.,* 1990) with the annotated proteins of the epibiont and the central bacterium. All primers were constructed containing four GCGC bp at

the 5' end to serve as a clamp for the added restriction site sequence and the start or stop sequence for the chosen region of the symbiotic protein. For Cag_1919 the restriction sites *Nco*I-*Bam*HI were added to the forward and reverse primer sequence enabling the cloning of the entire gene sequence into pQE60 (Qiagen, Venlo, Netherlands). Previously chosen sequence regions (3.3.1) of the genes Cag_1920, Cag_0614 and Cag_0616 were cloned as *Bam*HI-*Pst*I fragments into pQE30Xa (Qiagen, Venlo, Netherlands).

3.3.1 Sequence analysis of Cag_0614, Cag_0616 and Cag_1920

Due to the size of the symbiotic proteins, except for Cag_1919, segments for each protein were selected to be used as antigen in polyclonal antibody production. Cag_0614 and Cag_0616 possess regions of high sequence similarity which makes these amino acid positions redundant in regards to antibody production, due to cross reactions between the two proteins. Therefore these regions were excluded from further analyses. The amino acid sequences of Cag_0614, Cag_0616 and Cag_1920 were analysed regarding putative transmembrane (highly hydrophobic) segments and regions that are likely exposed on the surface of the protein (hydrophilic domains) and therefore potentially antigenic. To generate a hydrophobicity plot (web.expasy.org/protscale/), the protein sequence was scanned with a moving window and the hydrophobic index of the amino acids within the windows calculated. The hydrophobicity scale used, was determined by Kyte and Doolittle (Kyte & Doolittle, 1982). To identify amino acid sequences with a high probability of being located on the surface of the protein, the window size was set to 9 with a hydropathy score setting above 2 (Kyte & Doolittle, 1982). Possible transmembrane regions were also determined with a Kyte and Doolittle plot changing the window size to 19. A suitable hydrophilic region was chosen and enclosed between the forward and the reverse primer (primer nucleotide positions see Tab. 8).

Table 8: Nucleotide positions of the primers within the epibiont genome.

Epibiont gene	Plasmid	Nucleotide position of the primer sequence
Cag_1919	pQE1919	1 - 4578
Cag_1920	pQE1920	1395 - 2061
Cag_0614	pQE0614a	19810 - 21489
Cag_0614	pQE0614b	41410 - 41994
Cag_0616	pQE0616a	742 - 1668
Cag_0616	pQE0616b	20434 - 21489

3.4 Molecular biology techniques

3.4.1 Plasmid preparation

For a plasmid preparation a 5 ml overnight culture was inoculated with one colony of the appropriate strain. Antibiotics were added depending on the strain and the plasmid. On the following day the plasmid was extracted with a plasmid miniprep kit (Qiagen, Venlo, Netherlands) following the manufacturer's instructions.

3.4.2 PCR (polymerase chain reaction)

The amplification of the gene fragments of *Cag_0614*, *Cag_0616*, *Cag_1920* and the gene *Cag_1919* was carried out with 1 µl of chromosomal epibiont DNA. In order to obtain the template DNA 10 ml of cells with an OD_{650} = 1 was centrifuged at 10000 g for 5 min. The pellet was then washed and resuspended in 1 ml of 10 mM Tris·HCl pH 8.5. After placing the cells five times alternatingly in ice water and boiling water for 5 min, they were centrifuged at 10,000 g for 10 min. The supernatant was used as template material in PCR reactions, yielding ~100 ng DNA. When amplifying the gene *Cag_1919,* the PCR reaction comprised 0.25 µM of each primer, 10 µl of 5x Herculase II reaction buffer, 0.25 mM of each dNTP, 1 µl Herculase II fusion DNA polymerase (Agilent Technologies, CA, USA) and 2 % DMSO in a total volume of 50 µl. In the PCR reactions for the three other genes 0.5 µl DNA polymerase was used. All amplifications were performed in a GeneAMP thermo cycler PCR system 9700 (Applied Biosystems) (Tab. 9) and analyzed by standard agarose gel electrophoresis. DNA was amplified until sufficient quantities of DNA were gained for enzyme digestion and further cloning.

Table 9: PCR conditions. Each PCR started with 95°C for 2 min and ended with 72°C for 4 min.

Target	**Plasmid**	**Primer combination**	**Melting**	**No. of cycles: 30**	
				Annealing	**Extension**
Cag_1919	pQE1919	pQE60RTX_for pQE60RTX_rev	95°C, 20 s	62°C, 20 s	72°C, 150 s
Cag_1920	pQE1920	1920-pQE80_for 1920-pQE80_rev	95°, 20 s	62°C, 20 s	72°C, 60 s
Cag_0614	pQE0614a	0614-pQE80-2_for 0614-pQE80-2_rev	95°C, 20 s	63°C, 20 s	72°C, 60 s
	pQE0614b	0614-pQE80-1_for 0614-pQE80-1_rev	95°C, 20 s	61°C, 20 s	72°C, 60 s

Cag_0616	pQE0616a	0616-pQE80-1_for 0616-pQE80-1_rev	95°C, 20 s	61°C, 20 s	72°C, 60 s
	pQE0616b	0616-pQE80-2_for 0616-pQE80-2_rev	95°C, 20 s	63°C, 20s	72°C, 60 s

3.4.3 Agarose gel electrophoresis

Small horizontal agarose gels were made with 1 % agarose dissolved in 1x TAE. Before the DNA samples were loaded, 5x DNA loading dye was added. The samples were run with a 10kb or 1kb ladder at 100V between 15 to 60 mins. The gel was then stained with ethidium bromide and placed under ultraviolet light to visualize DNA.

3.4.4 DNA extraction from agarose gel

Bands containing the correct size of DNA molecules, were cut out of the gel with a scalpel and placed in a 1.5 ml eppendorf tube. The DNA was extracted using a gel extraction kit (Qiagen, Venlo, Netherlands) following the manufacturer's instructions.

3.4.5 DNA digestion

Plasmid and amplified DNA were cut with restriction enzymes to create complementary ends. The correct restriction sites at both ends of the amplified DNA were added in the PCR reaction by placing the restriction sequence in the primer sequence. All restriction enzymes were obtained from Thermo Fisher Scientific (Waltham, USA), and used in the following combination:

Plasmid	FastDigest enzymes
pQE60 based plasmids:	BamHI – NcoI
pQE30Xa based plasmids:	BamHI - PstI

Plasmid DNA was digested using the following protocol:

Plasmid DNA:	up to 1 µg (1-2 µl)
10x FastDigest buffer:	2 µl
Enzyme (10U/µl):	1 µl
ddH_2O:	to 20 µl

Digest at 37°C for 5 min.

If the plasmid was used for DNA ligation it was dephosphorylated with alkaline phosphatase (Thermo Fisher Scientific, Waltham, USA) which selectively cleaves terminal phosphate groups from oligonucleotides.

The following protocol was used:

Digested plasmid DNA:	1 µl
Alkaline phosphatase:	1 µl
10x buffer:	2 µl
ddH_2O:	to 20 µl

Incubate at 37°C for 10 minutes.

Chromosomale DNA was digested using the following protocol:

Genomic DNA:	5-10 µg (1-2 µl)
10x FastDigest buffer:	5 µl
Enzyme (10U/µl):	1 µl
ddH_2O:	to 50 µl

The digested DNA was purified via gel electrophorese.

3.4.6 DNA ligation

DNA ligation was used to ligate an insert a DNA molecule into a plasmid. The plasmid and DNA fragment were individually cut to yield complementary ends before the ligation. A 10 µl ligation mix containing approximately 10 ng plasmid DNA was prepared with the following quantities (buffer and enzyme: Thermo Fisher Scientific, Waltham, USA):

1 µl 10x T4 ligase buffer

1 µl T4 ligase

25 ng plasmid DNA

150 ng insert DNA

8 µl minus the vector and insert volume of ddH_2O

The ligation reaction was incubated for 3-4 hours at room temperature with the exception of the ligation reaction containing Cag_1919 which was incubated overnight at 4°C.

3.4.7 DNA sequencing

DNA sequencing was performed by the faculty biology genomics service unit of the LMU Munich using their "cycle, clean and run BigDye v3.1" protocol. The following reaction mixes was prepared:

Template DNA:	10 - 40 ng (200-500 bp)
	20 - 50 ng (500-1000 bp)
	40-100 ng (1000-2000 bp)
	50 – 150 ng (> 2000 bp)
Primer:	3.2 pmol
10 mM TrisHCl pH 8.5:	to 7 µl

3.4.8 Preparation of competent cells and transformation

The required *E. coli* strain was grown in LB supplemented with antibiotics overnight. The following day the culture was diluted 1:100 in 5 ml LB and incubated at 37°C with shaking until the cells had reached early log phase. The cell culture was then spun down at 5000 g for 7 mins. The cell pellet was resuspended in 1 ml TSB and kept on ice or stored at -80°C.

Between 50 and 100 µl of cells were incubated with 1-2 µl DNA (~100-400 ng) in eppendorf tubes on ice for 30 mins. The cells were then heat shocked in a 42°C water bath for 90 s and placed back on ice for 10 minutes. After this 1 ml LB was added and the transformation incubated in a 37°C heat block for 1 hour. The cells were spun down in a benchtop eppendorf centrifuge at 10 000 g for 1 minute and resuspended in 100-200 µl LB. The transformation was plated on agar plates containing an antibiotic for positive selection of the transformed cells.

3.4.9 Cell fractionation

In order to obtain different cell fractions for the negative control, 2 g of a XL-1 Blue cell pellet was washed with 50 mM Tris-HCl buffer pH 7.5. To maintain sphaeroplast integrity after the removal of the cell wall, the pellets were resuspended in 50 mM Tris-HCl buffer with 40 % (v/v) sucrose. 20 µl of 250 mM ethylenediamine tetraacetic acid (EDTA) and 10 µl of lysozyme (0.06 g/l) were added and the digest incubated for 30 min at 37°C. The sphaeroplasts were spun down and the supernatant was collected as the periplasmic fraction. The pellet was resuspended in 1 ml Tris-HCl buffer and the sphaeroplasts were lysed by osmotic shock. The suspension was homogenised, sonicated (Bandelin Sonopuls HD 2070) and centrifuged at 20,000 g at 4°C for 20 min. The supernatant was then ultracentrifuged at 160,000 g at 4°C for 30 min to pellet the cell membranes. Membranes were solubilised in MBE and the supernatant was collected as the cytoplasmic fraction.

The protocol to obtain cell fractions for the consortia and the epibiont was adjusted as follows. 1 g of cell pellet were washed with PBS and resuspended in 0.3 M Tris-HCl buffer with 40 % (v/v) sucrose. 1 mM EDTA and 1 mg of lysozyme were added to the buffer. The periplasmic fraction was collected as described above. After the sphaeroplasts were lysed by osmotic shock the cell pellet was resuspended in CBC, the suspension was sonicated and centrifuged at 1700 g at 4°C and for 20 min. The supernatant was ultracentrifuged at 160,000 rpm and at 4°C for three hours to pellet the cell membranes. The resulting supernatant was collected as the cytoplasmic fraction and the pellet solubilised with MBC.

3.4.10 Measurement of the protein concentration via Lowry assay

Protein concentration of a sample was determined with serum albumin standards (BSA 2 mg ml^{-1}) using 0, 2, 4, 6, 8, 10 mg ml^{-1} as reference. The standards and if required the samples were diluted in 2 % SDS of which 5 µl were pipetted into a 96 well test plate in triplicate. 25 µl of reagent A (Bio-Rad, California, USA) and 200 µl of reagent B (Bio-Rad) were added to each well containing a sample. The plate was left to incubate in the dark for 15 min. The absorbance was read with the multimode reader Infinite M200 (Tecan, Männedorf, Schweiz) at 750 nm.

3.4.11 SDS PAGE

SDS PAGE was conducted with the Bio-Rad system and performed with the Laemmli buffer system (Laemmli, 1970). Vertical gels were poured with glass plates (0.75 mm) standing in a casting stand. The concentration of polyacrylamide in the separating gel depended on the size of the protein of interest.

Protein	Polyacrylamide concentration [%]
Cag_1919	10
Cag_0614 segments	12
Cag_0616 segments	12
Cag_1920 segment	12

Gels were placed in a tank filled with 1x SDS running buffer. When whole cell samples were analysed, 2 ml of cells with an OD_{595} = 0.7 was boiled in Laemmli sample buffer (Serva Electrophoresis, Heidelberg, Germany) for 5 min, centrifuged at 20,000 g for 5 min and the supernatant used for loading the gel. If a cell fraction or previously treated sample was used, the sample would be diluted 1:1 with Laemmli sample buffer and processed as above.

The gel was run at 80 V until the samples reached the separating gel, after which the voltage was raised to 120 V. The gel electrophoresis was stopped as soon as the bromophenol blue front had passed through the separating gel. For the analysis of the production of recombinant protein, the gel was stained with Coomassie Brilliant Blue R-250. Afterwards the gel was photographed or dried in gel drying frames between two sheets of cellophane (Maxi frames, Carl Roth, Karlsruhe, Germany).

3.5 Production of antibodies targeting symbiotic proteins of the epibiont

3.5.1 Establishing a production protocol for recombinant protein expression

3.5.1.1 Small-scale expression cultures

Optimum conditions for recombinant protein expression were determined with a screening method adapted from the QIAexpressionist (Qiagen, Venlo, Netherlands) handbook. 50 ml culture medium (Tab. 3) was inoculated with 0.5 – 6 ml overnight culture depending on the growth temperature which was being tested. In addition the culture media contained ampicillin (100 µg ml^{-1}) to maintain a pQE plasmid construct, kanamycin (50 µg ml^{-1}) when the *E. coli* strain also contained the pRep4 vector or tetracyclin (50 µg ml^{-1}) when the *E. coli* strain XL-1 Blue was used. Recombinant protein expression was induced by adding isopropyl-β-D-1-thiogalactopyranoside (IPTG) to a final concentration of 1 mM as soon as the cultures had grown to an optical density of $OD_{595} = 0.7$ with vigorous shaking.

Expression levels of recombinant protein were monitored by removing 2 ml aliquots over a course of two days or more. The cells were spun down at 10,000 g for 5 min, washed with 0.5 M TrisHCl, spun down again and frozen at -20°C. The aliquots were collected, processed and the resulting fractions analysed with SDS PAGE.

3.5.1.2 Determination of target protein solubility

The collected cell pellets of a protein expression experiment were thawed on ice and resuspended in 5 ml lysis buffer. The samples were sonicated 5 x 30 s with 10 s pauses at 60 % amplitude (Bandelin Sonopuls HD 2070) and centrifuged at 10 000 g for 20 min at 4°C. The supernatant was collected as the soluble fraction, while the insoluble protein fraction was obtained by resuspending the pellet in 5 ml lysis buffer. 5 µl of the sample was diluted with 5 µl Laemmli buffer and heated at 99°C for 5 min. The samples were centrifuged at 15 000 g for 1 min and 10 µl loaded on a SDS PAGE gel. The gel was run as described in chapter 3.4.11 and stained with Coomassie Brilliant Blue R-250 to visualize the protein bands. Recombinant protein expression was followed by comparing protein bands of the calculated protein size with the protein bands of a non-induced negative control.

3.5.2 Production and purification of inclusion bodies

The following protocol produced inclusion bodies in sufficient amounts for all recombinant proteins. 200 ml TB medium containing 100 µg ml^{-1} ampicillin and 75 µg ml^{-1} tetracyclin was inoculated with 6 ml overnight culture. The production of the recombinant protein product of Cag_1919 was only possible with the addition of the plasmid pRep4. To maintain the plasmid

50 µg ml^{-1} kanamycin was added. The culture was grown to an optical density of OD_{595} = 0.7 and the recombinant protein expression was started with 1 mM IPTG. The cells were harvested 50 to 72 h after induction and washed twice with 0.5 M Tris-HCl. Inclusion bodies were purified with BugBuster Protein Extraction Reagent (Novagen, Darmstadt, Germany) following the protocol for inclusion body preparation. Additionally, recombinant proteins were suspended in 8 M urea IB buffer and shaken for 1 h at 4°C. After centrifugation for 30 min at 20,000 g and 8°C the supernatant contained purified inclusion bodies.

3.5.3 Purification of recombinant proteins

3.5.3.1 6xHis-tagged protein minipreps under denaturing conditions

Cells were harvested from a 50 ml expression culture and washed twice with 0.5 M Tris-HCl. The cell pellet was resuspended in 2 ml buffer B (Tab. 5), sonicated and divided into 1 ml aliquots. From this point the manufacturer's protocol for Ni-nitrilotriacetic acid (Ni-NTA) spin columns (Qiagen, Venlo, Netherlands) with lysates under denaturing conditions was followed. Several variations and suggestions for adapting the protocol were also implemented. Elution fractions were collected and analysed to determine the purity of the Hi-tagged proteins with SDS PAGE and subsequent Coomassie staining of the gel.

3.5.3.2 Batch purification of 6xHis-tagged proteins under denaturing conditions

Batch purification was conducted with Ni-NTA solution (Qiagen, Venlo, Netherlands) which was directly combined with purified inclusion bodies to increase the possible binding time between the His-tagged protein and Ni-NTA. First 1 ml Ni-NTA was pipetted into a 2 ml Eppendorf tube and the Ni-NTA allowed to sediment. In order to equilibrate the Ni-NTA the upper phase was discarded, Ni-NTA mixed with 500 µl distilled water and again allowed to sediment. This step was repeated once with distilled water and once with buffer B (Tab. 5). Different dilutions starting at 1:5 of purified inclusion bodies and buffer B were then combined 1:1 with the Ni-NTA. The solution was shaken at 300 rpm at room temperature for one hour and then transferred to a suitable column. 500 µl of buffer C was applied twice to wash the Ni-NTA and subsequently three times 500 µl of buffer E to elute His-tagged proteins. The fractions were collected on ice and analysed on a SDS PAGE gel.

3.5.3.3 Purification of proteins with Äkta

Recombinant protein products of Cag_0614, Cag_0616 and Cag_1920 were purified using the Ni-nitrilotriacetic acid HisTrap FF 1ml column (GE Healthcare, Buckinghamshire, Great Britain) applying the Aektaprime plus system (GE Healthcare, Amersham, Great Britain).

First the system was washed with 20 % Ethanol by starting the manufacturer's pre-program "System Wash Methode". The process was repeated twice with distilled water and binding buffer (Tab. 5). A 2 ml sample loop was connected to the system, washed with 10 ml distilled water and filled with binding buffer. 300 µl of binding buffer was then displaced with 300 µl purified inclusion bodies (3.5.2). The following method was programed (Tab. 10) using the method Histidine-tag purification as template. It was applied to purify the recombinant proteins which were expressed with a His-tag.

Table 10: His-tagged protein purification program.

Step	Preprogramed steps	Programed
1	Injection	valve
2	Pressure limit	0.5 MPa
3	Flow rate	1 ml min^{-1}
4	Fraction size	0.5 ml
5	Equilibration size	5 ml
6	Sample volume	300 µl
7	Wash volume 1	15 ml
8	Elution volume	5 ml
9	Wash volume 2	15 ml

A UV measuring cell was used to monitor protein elution. The elution fractions containing the purified protein were combined and the Urea of the elution buffer (Tab. 5) removed by dialyse (3.5.4). The obtained proteins subsequently screened with a 12 % SDS PAGE gel and the concentration determined via Lowry assay.

In contrast the recombinant protein product of Cag_1919 could not be purified by its His-tag, therefore the protein was purified with the size exclusion column HiPrep 16/60 Sephacryl S-300 HR (GE Healthcare, Buckinghamshire, Great Britain). Following the manufacturer's instruction and using the method template for gelfiltration the conditions shown in table 11 was applied for size exclusion purification.

Table 11: Program for size exclusion purification of proteins on the Äktaprime plus.

Action	Step	Volume	Flow rate
Equilibration	1	240 ml	0.5 ml min^{-1}
Sample applification	2	Injection vol.: 1.2 ml	
Elution	3	120 ml	0.5 ml min^{-1}
Fraction size	3	5 ml	

The column was equilibrated, washed and stored as described in the manufacturer's instructions. The elution fractions were screened with a 10 % SDS PAGE gel.

3.5.4 Dialysis

All recombinant proteins were solubilised in 8 M urea buffers. The high concentration of urea had to be removed without precipitating the proteins. Therefore the samples were pipetted into a dialysis unit from Spectrum Labs (Los Angeles, USA) and placed in a glass beaker. The following buffer amounts were added in succession to 200 ml buffer I (Tab. 12).

Table 12: Dialyse steps and buffer volumes used during dialyse.

Step	Urea conc.	Buffer	Time	Total Vol
1	6 M	Buffer I	2 h	200 ml
2	5 M	Add 35 ml buffer II	2 h	236 ml
3	4 M	Add 50 ml buffer II	2 h	286 ml
4	2 M	Add 75 ml buffer II	2 h	361 ml
5	2 M	Add 120 ml buffer II	2 h	481 ml
6	1 M	Substract 250 ml, add 250 ml of buffer II	2 h	500 ml
7	0.5 M	Substract 250 ml, add 250 ml of buffer II	2 h	500 ml
8	0 M	Replace all with buffer II	2 h	500 ml
9	0 M	Replace all with buffer II	2 h	500 ml

3.5.5 Antibody production

Purified proteins were used as antigen for polyclonal antibody production. The Speedy 28 days program of Eurogentec (Seraing, Belgium) was chosen for antisera production and subsequent affinity purification. These purified polyclonal antibodies were employed as primary antisera in immunoblot, immunofluorescence and immunogold analyses.

3.5.5.1 Purification of pre-immune serum

The purification of preimmune sera, supplied with the antibodies by Eurogentec, was carried out with a HiTrap Protein A column (GE Healthcare, Buckinghamshire, Great Britain) run in the Äkta. The preimmune fractions were thawed on ice and 2 ml diluted with 3 ml binding buffer (Tab. 5Table 5). The Äkta machine was run with a 5 ml sample line which was filled with 5 ml sample by displacing previously administered sample buffer. The first six slots of the fraction wheel were supplied with six Eppendorf tubes filled with 50 µl sample buffer in order to neutralize the pH value of the elution fraction. The system was connected with the binding and elution buffer and the program Mab-purification Step elution for monoclonal antibodies started, as described in the Aektaprime plus manual. The OD value of each fraction was measured with the Eppendorf BioPhotometer and used to calculate the antibody

concentration with the standard OD = 1.45 amounting to 1 mg ml^{-1} protein concentration. Fractions containing antibodies were pooled and the buffer exchanged with 0.5 M PBS facilitating the HiTrap Desalting 5 ml column (GE Healthcare, Buckinghamshire, Great Britain), following the manufacturer's instruction.

3.5.6 Western blotting

Western blotting was carried out to detect the protein Cag_1919 in the sample of interest. SDS PAGE was used to separate the proteins which were then transferred to a polyvinylidene difluoride (PVDF) membrane (Carl Roth, Karlsruhe, Germany) and detected using antibodies specific to the Cag_1919 protein.

The gels were carefully removed from the glass plates and incubated in 1 x transfer buffer on a shaker for 10 min. The PVDF membrane was cut and activated with methanol for 10 minutes and then soaked in 1x transfer buffer. A test tube was then rolled across each layer to prevent formation of gas bubbles between the layers.

The transfer took place in a wet tank Bio-Rad system at 50 V for 3 h. The membrane was blocked overnight; incubated for 1 h with the primary antibody (diluted 1/1000 in PBST) and incubated for one hour with a horseradish peroxidase (HRP) conjugated secondary antibody (diluted 1/2000 with PBST). To visualise the protein the membranes were incubated for 5 min with chemiluminescent HRP substrate system Lumi-Light from Roche Diagnostics (Basel, Switzerland) and scanned with the photoimager Fujifilm LAS-3000.

3.5.7 Dot Blotting

Due to the size of the proteins Cag_0614 and Cag_0616 only dot blotting could be performed in order to localize the proteins in the samples of interest. A treated PVDF membrane was placed under a 96 well plate of the Bico BRL maschine (Life Technologies, CA, USA), and subsequently 100 µg protein per sample applied in 100 µl 1 M Tris HCl (pH 7.2). The membrane was washed three times with PBS in the dot blotter and dried for 1 h at room temperature. Visualization of the proteins was carried out as described in 3.5.6 with the respective antibodies.

3.6 Immunofluorescence

3.6.1 Sample preparation for high resolution microscopy

Consortia and epibionts for the immunofluorescence protocol were grown as described in 3.2.1, collected on black polycarbonate filters (0.2 µm pore size; Merck Millipore, MA, USA) and washed three times with PBS. The protocol developed by Buddelmeijer et al. (Buddelmeijer *et al.,* 1998) was adapted to be effective for the cells of consortia. For detection of Cag_0614 and Cag_0616 products, cells were fixed in 3.5% (v/v) formaldehyde and 0.008% (v/v) glutaraldehyde in PBS at room temperature for 4 h and for Cag_1919 products cells were fixed in 4% (v/v) paraformaldehyde overnight at 4°C. The filters were washed three times with PBS and incubated in 0.2% (v/v) Triton X-100 for 1 h at room temperature, washed again and incubated in PBS containing lysozyme (100 µg ml^{-1}) and 5 mM EDTA for 1 h at room temperature. Filters were blocked by incubation in 0.5% (w/v) blocking reagent (Boehringer, Ingelheim, Germany). The first antibody was applied in a 1:1000 dilution in PBST during overnight incubation of filters at 4°C. After washing the filters three times with PBS, the secondary antibody goat anti-rabbit antibody conjugated with Alexa Fluor 488 nm (Agilent Technologies) was diluted 1:2000 in PBS and applied for 1 h. Negative controls were performed with pre-immune sera and the secondary antibody.

3.6.2 Microscopy and image analysis

Filters were treated with 100 ng·ml^{-1} 4',6-diamidino-2-phenylindole (DAPI) for 10 min, washed three times with PBS and sectioned with a scalpel. One quarter of the filter was placed on a glass slide and layered with a drop of mounting media. On top of the filter a 22 x 22 mm cover slip (High Precision Glass 170 ± 5 µm, Carl Roth) was placed and sealed with nail varnish. The cells were photographed with the Andor camera DU-897X-4669 mounted on a Nikon Eclipse Ti high resolution microscope (Nikon, Tokyo, Japan). Each microscopic field was photographed first with a filter for immunofluorescence, followed with a filter to capture the autofluorescence of bacteriochlorophyll *c* of the chlorosomes in the epibiont cells and lastly with a DAPI filter (Tab. 13).

Table 13: Excitation and Emission values for three different filter systems used in the Nikon Eclipse Ti high resolution microscope.

Filter	Excitation	Emission
Immunofluorescence	442/46	525/45
Autofluorescence	430/24	760/50
DAPI	377/50	442/46

For every fluorescence filter a set of z-stack images with a distance of 0.1 µm was taken. The images were subsequently analysed with the Nikon program NIS-Elements AR 4.13.01 for deconvolution. The localization of the immunofluorescence signal was visualized through an overlay of the images which were taken with the three different filter sets.

3.7 Immunogold labelling

3.7.1 Sample preparation for immunogold localization

A higher resolution for the localization of the symbiotic proteins in "*C. aggregatum*" can be achieved by cryosectioning the consortia and applying antibodies conjugated with gold particles. Therefore the consortia were fixated by freeze-substitution in acetone containing 0.3 % uranyl acetate using the Leica EM HPM 100 (Leica, Vienna, Austria). The samples were heated to -90°C and remained at this temperature for 28 h. Subsequently the samples were heated to -60°C over 6 h, held at – 60°C for 4 h and then heated to -50°C over 2.5 h. The samples remained at – 50°C for the following steps: Samples were washed three times for 15, 30 and 45 minutes with pure acetone; emerged in a graded series of HM20/acetone mixtures: 25% HM20 for 1.5 h, 50 % HM20 for 2 h, 75% HM20 for 2.5 h and pure HM20 for 16 h, 3.5 h, and 4 h and subsequently polymerised with ultraviolet light for 48 h. The temperature was raised to 20°C during the next 14 h and the samples were again polymerised for 22 h. Cryosections were cut, washed twice with PBS containing 50 mM glycine, placed in blocking buffer (0.5 % BSA, 0.05 % gelatine, 0.01 % tween 20 in PBS) for 1 h and then incubated overnight at 4°C with the primary antibody (5 µg/ml of the pre-immune serum). Then the samples were washed six times for 5 minutes with blocking buffer and incubated with the secondary antibody, anti-rabbit conjugated with 6 nm gold particle (Dianova, Hamburg, Germany), for 90 minutes at room temperature. Subsequently the samples were twice washed for 5 minutes with blocking buffer, PBS containing glycine, PBS and water (Ampuwa, Fresenius). The described procedures were conducted by Sylvia Dobler and Prof. Gerhard Wanner at the LMU in Munich.

3.7.2 Analysis of immunogold localization

The immunogold labelling conducted with antiserum targeting each of the three putative symbiotic proteins was analysed statistically. The gold particles were allocated to the different compartments of the cells, which in this analysis included the cytoplasm and membrane regions of the central bacterium and the epibiont. Gold particles were allocated to the membrane when they were detected closer than a 25 nm distance from the membrane (approximate length of the antibody complex). In total 38 immunogold labelling pictures were

analysed including the incubations with the pre-immune sera. The statistical significance of the labels in regard to the negative controls was analysed using an unpaired t-test (GraphPad: http://www.graphpad.com/quickcalcs/). To determine if the differences in the labelling of the subcellular compartments of the cells were statistically significant, the average number of immunogold particles per μm^2 area was calculated for each subcellular location. Therefore the average number of immunogold particles per intercellular location could be analysed with a pair-wise comparison t-test using the R code command pairwise.t.test in Rstudio.

3.8 Mapping of short read transcriptome data

Transcriptome data of *Chl. chlorochromatii* was generated by Dr. Johannes Müller. Short read transcriptome data (fastq-files from an Illumina 37 bp single end run) was mapped by Dr. Boyke Bunk against the complete genome of *Chl. chlorochromatii* (GenBank Acc. No CP000108.1) using BWA (Burrows-Wheeler Aligner, (Li & Durbin, 2009). Sorting and indexing of the resulting bam-files was performed with Samtools (Li *et al.,* 2009). IGV (integrative genome viewer, (Robinson *et al.,* 2011) allowed for comparative display of all transcriptomes in order to delineate polycistronic features from raw read data.

3.9 Experimental procedures for the metabolic analysis of the two partners of "*Chlorochromatium aggregatum*"

3.9.1 Nanoscale secondary ion mass spectrometry (NanoSIMS)

To determine the transfer of ^{13}C and ^{15}N between the cells of consortia, the isotope composition of the epibonts and the central bacterium of consortia was analysed separately with nanoSIMS. For each experiment consortia biofilm was harvested and washed with K4 medium lacking $NaHCO_3$ and/or ammonium depending on the experimental setup. Washed cell suspensions were adjusted to an OD_{650} of 1.0 and incubated at 25 µmol quanta m^{-2} s^{-1} incident light intensity. For the analysis of carbon transfer in the presence of combined inorganic nitrogen, standard cultures were washed with K4 devoid of $NaHCO_3$ and $NaH^{13}CO_3$ was added to a final concentration of 10 mM. Consortia suspensions tested for transfer of carbon and nitrogen were pregrown without ammonia and washed with K4 medium lacking ammonia and $NaHCO_3$. Labelled $^{15}NH_4^+$ was added to a final concentration of 1 mM, which corresponds to the ammonia concentration in standard K4. Cultures tested for N_2 fixation and subsequent N-transfer were supplemented with $NaH^{13}CO_3$ and overlaid with a gas phase containing $^{15}N_2$ gas. After subsampling, aliquots were stopped with paraformaldehyde (final concentration of 2 % v/v). Subsamples were incubation overnight in paraformaldehyde and then washed twice with 1x PBS and were filtered onto 0.2 µm polycarbonate filters

(Millipore, Billerica, USA). After two more washing steps with 1 x PBS, filters were cut with a scalpel to fit on a polylysine coated glass slide. The filter pieces were dried on the glass slide and then carefully removed leaving the consortia attached to the glass slide. At least five consortia that still consisted of the clearly visible central bacterium and epibionts were selected for each time point. The glass slides were sputtered with gold at CalTech, (L.A., USA).

3.9.1.1 NanoSIMS image processing

NanoSIMS images were collected in both Image and Isotope mode on the CAMECA NanoSIMS 50L by Dr. Shawn McGlynn at Caltech (L.A., USA), with a resolving power of ~5,000. The four secondary ions $^{12}C^-$, $^{13}C^-$, $^{12}C^{14}N^-$, and $^{12}C^{15}N^-$ were simultaneously measured. In Image mode, a ~2.5 pA primary Cs^+-beam with a nominal spot size of ~100-200 nm was used. Depending on the size of the target, the beam rastered at 256 x 256 pixel resolution over square regions of 5 to 20 µm edge length. Measurements in Isotope mode were collected with an ~30-40 pA primary Cs^+-beam over square regions of the same size but typically with a reduced resolution of 128 x 128 pixels, a per frame acquisition time of 30 seconds, and a total acquisition time of one to three hours. NanoSIMS images were processed with the MatLab based program Look@NanoSIMS (Polerecky *et al.,* 2012). Each series of frames was corrected for drift. Discrete regions of Interest (ROI's) were hand-drawn on the ion images guided by the corresponding microscope images. Isotope ratios and the corresponding Poisson errors (σ) were determined for each frame. Weighted means were calculated separately for the central bacterium and the epibionts according to

$$\mu_W = \frac{\sum(x_i/\sigma_i^2)}{\sum(1/\sigma_i^2)} \qquad (\sigma = \text{Poisson error})$$

3.10 Zaragozic acid experiment

The stability of consortia was tested with the biofilm inhibiting substance zaragozic acid (López & Kolter, 2010).

The consortia biofilm was carefully harvested with K4 medium which was used to inoculate six subsequent cultures with an OD_{650} of 0.434. Before the cultures were placed in front of 25 mmol quanta m^{-2} s^{-1} incident light intensity, 0, 30 and 60 µmol of zaragozic acid were added yielding one parallel for each concentration. Samples were taken after 0h, 6h, 24h and 52h and fixated with a final concentration of 2 % paraformaldehyde overnight at 4°C. After the samples were washed twice with 1x PBS, 4.8 µl of each sample was pipetted on a glass slide and the cover slip sealed with nail varnish. Single consortia and single epibionts were counted under a 63x magnification objective with a counting grid in the ocular.

References

Altschul, S. F., **Gish, W.**, **Miller, W.**, **Myers, E. W. & Lipman, D. J. (1990).** Basic local alignment search tool. *Journal of Molecular Biology* **215**, 403–410.

Buddelmeijer, N., **Aarsman, M. E.**, **Kolk, A. H.**, **Vicente, M. & Nanninga, N. (1998).** Localization of cell division protein FtsQ by immunofluorescence microscopy in dividing and nondividing cells of Escherichia coli. *J. Bacteriol.* **180**, 6107–6116.

Gottesman, S., **Halpern, E. & Trisler, P. (1981).** Role of sulA and sulB in filamentation by lon mutants of *Escherichia coli* K-12. *Journal of Bacteriology* **148**, 265–273.

Kanzler, B. E., **Pfannes, K. R.**, **Vogl, K. & Overmann, J. (2005).** Molecular characterization of the nonphotosynthetic partner bacterium in the consortium "*Chlorochromatium aggregatum*". *Appl. Environ. Microbiol.* **71**, 7434–7441.

Kyte, J. & Doolittle, R. F. (1982). A simple method for displaying the hydropathic character of a protein. *J. Mol. Biol.* **157**, 105–132.

Laemmli, U. K. (1970). Cleavage of structural proteins during the assembly of the head of bacteriophage T4. *Nature* **227**, 680–685.

Li, H. & Durbin, R. (2009). Fast and accurate short read alignment with Burrows-Wheeler transform. *Bioinformatics (Oxford, England)* **25**, 1754–1760.

Li, H., **Handsaker, B.**, **Wysoker, A.**, **Fennell, T.**, **Ruan, J.**, **Homer, N.**, **Marth, G.**, **Abecasis, G. & Durbin, R. (2009).** The Sequence Alignment/Map format and SAMtools. *Bioinformatics (Oxford, England)* **25**, 2078–2079.

López, D. & Kolter, R. (2010). Functional microdomains in bacterial membranes. *Genes & development* **24**, 1893–1902.

Pfannes, K. R., **Vogl, K. & Overmann, J. (2007).** Heterotrophic symbionts of phototrophic consortia: members of a novel diverse cluster of Betaproteobacteria characterized by a tandem rrn operon structure. *Environ. Microbiol.* **9**, 2782–2794.

Polerecky, L., **Adam, B.**, **Milucka, J.**, **Musat, N.**, **Vagner, T. &** Kuypers, Marcel M M **(2012).** Look@NanoSIMS--a tool for the analysis of nanoSIMS data in environmental microbiology. *Environmental Microbiology* **14**, 1009–1023.

Robinson, J. T., **Thorvaldsdóttir, H.**, **Winckler, W.**, **Guttman, M.**, **Lander, E. S.**, **Getz, G. & Mesirov, J. P. (2011).** Integrative genomics viewer. *Nature biotechnology* **29**, 24–26.

Stueber, D., **Matile, H. & Garotta, g. (1990).** System for high-level production in *Escherichia coli* and rapid purification of recombinant proteins: application to epitope mapping, preparation of antibodies, and structure-function analysis. *Immunological Methods* **4**, 121–152.

Villarejo, M. R. & Zabin, I. (1974). Beta-galactosidase from termination and deletion mutant strains. *J. Bacteriol.* **120**, 466–474.

Chapter 4

Optimization of recombinant protein expression

4.1 Results

4.1.1 Recombinant protein production

The symbiotic genes Cag_1919 and segments of Cag_0614, Cag_0616 and Cag_1920 were cloned into pQE vectors due to the low copy number of the plasmid in the cell (15-20 copies per cell, (Lin-Chao, 1986)). Especially the protein sequences of Cag_0614 and Cag_0616 possess an overall hydrophobic character and could not be totally avoided in the chosen segments. Hydrophobic regions can often have a toxic effect on the host cells, likely due to association of the protein with membrane systems. Small-scale cultures were used to determine the optimal conditions for expressing recombinant proteins. The conditions tested included different *E. coli*, media, growth temperature and IPTG and tetracycline concentrations (Tab. 14).

Protein production was monitored over a time period and the soluble and insoluble protein fractions were than analyzed with a SDS PAGE gel. Figure 4 and 5 show examples of an SDS PAGE gel, loaded with the soluble (Fig. 4 A and Fig. 5 A) and insoluble protein fraction (Fig. 4 B and Fig 5 B) of XL-1 Blue, containing the plasmid pQE0616a, at different temperatures. As negative control the *E. coli* which was used for the experiment, containing an empty plasmid, was used. First, lower growth temperatures were tested with the aim to produce recombinant proteins in the soluble protein fraction. When the conditions listed in table 14 were not yielding recombinant proteins, the growth temperature was raised.

Table 14: Different growth conditions und supplements tested for recombinant protein production at 25°C and lower.

	Conditions tested
E. coli	M15
	SG13009
	XL-1 Blue
Media	LB
	TB
	NZCYM
	2x YT
Medium supplements	0.5 M sucrose
	0.05 - 0.5 M NaCl
IPTG (mM)	0.1
	0.5
	1

Figure 5 shows, in comparison to the negative control and to figure 4, a slight increase of strength in a protein band (square box), running parallel with the 40 kDa protein marker. This size corresponds with the theoretical protein mass of the recombinant protein of 0616a.

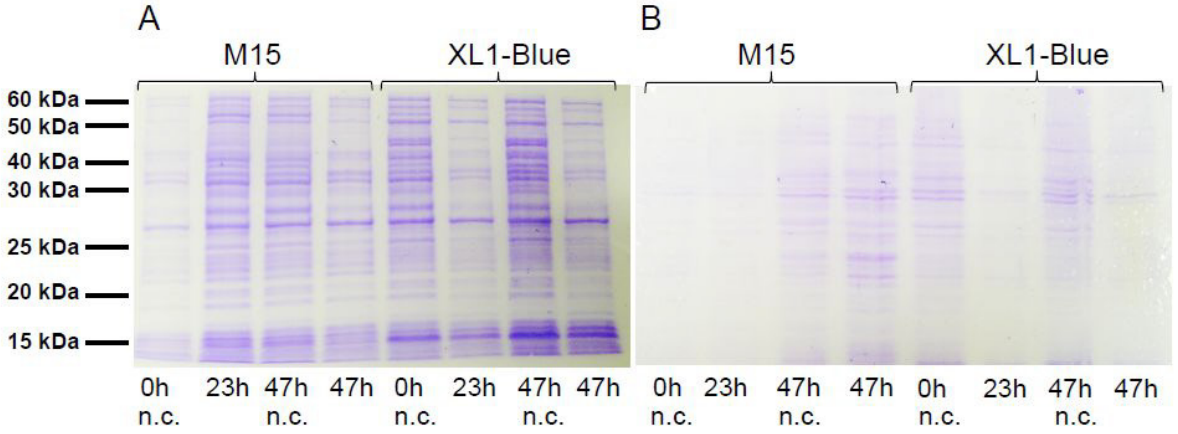

Figure 4: Recombinant protein production trial of the protein 0616a at 25°C (Xl-1 Blue in TB supplemented with 50 µg μl^{-1} tetracycline and 1 mM IPTG); n.c.: negative control. A: soluble protein fraction B: insoluble protein fraction**.**

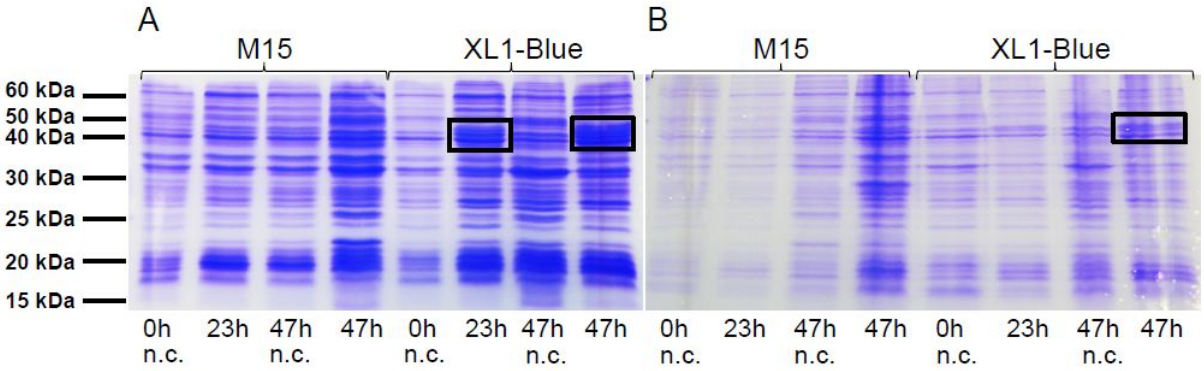

Figure 5: Recombinant protein production trial of the protein 0616a at 32°C (Xl-1 Blue in TB supplemented with 50 µg µl-1 tetracycline and 1 mM IPTG); n.c.: negative control. A: soluble protein fraction B: insoluble protein fraction.

As soon as the SDS PAGE gel showed a stronger signal in one of the bands compared to the negative control, inclusion bodies (Fig. 6) were distinguishable under the microscope and further adjustments had to be made to increase the protein stored in the inclusion bodies. An example for a good protein production is shown in figure 7.

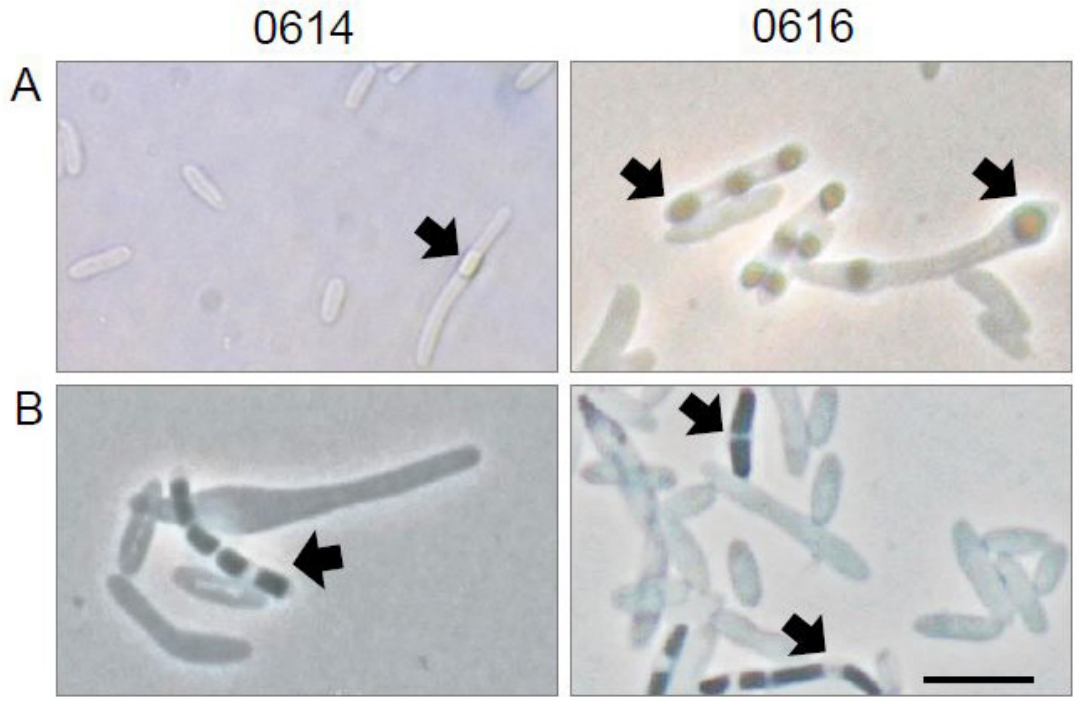

Figure 6: XL-1 Blue with formed inclusion bodies expressing the two segments of Cag_0614 and Cag_0616 47 h after induction; scale bare 5 µm.

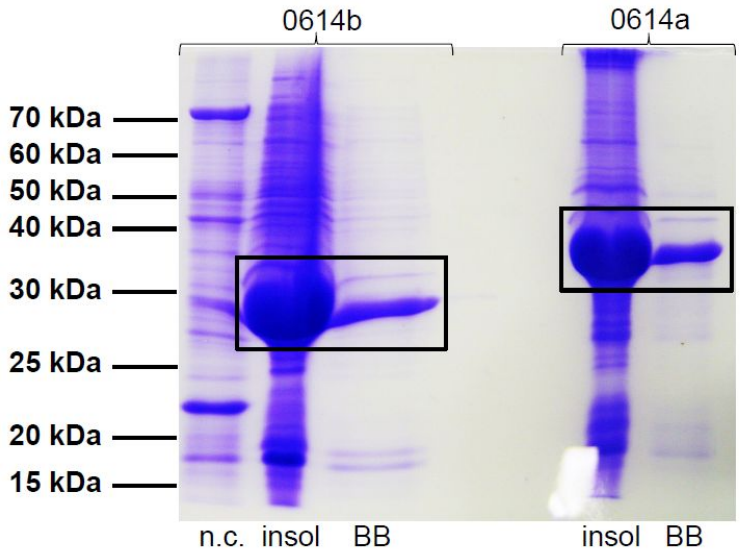

Figure 7: 12 % SDS gel showing the recombinant proteins 0614a and 0614b as inclusion bodies in the crude insoluble fraction (insol) and purified with the BugBuster (BB) protocol; n.c.: negative control.

A sufficient expression of the protein segments generated from sequences of Cag_0614 and Cag_0616 was achieved in Xl-1 Blue grown in terrific broth at 28°C. The tetracyline concentration in the media had to be raised to 75 µg μl^{-1} and the production of the proteins given a 48 h time period. The expression of the protein product of Cag_1919 had the further difficulty that its protein sequence contained a transmembrane region. Expression was achieved after the addition of the plasmid pRep4 to XL-1 Blue. Figure 8 shows the comparison between XL-1 Blue cells which do (B) and do not contain (A) pRep4.

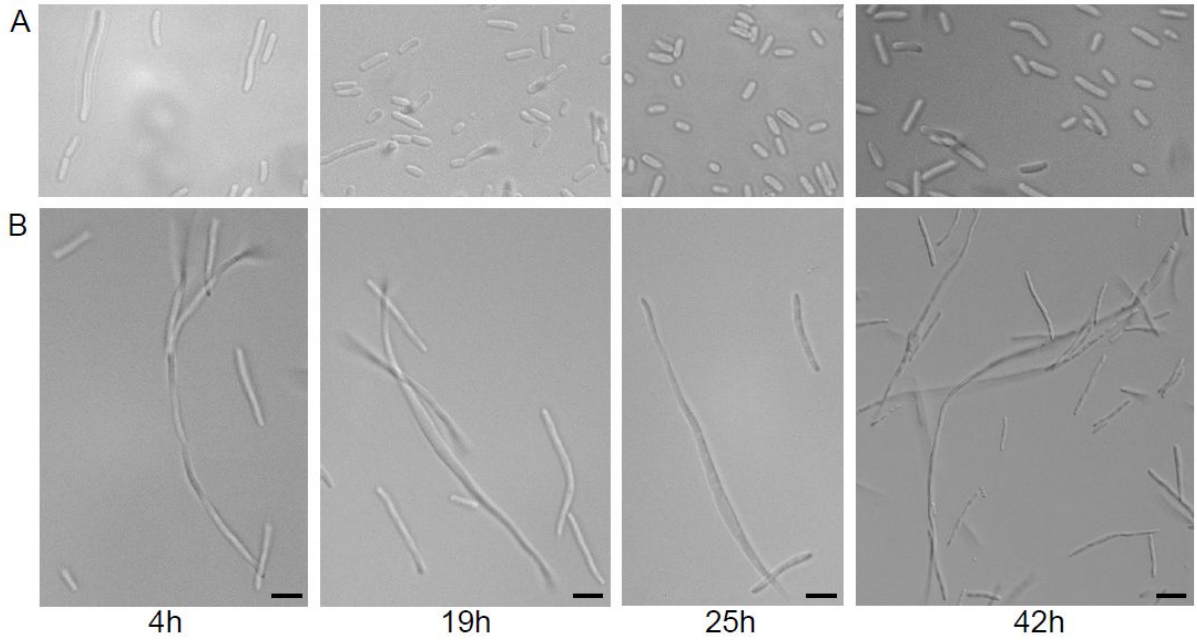

Figure 8: XL-1 Blue cells containing the plasmid pQE1919, growing in terrific broth medium at 28°C. Samples were taken after the induction with IPTG. (A): without pRep4; (B): with pRep4; scale bar 5 µm.

The first difference in protein expression could be seen after 4h. XL-1 Blue cells are clearly elongated and show signs of inclusion bodies after 19h. The cells are clearly stressed by the protein production, but are able to produce 1919 in a sufficient amount for purification and subsequent antibody production. The protein fragment of Cag_1920 could be produced in XL-1 Blue and M15 cells, when grown in terrific broth medium. Interestingly the production of the 1920 fragment yielded branched M15 cells (Fig. 9 A) and the production of the protein 1919 yielded extremely elongated XL-1 Blue cells (Fig. 9 B).

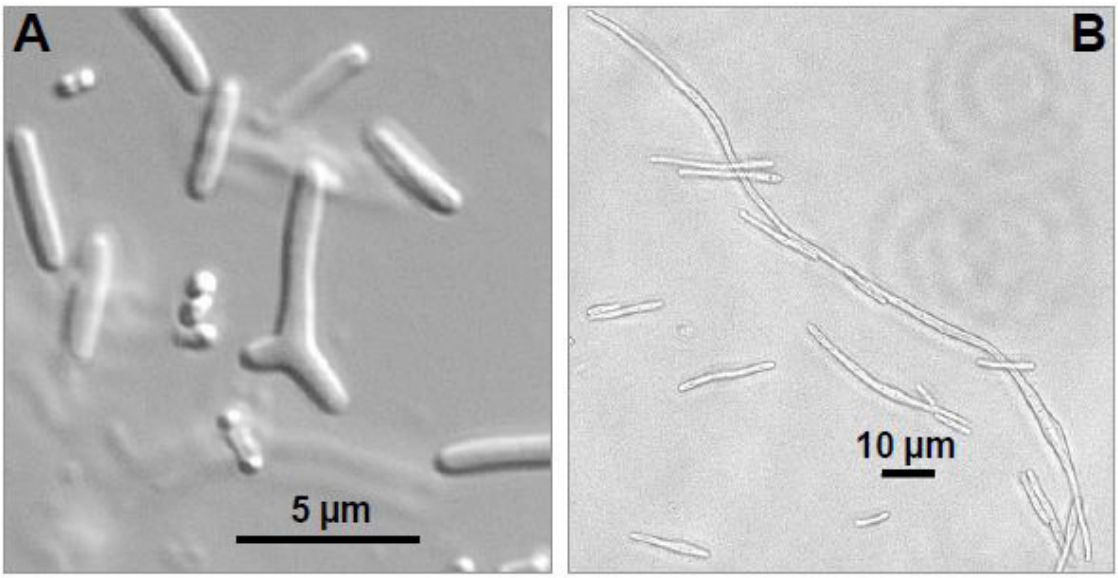

Figure 9: M15 expressing the protein fragment of 1920; B: XL-1 Blue expressing the protein 1919.

In summary the recombinant expression of the epibiont's symbiotic proteins and protein segments was successful when conducted in the *E. coli* XL-1 Blue and grown in terrific broth medium at 28°C for 48 h. The medium had to be supplemented with 75 µg μl^{-1} tetracycline and in the case of the recombinant protein Cag_1919 the plasmid pRep4 had to be present in the expressing cell.

4.1.2 Recombinant protein purification

Purified recombinant proteins had to be purified in order to serve as a pure antigen for the antibody production. All recombinant expressed proteins were found in the insoluble fraction of the cells and could be collected as inclusion bodies. Inclusion bodies were than concentrated and cleaned with the BugBuster protocol and the proteins solubilised in an 8 M Urea buffer (example Fig. 10). The pQE vectors used for cloning in this project contain a 6x His-Tag for purification. The Miniprep spin columns from Qiagen and batch purification system with Ni-NTA agarose were not able to purify any of the recombinant proteins. Standard conditions recommended by the manufacturer resulted in a low recovery of the recombinant protein and an overall high impurity due to accompanying proteins. Further modifications in order to improve the binding of the His-tag to the Ni-NTA or lessen the binding of the non-recombinant proteins resulted in a higher yield of the recombinant proteins and the non-recombinant proteins.

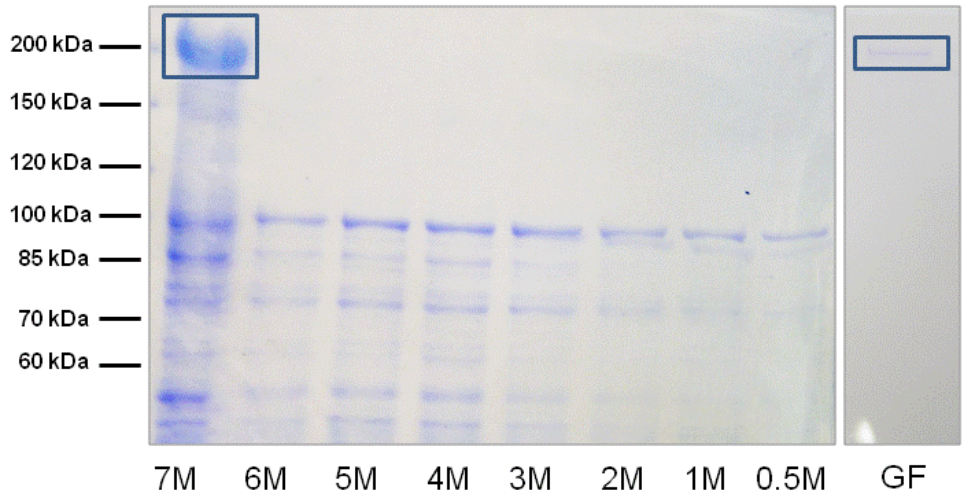

Figure 10: A: Solubility of the protein 1919 in different concentrations of Urea; GF: elution fraction of the gelfiltration purification of the protein 1919.

All the recombinant proteins were purified, with the exception of the protein Cag_1919, with the HisTrap FF 1ml column in the Äktaprime plus system (Fig. 11).

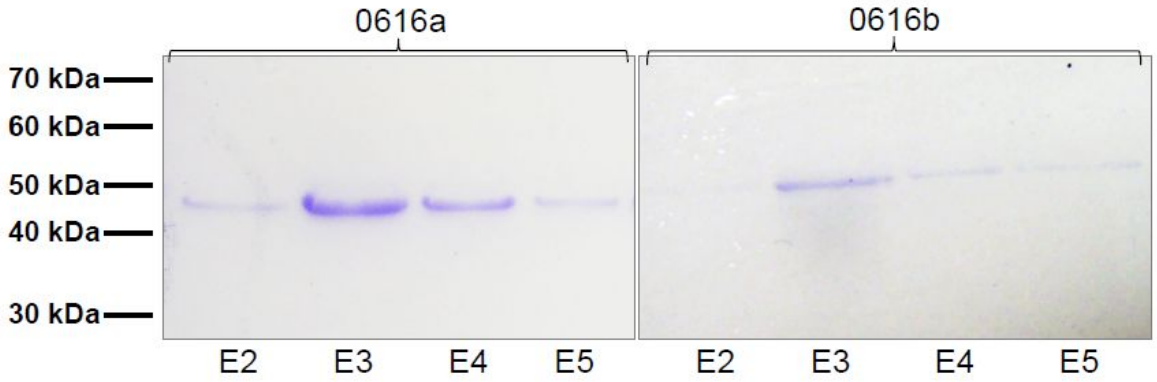

Figure 11: 12% SDS gel showing the elution fractions of the purification of the proteins 0616a and 0616b.

The size exclusion column HiPrep 16/60 Sephacryl S-300 HR was successfully used to purify the protein 1919 (Fig. 10) and best results were obtained loading a 1.2 ml sample. Removal of the high concentration of urea had to be carried out slowly overnight at 4°C via dialysis from all purified protein sample. The proteins were than concentrated with the use of an absorbent.

4.2 Summary

The protein product of Cag_1919 and the segments expressed from the giant proteins were highly instable and caused high stress levels for the expressing *E. coli*. Nevertheless, the conditions were adapted to produce sufficient amounts of recombinant protein. The conditions included the medium TB, slow growth at 28°C and high amounts of the antibiotic tetracycline. The 6xHis tag was probably insufficient for the purification of these proteins, due to their size and hydrophobicity. But the extended binding time in the Äkta purification method, with better quality columns, was able to counteract this disadvantage. The recombinant protein Cag_1919 was not able to sufficiently bind to any form of Ni-NTA. The protein might have been partially folded due to its RTX domain.

The recombinant proteins were localized in the membrane of XL-1 Blue cells, when conducting immunofluorescence experiments (Fig. 12). Insertion of the recombinant proteins into the membrane must have prevented correct membrane organization during cell growth and division, explaining the extremely elongated cells.

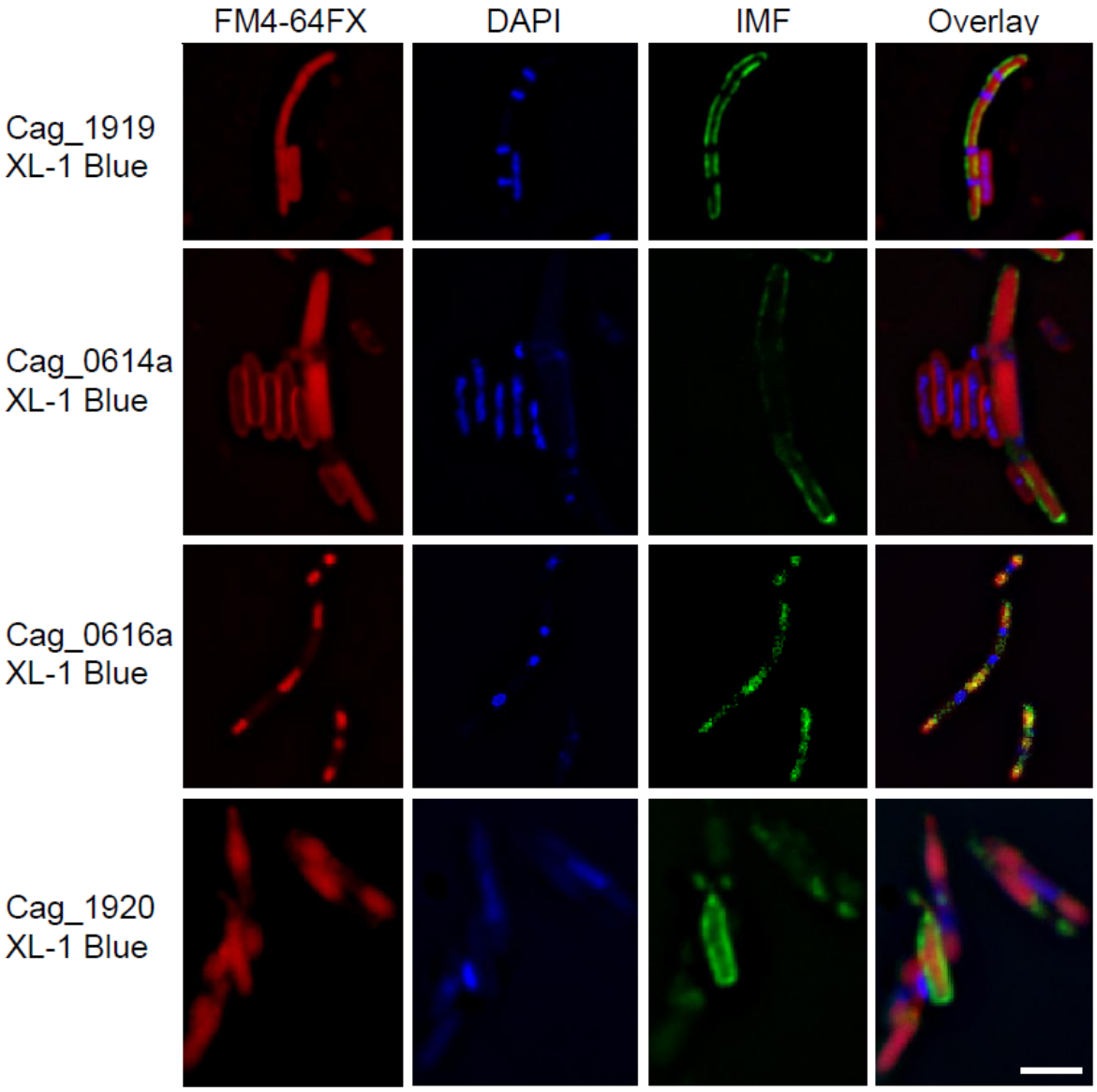

Figure 12: Immunofluorescence analysis of XL-1 Blue cells which expressed the recombinant proteins 1919, 0614a, 0616a and 1920 with anitsera targeting the protein products of Cag_ 1919, Cag_0614, Cag_ 0616 and Cag_1920. FM4-64FX = fixable analogue of the FM4-64FX membrane stain (Thermo Fisher, Waltham, USA**)**, DAPI = DNA stained with DAPI, IMF = immunofluorescence signal of the expressed proteins and an overlay of the three different fluorescence signals. Scale bar 5 µm.

4.3 References

Lin-Chao, S. & Bremer, H. (1986). Effect of the bacterial growth rate on replication control of plasmid pBR322 in Escherichia coli. *Molecular & general genetics : MGG* **203**, 143–149.

Chapter 5

Analysis of symbiotic proteins of *Chlorobium chlorochromatii*

5.1 Results

5.1.1 Results for the localization of symbiotic proteins

5.1.1.1 Western blot analysis of the protein product of Cag_1919

Western blot analysis of the protein product of Cag_1919 (Fig. 13) showed a single band between 150 and 250 kDa, which corresponds to the predicted protein size of 155 kDa. The consortia culture "*C. aggregatum*" and the pure culture of *Chl. chlorochromatii* both contain the protein product of Cag_1919 in a similar concentration (Fig. 13 A). Furthermore, the product of Cag_1919 was localized in the different cell fractions. In the first analysis containing the cell fractions the western blot analysis was conducted with the same total protein concentration for each cell fraction, revealing that the Cag_1919 product constituted the largest fraction among proteins of the periplasm of the consortium and the epibiont. Smaller amounts were detectable in the cytoplasm and traces were detected in the membrane of "C. aggregatum" (Fig. 13 B). When the amounts loaded were normalized to the relative

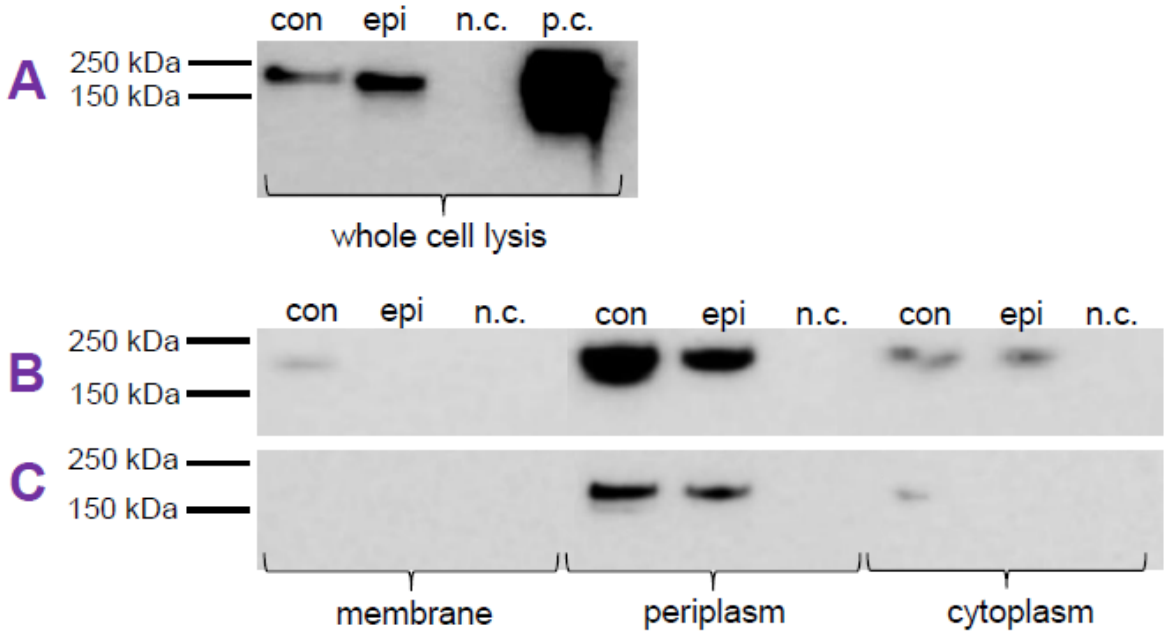

Figure 13: Detection of the Cag_1919 protein product in "*C. aggregatum*" and *Chl. chlorochromatii* through western blot analysis. Abbreviations stand for: con = consortium, epi = epibiont, n.c. = negative control (XL-1 Blue) and p.c. = positive control (purified recombinant protein of Cag_1919). (A) Comparison of the whole cells lysis of "*C. aggregatum*", *Chl. chlorochromatii* and XL-1 Blue. (B) Comparison of the membrane, periplasm and cytoplasm fractions of "C. aggregatum", *Chl. chlorochromatii* and XL-1 Blue. Each fraction contains the same total protein concentration. (C) Comparison of the different cell fractions as in (B); protein concentrations have been normalized to the relative amounts per cell.

amounts per cell (Fig. 13 C), the major fraction of the product of Cag_1919 was located in the cytoplasm of the consortium, whereas the signal for the cytoplasm fraction of the epibiont decreased. A reduced chemiluminescence signal was still detected for the periplasm fraction of the consortia.

5.1.1.2 Dot blot analysis of the protein products of Cag_0614 and Cag_0616

The protein products of Cag_0614 and Cag_0616 could not be analysed with western blot analysis due to their size.

Dot blot analysis of the protein products of Cag_0614 (Fig. 14) and Cag_0616 (Fig. 15) fragments showed the same result for both proteins. First the cell fractions were compared using the same total protein concentration for each fraction. The cytoplasmic fractions yielded the strongest signal, while the periplasmic fraction of "*C. aggregatum*" contains a weak signal. After normalising the protein concentrations per cell, the signal for the periplasm fraction of "*C. aggregatum*" decreased in the blots generated with antisera targeting 0614a, 0616a and especially for 0616b (Fig. 15). It was not possible to detect the protein product Cag_1920 with western blot or dot blot analysis.

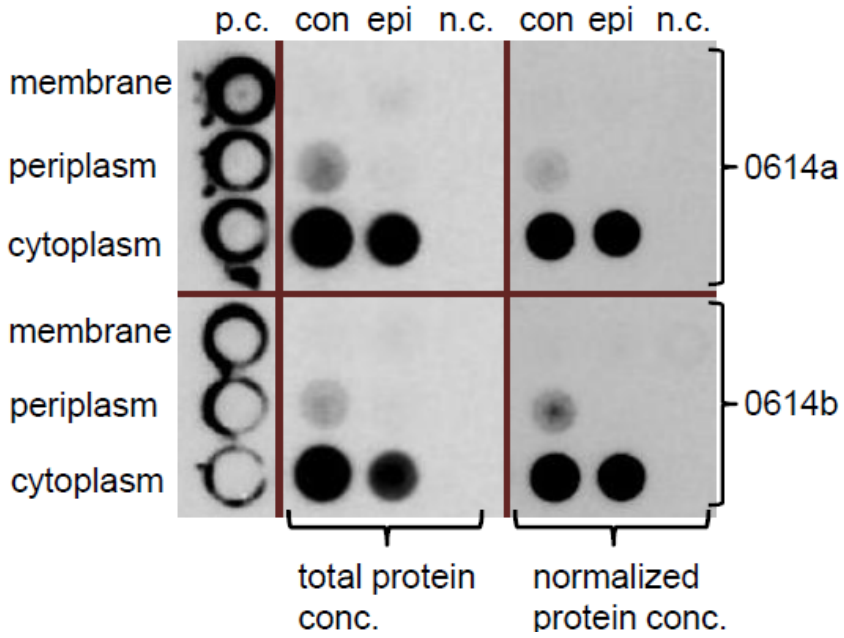

Figure 14: Dot blot analysis of the protein product of Cag_0614 in the cytoplasm, periplasm and membrane cell fractions of "*C. aggregatum*" and the pure culture of *Chl. chlorochromatii*. Abbreviations stand for: con = consortium, epi = epibiont, n.c. = negative control (XL-1 Blue) and p.c. = positive control (purified recombinant protein segments of Cag_0614).

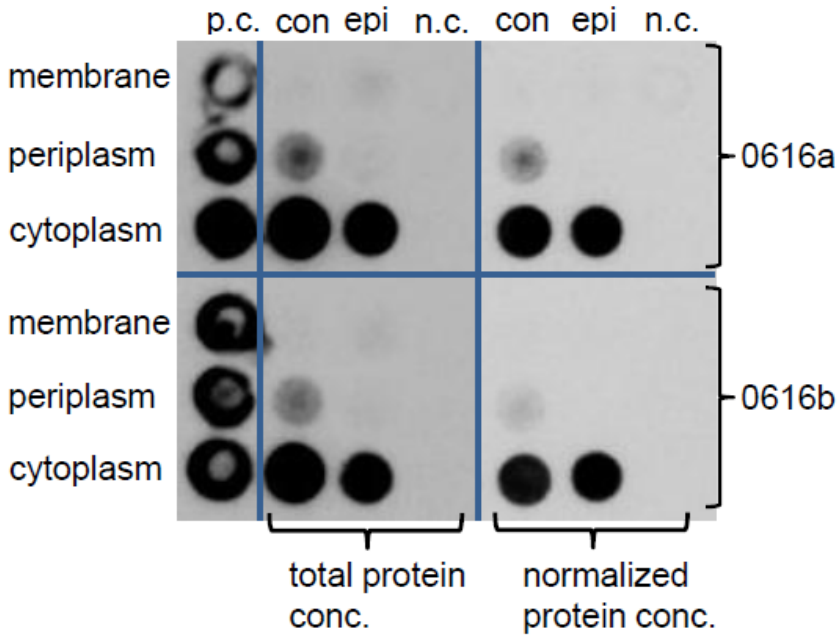

Figure 15: Dot blot analysis of the protein product of Cag_0616 in the cytoplasm, periplasm and membrane cell fractions of "*C. aggregatum*" and the pure culture of *Chl. chlorochromatii*. Abbreviations stand for: con = consortium, epi = epibiont, n.c. = negative control (XL-1 Blue) and p.c. = positive control (purified recombinant protein segments of Cag_0616).

5.1.1.3 Immunofluorescence microscopy

Chl. chlorochromatii contains bacteriochlorophyll *c* (BChl *c*) which can be visualized as an autofluorescence signal (Fig. 16). The colocalization of the immunofluorescence signal with epibiont cells was therefore facilitated by their autofluorescence signal and the colocalization with the central bacterium by the absence of BChl *c* autofluorescence.

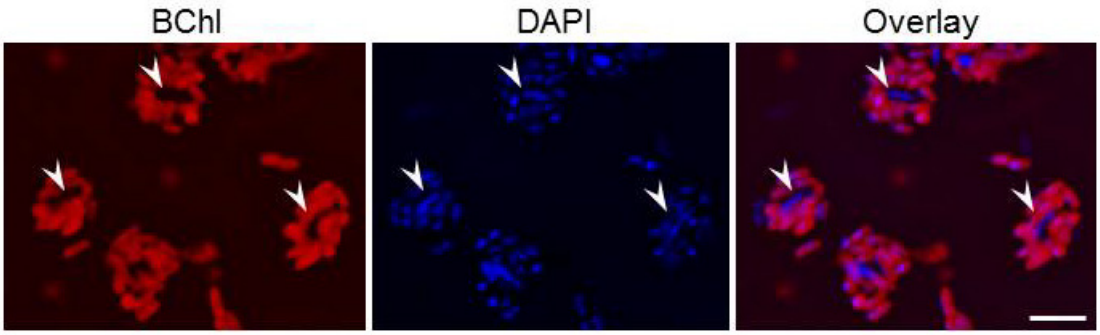

Figure 16: Example of the visualization of bacteriochlorophyll c in Chl. Chlorochromatii; BChl = autofluorescence of bacteriochlorophyll *c* of the chlorosomes in the epibiont cells and DAPI = DNA stained with DAPI. Arrows indicate the position of the central bacterium in each image. Scale bar 5 µm.

It was possible to establish an immunofluorescence protocol with the antisera generated against the recombinant proteins Cag_1919, Cag_0614a and Cag_0616a, whereas antisera generated against the recombinant proteins of Cag_0614b, Cag_0616b could not be used to establish an immunofluorescence protocol (data not shown). The following figures show individual images of BChl *c*, DAPI, immunofluorescence (IMF) and the overlay of all three fluorescence signals. Two different fluorescent-labelling patterns can be seen between the three symbiotic proteins (Fig. 17 – Fig. 19). The immunofluorescence signals for Cag_1919 (Fig. 17) are located in condensed areas between the DAPI stained DNA of the central bacterium and the autofluorescence of the epibiont. The negative controls (bottom lane) performed with pre-immune serum did not yield any immunofluorescence signal. In contrast to Cag_1919 the immunofluorescence signals of Cag_0614 (Fig. 18) and Cag_0616 (Fig. 19) are more co-localised with the DAPI stain of the central bacterium. Consortia treated with pre-immune sera, collected during antibody production against 0616a and 0614a, did not yield any immunofluorescence signal (negative controls: see last lanes of Fig. 18 and Fig. 19). Based on these results it could be shown that the proteins Cag_0614 and Cag_0616 are located most likely in the cytoplasm of the central bacterium.

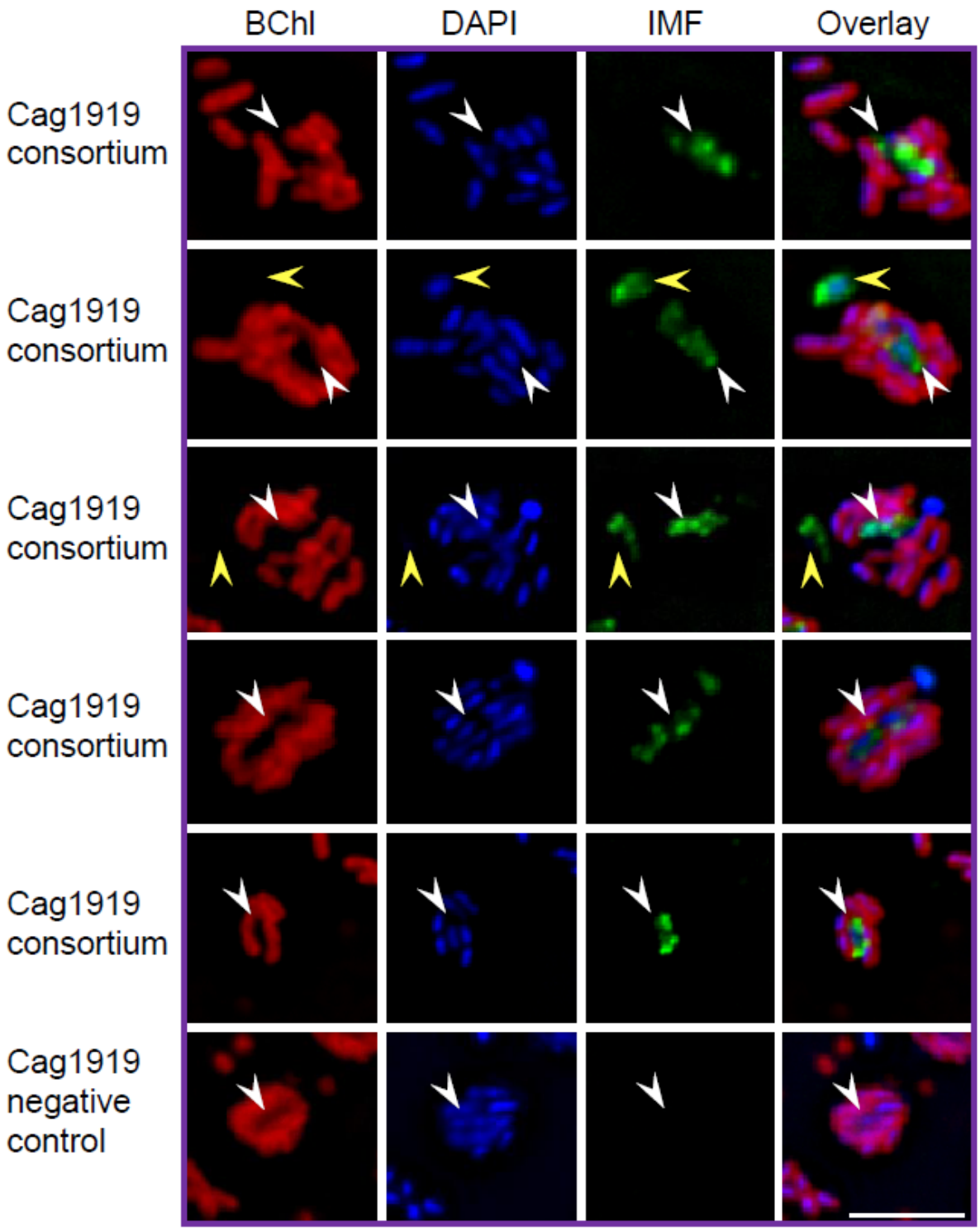

Figure 17: Immunofluorescence analysis of "*C. aggregatum*" with anitsera and pre-immune sera against the protein product of Cag_1919. BChl = autofluorescence of bacteriochlorophyll *c* of the chlorosomes in the epibiont cells, DAPI = DNA stained with DAPI, IMF = immunofluorescence signal of the targeted symbiotic proteins and an overlay of the three different fluorescence signals. Arrows indicate the position of the central bacterium in each image. Yellow arrow indicates a single central bacterium. Scale bar 5 µm.

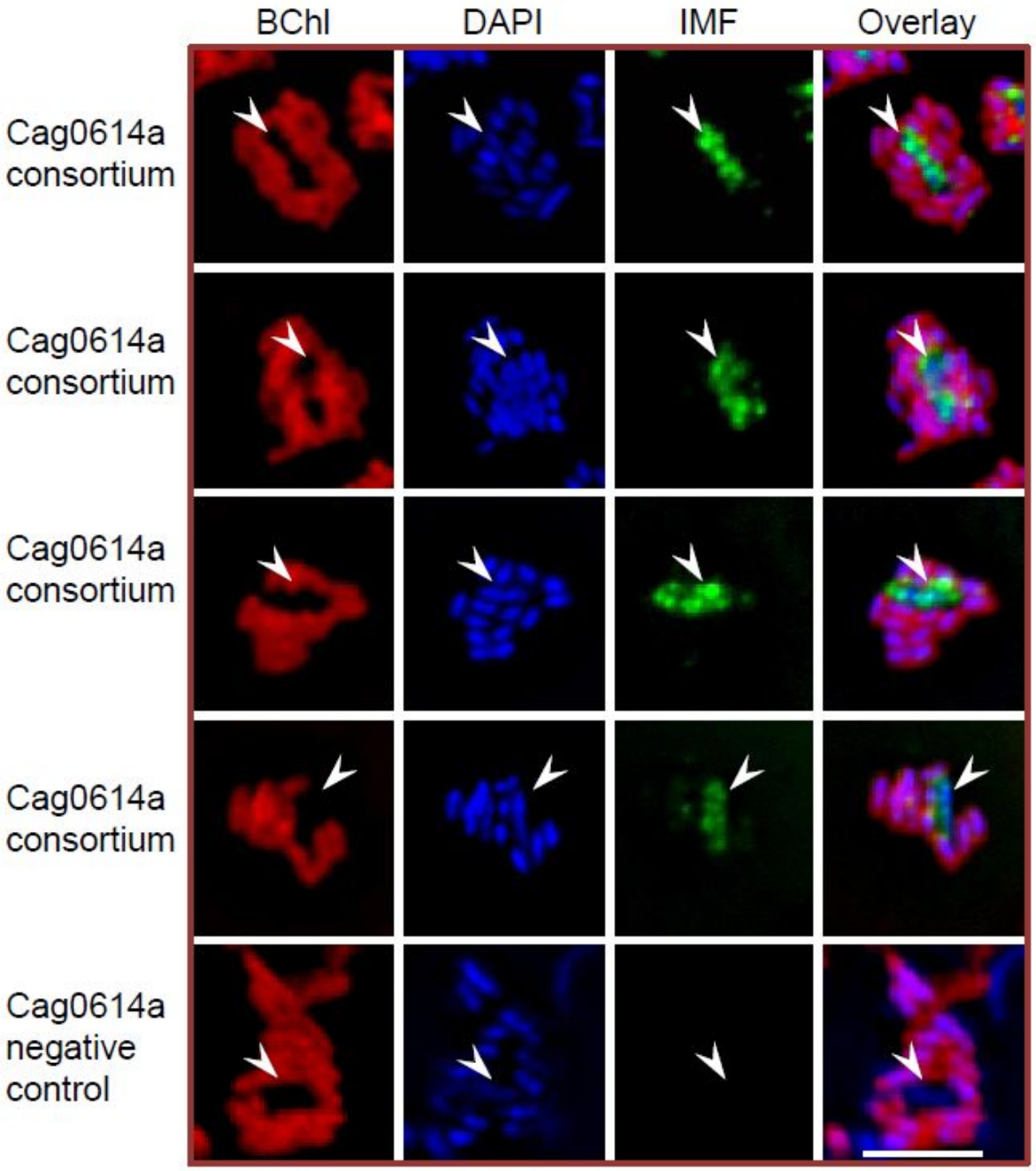

Figure 18: Immunofluorescence analysis of "*C. aggregatum*" with anitsera and pre-immune sera against the protein product of Cag_0614. BChl = autofluorescence of bacteriochlorophyll *c* of the chlorosomes in the epibiont cells, DAPI = DNA stained with DAPI, IMF = immunofluorescence signal of the targeted symbiotic proteins and an overlay of the three different fluorescence signals. Arrows indicate the position of the central bacterium in each image. Scale bar 5 µm.

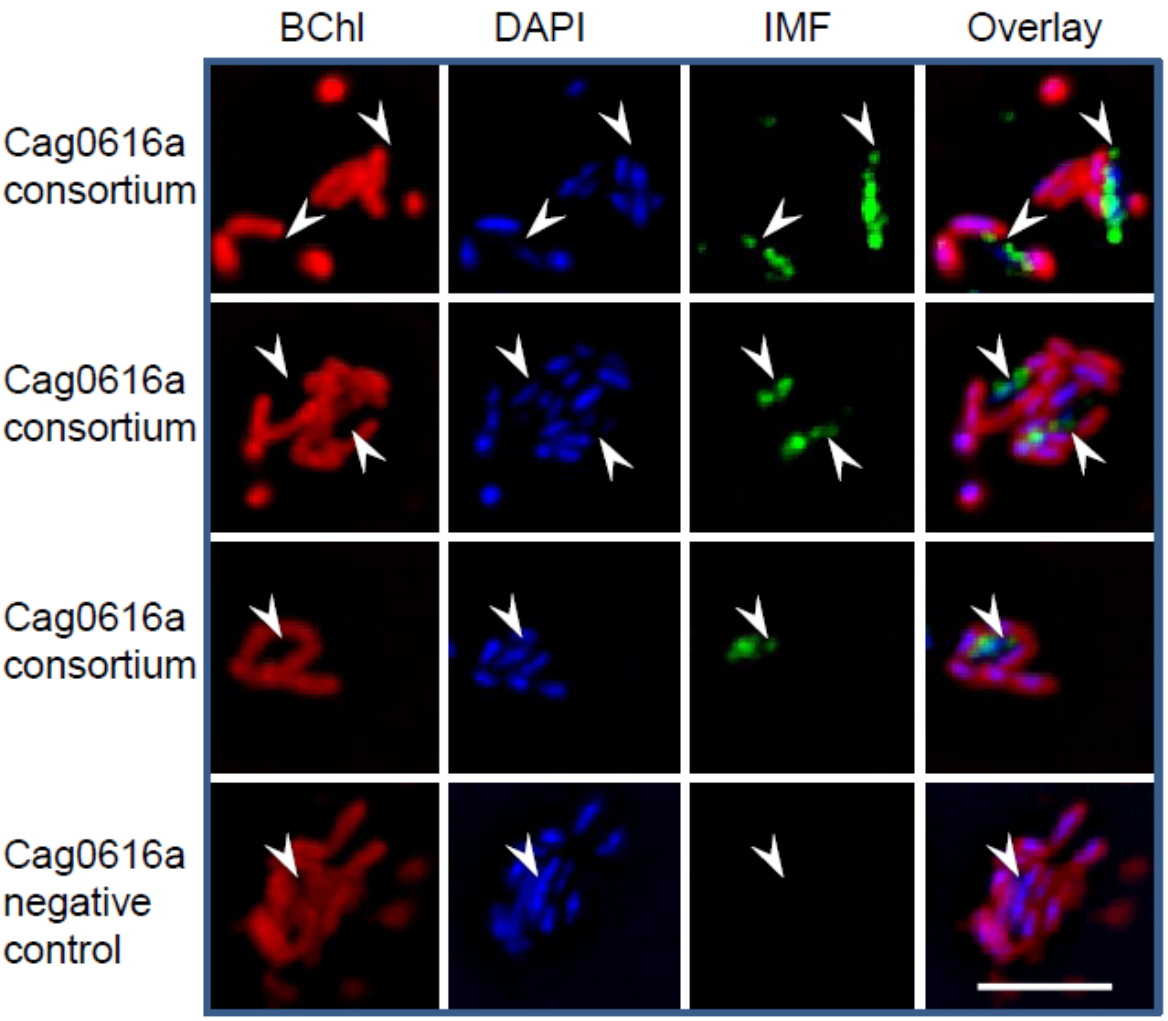

Figure 19: Immunofluorescence analysis of "*C. aggregatum*" with anitserum and pre-immune serum against the protein product of Cag_0616. BChl = autofluorescence of bacteriochlorophyll *c* of the chlorosomes in the epibiont cells, DAPI = DNA stained with DAPI, IMF = immunofluorescence signal of the targeted symbiotic proteins and an overlay of the three different fluorescence signals. Arrows indicate the position of the central bacterium in each image. Scale bar 5 µm.

In the preparations it was possible to observe central bacteria which were partially stripped off their epibionts. The location of all immunofluorescence signals remained with the central bacterium (Fig. 20), which is especially interesting for the immunofluorescence signal regarding the protein product of Cag_1919.

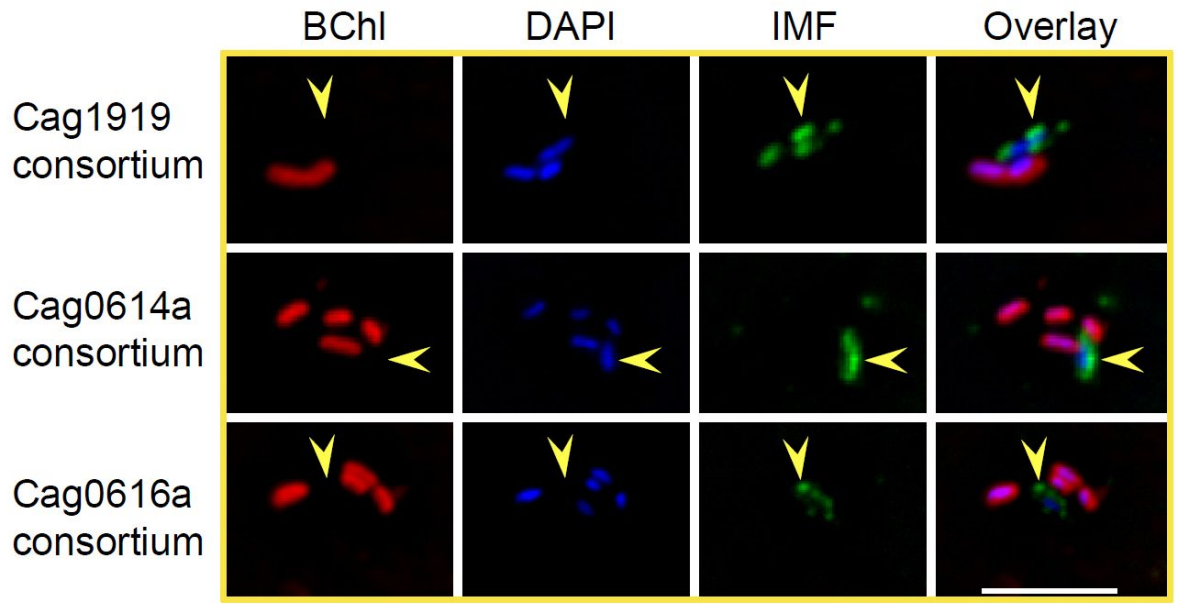

Figure 20: Immunofluorescence analysis of "*C. aggregatum*" with antisera against the proteins Cag_1919, Cag_0614a and Cag_0616a. BChl = autofluorescence of bacteriochlorophyll *c* of the chlorosomes in the epibiont cells, DAPI = DNA stained with DAPI, IMF = immunofluorescence signal of the targeted symbiotic proteins and an overlay of the three different fluorescence signals. Arrows indicate the position of the central bacterium in each image. Scale bar represents 5 µm.

When the pure epibiont culture was analysed using the antiserum targeting the product of Cag_1919, 44% (±7.2%) of the epibiont cells exhibited an immunofluorescence signal. These immunofluorescence signals were localized on the outer edge of the epibiont autofluorescence (Fig. 21). Immunofluorescence analyses of the proteins Cag_0614a and Cag_0616b revealed two localizations (Fig. 22 and 23). Either the whole epibionts cell contained the immunofluorescence signal or small circular immunofluorescence signals could be discerned directly at the cell envelope. In contrast to Cag_1919 only 4% and 3.8 % of the epibiont cells treated with antiserum targeting Cag_0614a and Cag_0616b, respectively, contained an IMF signal. The negative controls for this procedure did not show any immunofluorescence signal (Fig. 22 and 23).

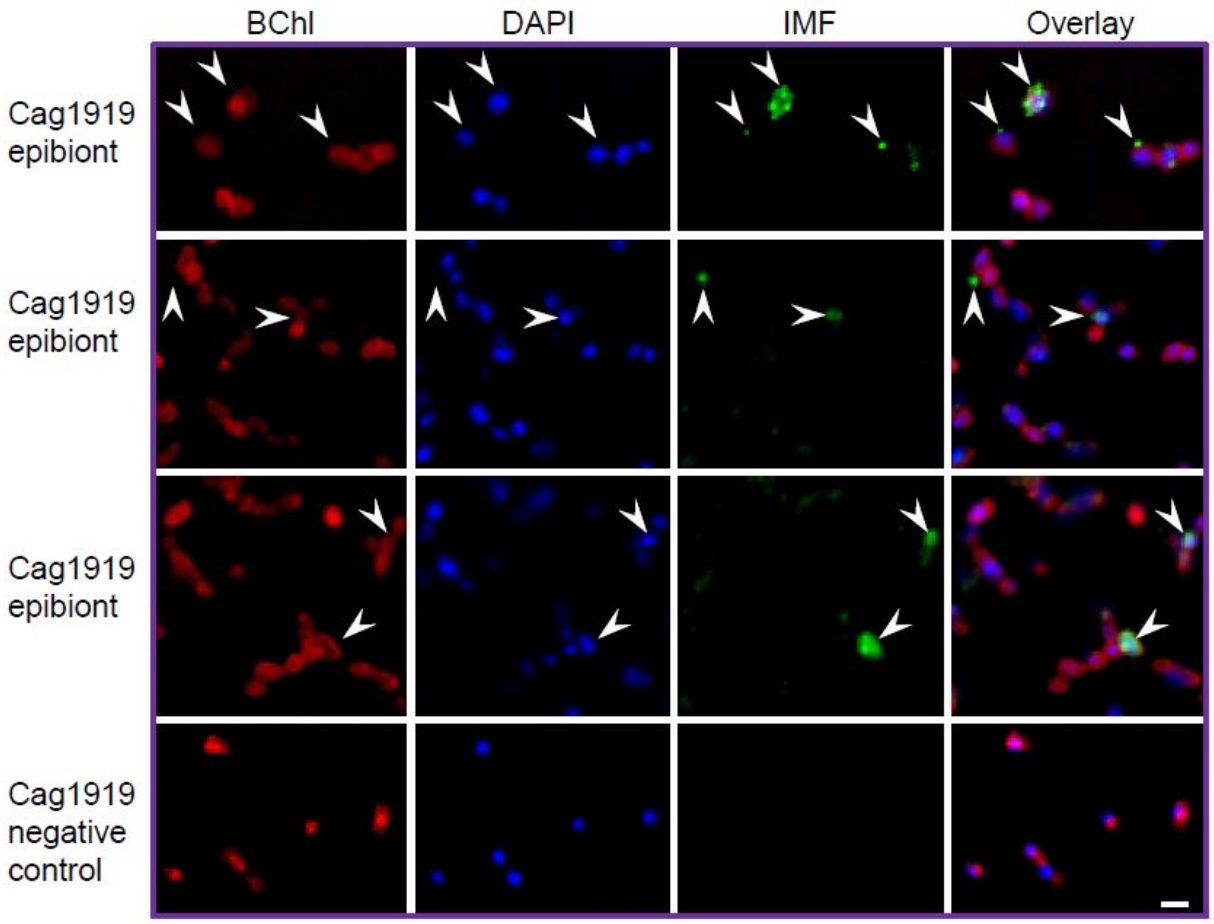

Figure 21: Immunofluorescence analysis of *Chl. chlorochromatii* with antiserum and pre-immune serum against the protein product of Cag_1919. BChl = autofluorescence of bacteriochlorophyll *c* of the chlorosomes in the epibiont cells, DAPI = DNA stained with DAPI, IMF = immunofluorescence signal of the targeted symbiotic proteins and an overlay of the three different fluorescence signals. Scale bar 5 µm

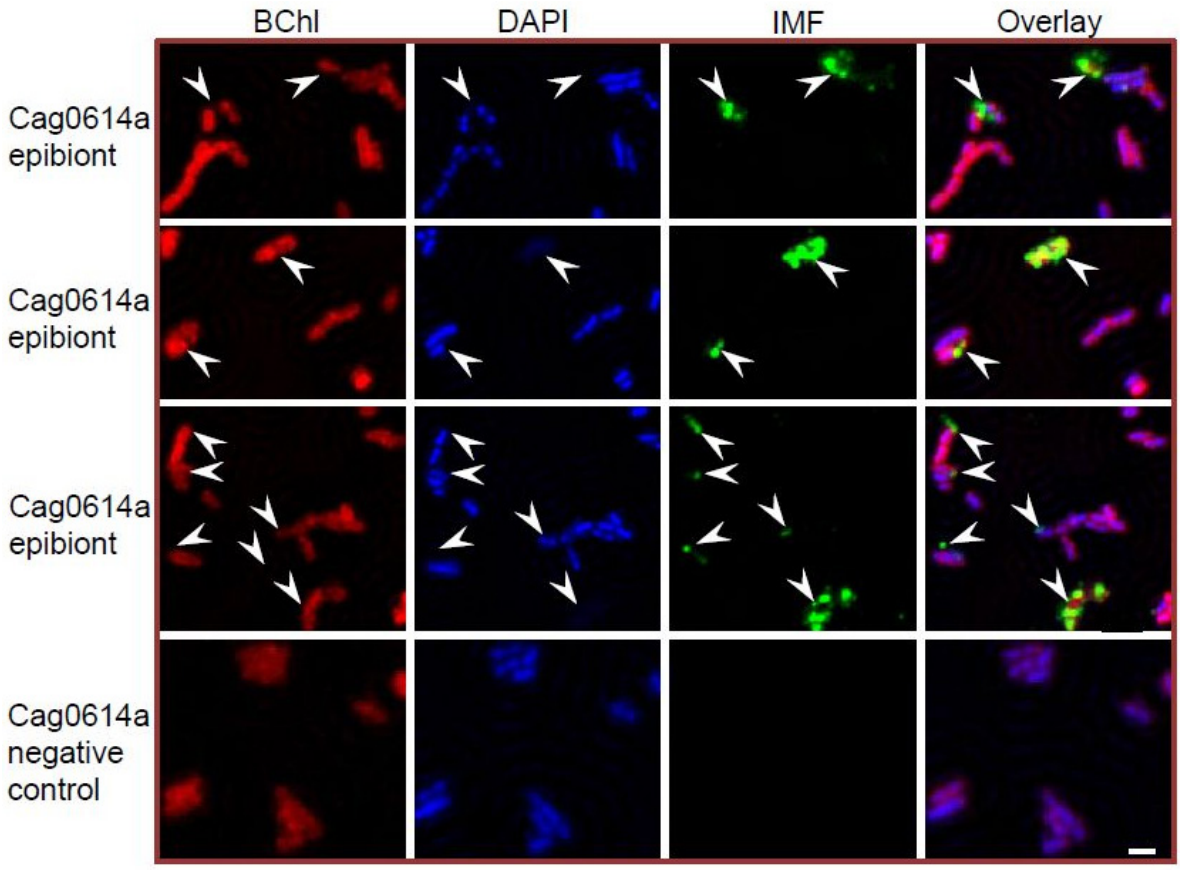

Figure 22: Immunofluorescence analysis of *Chl. chlorochromatii* with antiserum and pre-immune serum targeting Cag_0614a. BChl = autofluorescence of bacteriochlorophyll *c* of the chlorosomes in the epibiont cells, DAPI = DNA stained with DAPI, IMF = immunofluorescence signal of the targeted symbiotic proteins and an overlay of the three different fluorescence signals. Scale bar 5 µm

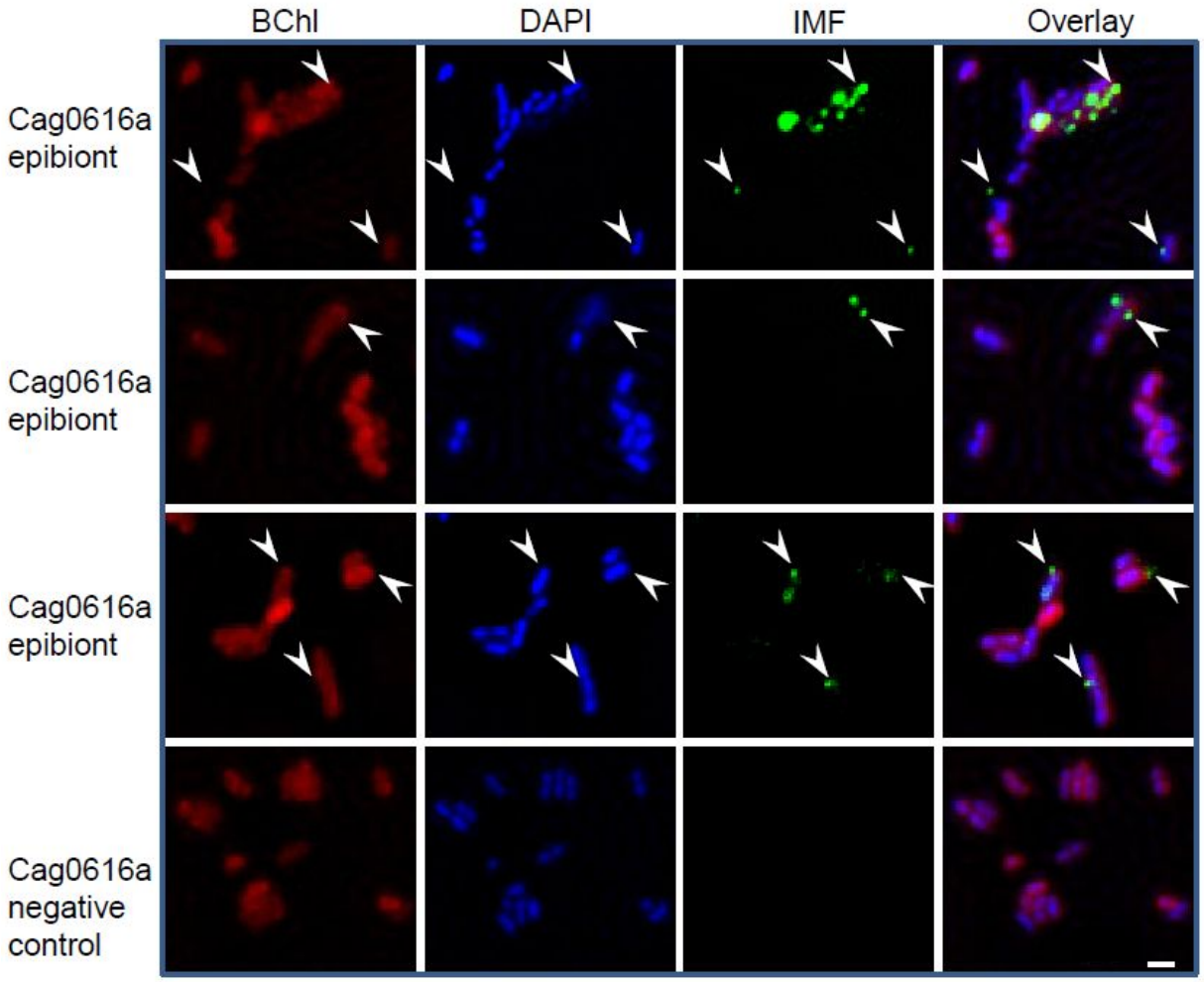

Figure 23: Immunofluorescence analysis of *Chl. chlorochromatii* with antiserum and pre-immune serum targeting Cag_0616a. BChl = autofluorescence of bacteriochlorophyll *c* of the chlorosomes in the epibiont cells, DAPI = DNA stained with DAPI, IMF = immunofluorescence signal of the targeted symbiotic proteins and an overlay of the three different fluorescence signals. Scale bar 5 µm

5.1.1.4 Immunogold analysis

The antisera targeting the proteins products of Cag_1919 (Fig. 24), Cag_0614 (Fig. 25) and Cag_0616 (Fig. 26) were used for immunogold labelling of cryosectioned consortia in order to determine their localization at higher resolution.

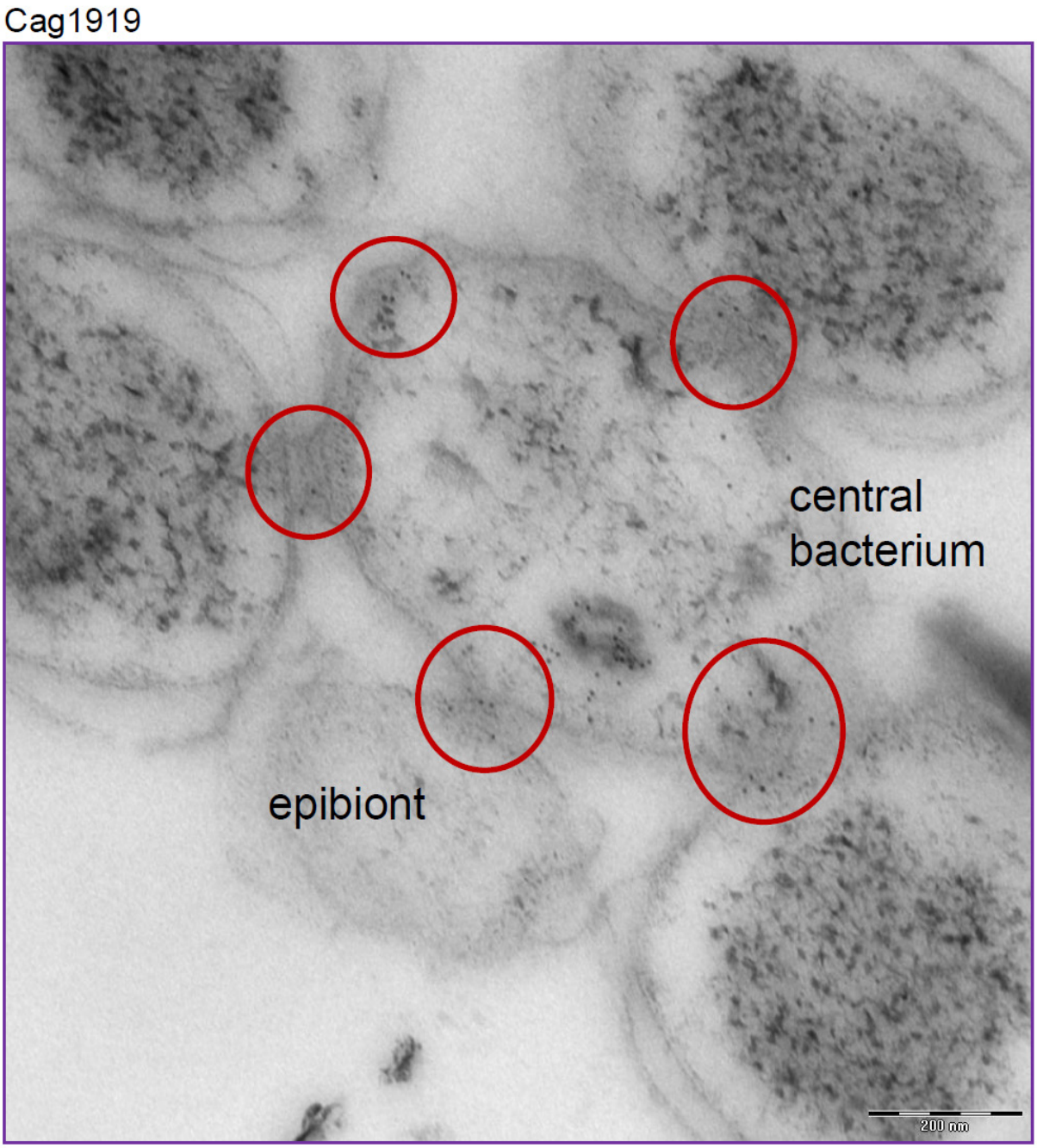

Figure 24: Examples for immunogold labelling with the antiserum targeting the protein product of Cag_1919 in *"C. aggregatum"* crysections. Red circles indicate accumulations of immunogold particles.

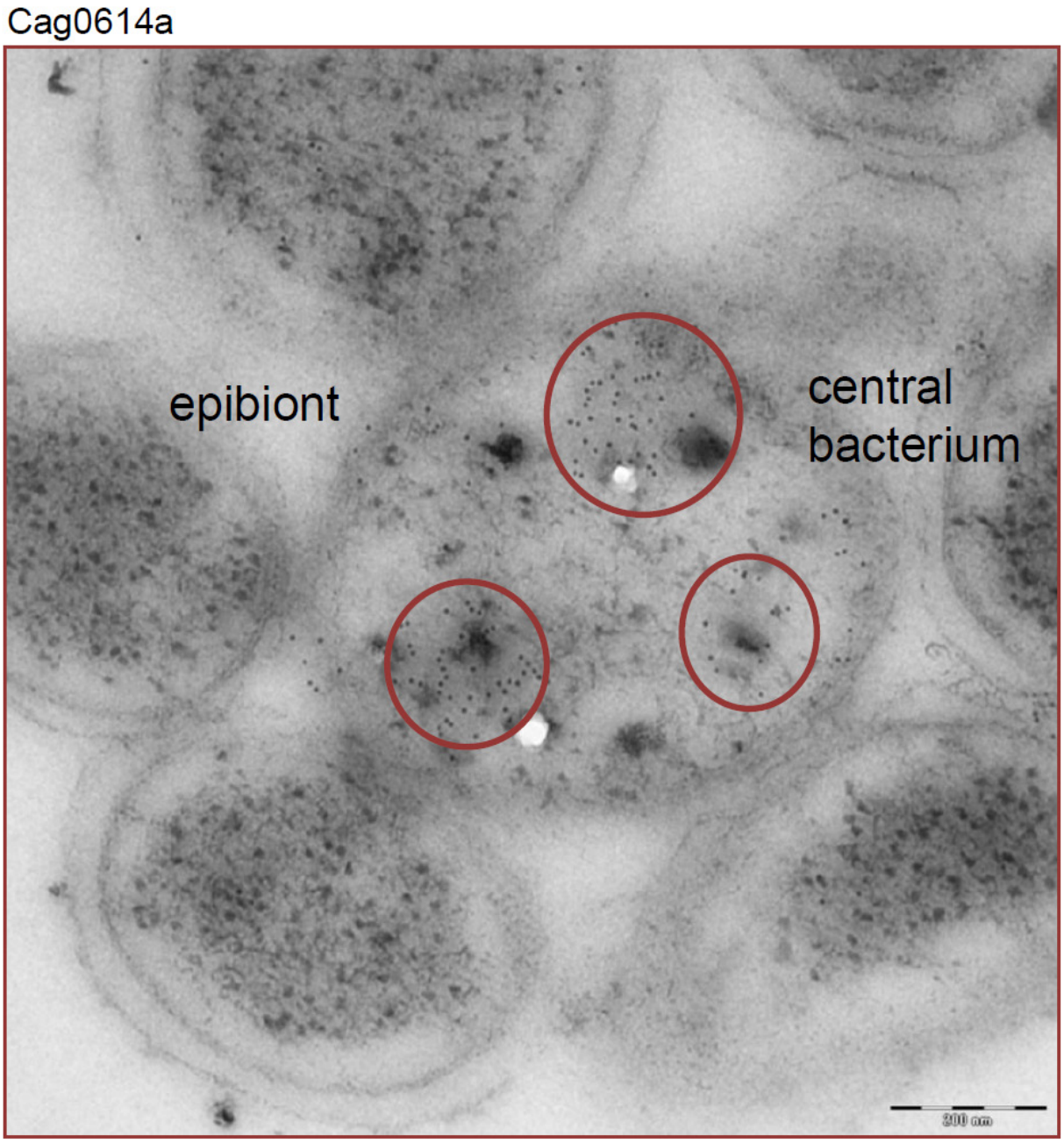

Figure 25: Examples for immunogold labelling with the antiserum targeting the protein product of Cag_0614 in cryosections of *"C. aggregatum"*. Red circles indicate accumulations of immunogold particles.

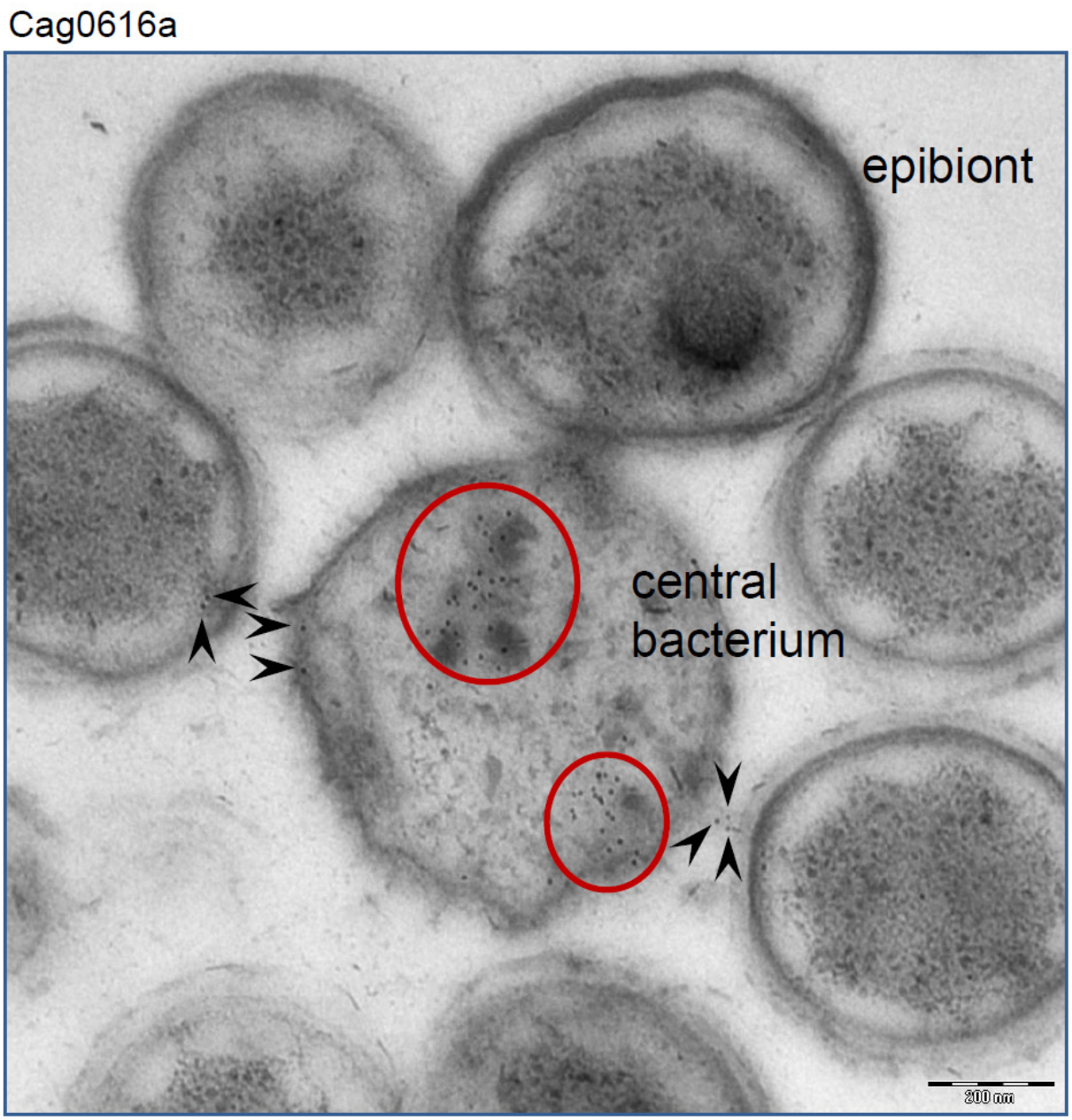

Figure 26: Examples for immunogold labelling with the antiserum targeting the protein product of Cag_0616 in cryosections of *"C. aggregatum"*. Red circles indicate accumulations of immunogold particles.

For this analysis the immunogold particles were either allocated to the cytoplasm or the membrane region of either the central bacterium or the epibiont. The significance of the immonugold particle count for the three different proteins was then calculated using the particle count of immunogold labelling generated with pre-immune sera as a control.

The immunogold labelling for the analyzed regions was significantly different compared to the labelling generated with pre-immune sera (Fig. 27) regarding all three proteins. Exceptions were the immunogold labellings of the epibiont's membrane regions for each of three proteins. These labellings were very low and could not be distinguished from the negative controls.

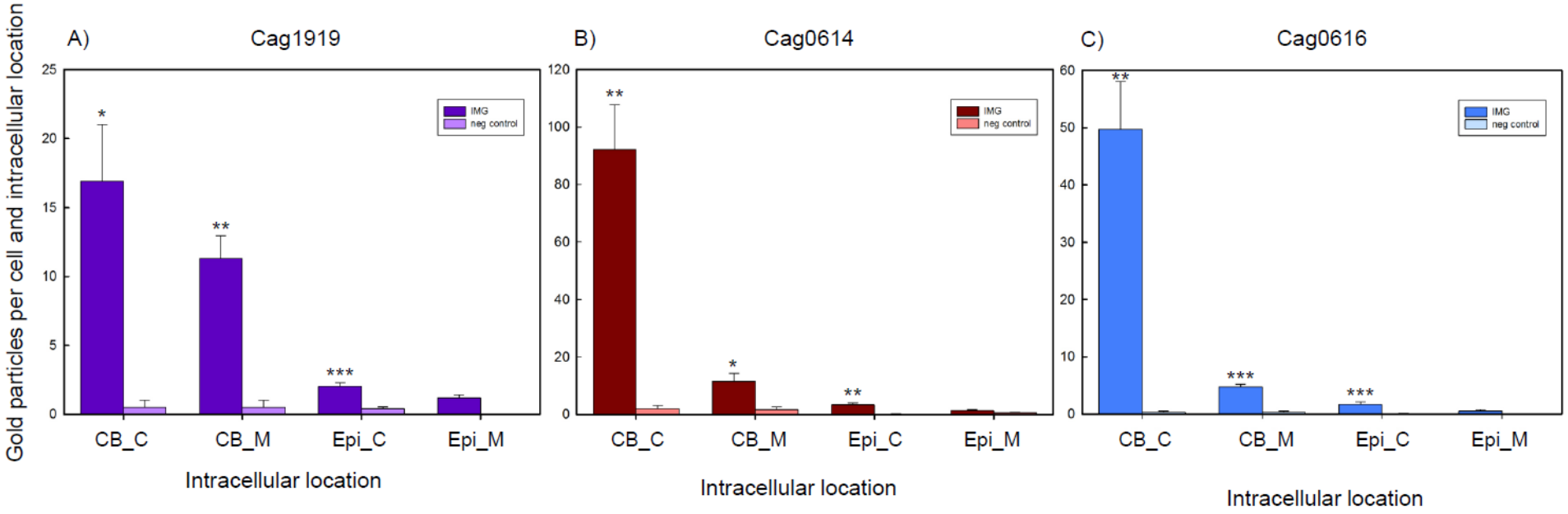

Figure 27: Average immunogold particles per cell per localization in "*C. aggregatum*" using the serum and pre-immune serum targeting the protein products of Cag_1919 (A), Cag_0614 (B) and Cag_0616 (C). The significance of the cell location (CB_C and CB_M = cytoplasm and membrane of the central bacterium; Epi_C and Epi_M = cytoplasm and membrane of the epibiont) labelling was determined with an unpaired t-test. A P-value between 0.05 and 0.01 is considered significant (*), 0.01 and 0.0001 very significant (**) and less than 0.0001 extremely significant (***).

The average number of immunogold particles for the previously defined localizations of the cells was determined per μm^2 of the respective area. First, a pair-wise comparison t-test was conducted between the values calculated for the central bacterium and the epibiont. For Cag_1919 (P-value = 1.5×10^{-4}) and Cag_0614 (P-value = 1.6×10^{-4}) the immunogold labelling is very significant and for Cag_0616 (P-value = 2.4×10^{-5}) extremely significant for the central bacterium compared to the epibiont.

A pair-wise comparison t-test between the regions of the central bacterium was conducted next to test for statistically significant values (Fig. 28). For Cag_1919 the average number of immunogold particles was statistically higher in the membrane than in the cytoplasm (Fig. 28 A). The highest immunogold particle value was found in the cytoplasm of the central bacterium targeting the product of Cag_0614 (Fig. 28 B) and cannot be statistically distinguished from the labelling of the membrane region. Therefore, the protein product of Cag_0614 could be localized in the cytoplasm and the membrane region of the central bacterium. The Cag_0616 protein product is clearly localized in the cytoplasm of the central bacterium (Fig. 28 C).

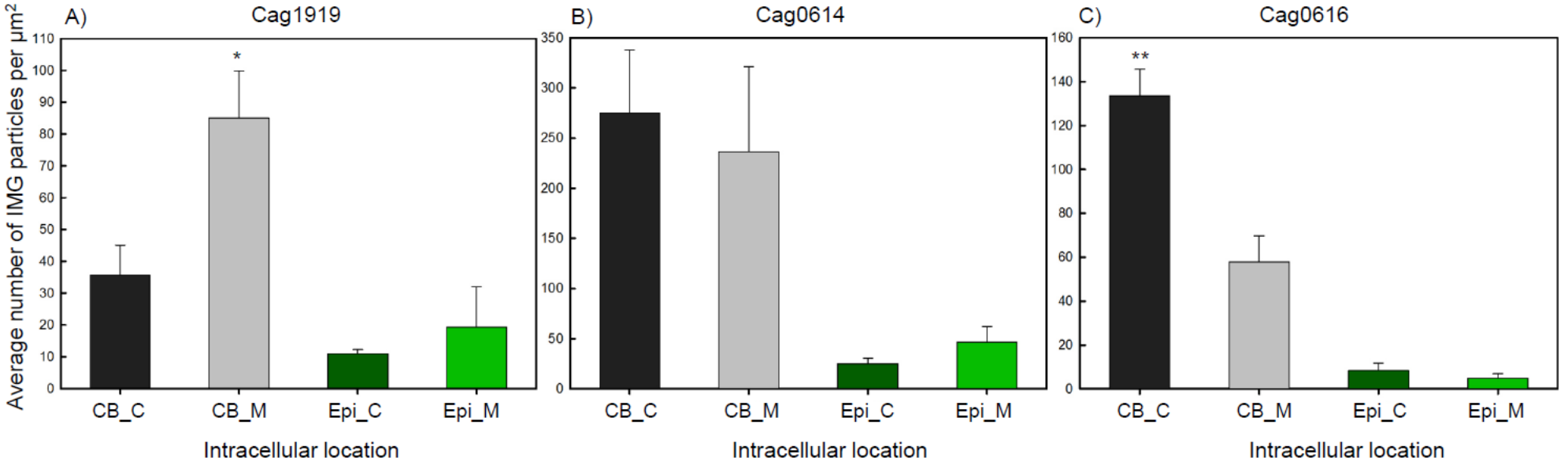

Figure 2: Immunogold labelling in *"C. aggregatum"* using antisera targeting the protein product of Cag_1919 (A), Cag_0614 (B) and Cag_0616 (C). The significance of the cell location (CB_C and CB_M = cytoplasm and membrane of the central bacterium; Epi_C and Epi_M = cytoplasm and membrane of the epibiont) labelling was determined with a pair-wise comparison t-test. A P-value between 0.05 and 0.01 is considered significant (*), 0.01 and 0.0001 very significant (**) and less than 0.0001 extremely significant (***).

5.1.2 Sequence analysis and putative transport of the gene products of Cag_0614, Cag_0616 and Cag_1919

5.1.2.1 Sequence analysis of the gene product of Cag_1919

Cag_1919 was identified as a repeats-in-toxin-(RTX) like protein by Vogl *et al*. The Phyre2 software was able to model such a β roll structure for the C-terminal end of Cag_1919 (Fig. 29, Kelley & Sternberg, Michael J E, 2009), in accordance to RTX modules of various proteobacterial proteins (Vogl *et al.,* 2008).

Further structural analysis of Cag_1919 revealed a 285 kDa multi-domain protein with a similar distribution of motifs in *Shewanella oneidensis* (Theunissen *et al.,* 2010). The biofilm-promoting factor A (BpfA) features structural motifs that can be found in biofilm-associated

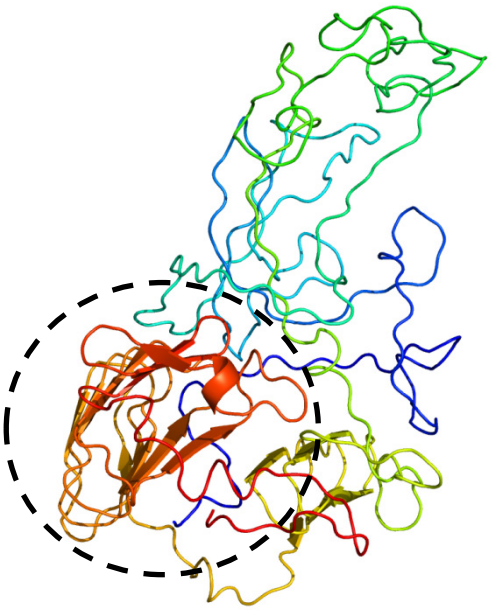

Figure 29: Three-dimensional model of the C-terminal end (spanning 1325 aa) of the gene product of Cag_1919 predicted by Phyre2; dashed line encircles modelled β roll.

proteins (BAP) and RTX proteins and is secreted by the a type I secretion system to the cell surface. Motif search conducted with the KEGG Blast revealed six SWM_repeats and six Big_3_4 motifs for the BAP domain and 9 nonarepeats for the RTX domain of BpfA. The SWM_repeats and Big_3_4 motifs are found in surface proteins. Cag_1919 is overall smaller than BpfA, but still contains 4 SWM_repeats and six nonarepeats, matching the motif organization of BpfA.

5.1.2.2 Putative transport of the protein product of Cag_1919

The C-terminal end also contains the conserved motif DPAFV (DXXXX, where X are hydrophobic residues) which serves as a type I secretion signal (Ghigo & Wandersman, 1994). The signal analyzing software SignalP (Dyrløv Bendtsen *et al.,* 2004) and PrediSi (Hiller *et al.,* 2004) did not indicate any other secretion signals. As all RTX proteins are known to be transported through a type I secretion system and the product of Cag_1919 was detected outside of the epibiont, the genome of *Chl. chlorochromatii* was searched for the components of the secretion system I (T1SS). The T1SS in Gram-negative bacteria transports unfolded RTX related proteins of various sizes from the cytoplasm to the extracellular medium in a single step. All the necessary components of T1SS were found upstream of Cag_1919 (Fig. 30).

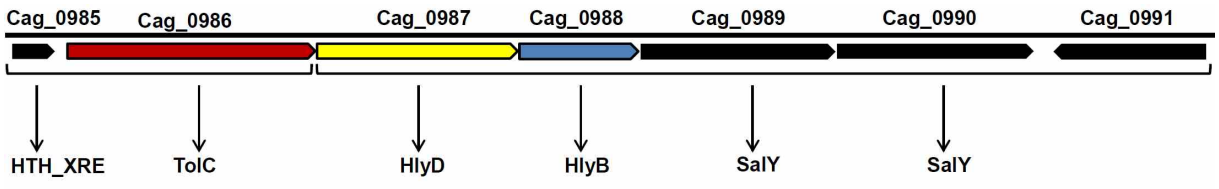

Figure 30: Depiction of a putative secretion system I genes in *Chl. chlorochromatii.* Bioinformatics analysis of the gene products Cag_0985 – Cag_0990 revealed the following sequence homologies with *E. coli* proteins: Cag_0985 = transcriptional regulator; Cag_0986 = TolC; Cag_0987 = HlyD; Cag_0988 = HlyB; Cag_0989 = SalY; Cag_0990 = SalY.

Cag_0986 represents the outer membrane protein, Cag_0987 the periplasmic adaptor or membrane fusion protein and Cag_0988 the ABC transporter. Analysis of transcriptome data of this sequence region showed that the genes Cag_0985-Cag_0986 and Cag_0987-Cag_0990 are probably transcribed into two mRNAs (Suppl. Fig. S1 and Suppl. Fig. S2). The coverage of this region in all three transcriptomes is not efficient to draw a definite conclusion. Cag_0985 was identified as a XRE family transcriptional regulator and Cag_0989 and Cag_0990 as two further ABC transporters, related to SalY. Cag_0991 was only identified as a hypothetical protein, but contains a transposase protein domain identified by DELTA-BLAST, which have been found near transporters and membrane proteins.

It could be argued that the best known model from *E. coli*, the *hly* operon contains the transported substrate HlyB. Another Type I system, the *sla*-operon from *Serratia marcescens*, on the other hand, includes two more substrates localized outside the operon (Kawai *et al.,* 1998). Thereby the localization of the substrate of the Type I transportation system is not relevant regarding its transport with T1SS in an organism. The T1SS operon of the epibiont also contains two further ABC transporters. *Vibrio cholera's* T1SS also contains an additional

ABC transporter (*rtxE*), which is required for the export of an RTX protein (Boardman & Satchell, 2004) and hypothesized to form a heterodimer with another ABC transporter (RtxB).

5.1.2.3 Sequence analysis of the gene products of Cag_0614 and Cag_0616

With 61,938 and 110,418 bp, Cag_016 and Cag_0614 are two of the biggest known ORFs to date and have to cross the epibiont membrane into the central bacterium. Cag_0616 and Cag_0614 share three almost identical sequence regions (Vogl *et al.,* 2008) (Fig. 31) and show an overall β helical character (Inter Pro Scan) with up to 30 predicted parallel beta helix repeats for Cag_0614. Due to their unique size only relative small parts of the amino acid sequence could be matched. Therefore the bioinformatics analysis focused on the unique composition of conserved domains (Fig. 31). DELTA-BLAST revealed a flagellin, a long tail fiber and an FhaB domain at the C-terminus for both proteins. In addition Cag_0616 contains a Hia domain which is characterized as an autotransporter adhesin. Two Greek key motifs, which also harbor Ca^{2+} binding sites, and three RGD tripeptide motifs, were previously identified in Cag_0616. Cag_0614 harbours one RGD tripeptide motif (Vogl *et al.,* 2008).

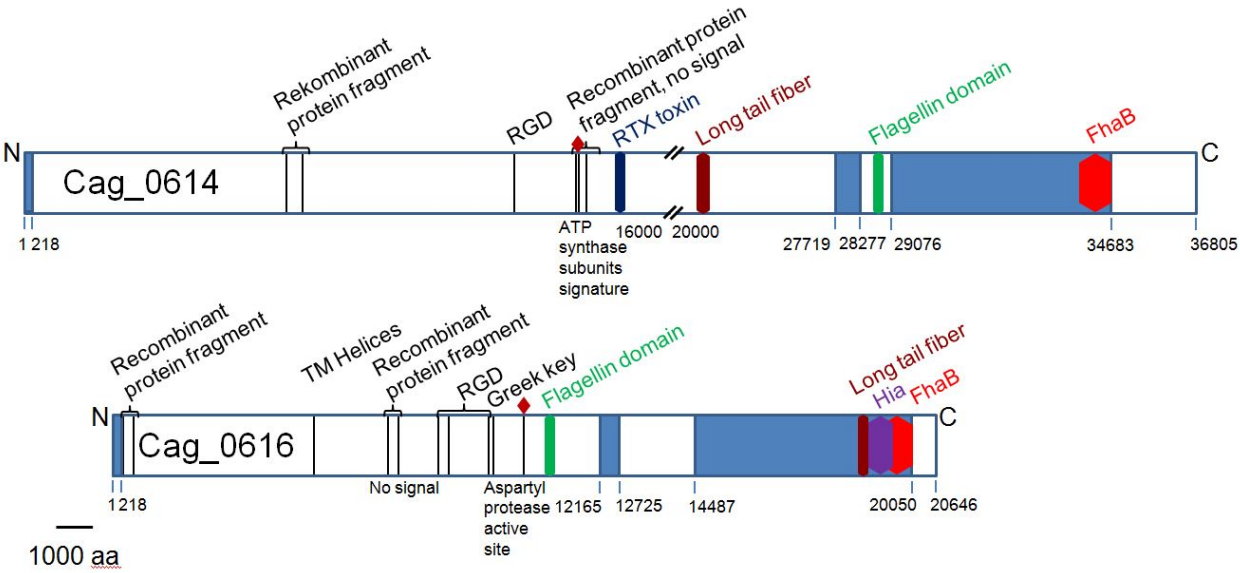

Figure 31: Bioinformatic analysis of the products of ORFs Cag_0614 and Cag_0616. High sequence similarity between the two ORFs is coloured in blue and spans the amino acid regions 1 - 218, 27 719 – 29 076 and 34 683 – 36 805 for Cag_0614 and 1-218, 12 165 – 12 725 and 14 487 – 20 050 for Cag_0616. Protein domains are indicated with coloured hexagons, sequence motifs, like RGD and Greek key, with black bars and sequence motifs for the aspartyl protease active site and the ATP synthase subunits are additionally marked by red squares. The positions of the chosen fragments for antibody production are also indicated with two black bars. Size bar represents 1000 aa.

When analyzing the sequences with Pro Site Scan an aspartyl protease active site and signature sequences for α and β-ATP synthase subunits were detected for Cag_0616 and Cag_0614, respectively. The units of the ATPase synthase (EC 3.6.3.14) are usually found in the cytoplasmic membrane of eubacteria. A protein highly similar to the β ATPase synthase

subunit in bacteria, FliL, was first documented in *Salmonella typhimerium* as a flagellar component (Dreyfus *et al.,* 1993). Aspartyl proteases are a widely distributed family of proteolytic enzymes, in this context however it should be noted that a so-called type IV prepilin peptidase is also an aspartate protease and involved during the process of protein secretion (LaPointe & Taylor, 2000). The type IV prepilin peptidase and its homologs play a central role in type IV pilus biogenesis and in toxin and enzyme secretion (Hobbs & Mattick, 1993).

5.1.2.4 Transcriptome analysis of the sequence region of Cag_0614 and Cag_0616

The analysis of transcriptome data revealed two polycistronic messengers for Cag_0611-Cag_0615 and Cag_0616-Cag_0620, placing the two symbiotic proteins into two different operons (Suppl. Fig. S3 – Suppl. Fig. S5). Cag_0611 encodes an anti-sigma regulatory factor which inhibits the transcriptional activity of sigma factors.

Cag_0612 encodes a glucose-6-phosphate isomerase. Cag_0613 was annotated as a SapC protein which is transported by the type I transportation system and forms part of a paracrystalline surface layer (S-layer) in *Campylobacter fetus* (Thompson *et al.,* 1998). Between the ORF of Cag_0614 and Cag_0616 the outer membrane component of different transporters, TolC, is localized. Cag_0617 is an ORF of unknown function while the ORFs of Cag_0618-Cag_0620 encode different subunits of the polysulfide reductase (Lengeler *et al.,* 1999). Cag_0618 represents the hydrophobic subunit which anchors the enzyme in the membrane; Cag_0619 is one of the two hydrophilic subunits encoding an iron-sulfur protein and Cag_0620, the second subunit, encodes a molybdopterin-binding protein.

5.2 Discussion

5.2.1 Localization of the symbiotic proteins

The results of this study showed that the three protein products of Cag_1919, Cag_0614 and Cag_0616 are transported from the epibiont to the central bacterium in the consortium.

5.2.1.1 Localization of the protein product of Cag_1919

Since Cag_1919 contains a signal sequence for T1SS transport, a putative T1SS transport system is encoded in the epibiont's genome and the protein product of Cag_1919 was localized outside of the epibiont, the transport of this protein occurs very likely with the T1SS system (Fig. 32). The additional ABC transporters in the putative T1SS transport operon could either be necessary to form heterodimers for the transportation system or recognize different substrates for transportation as the ABC transporters also contain part of the substrate recognition sequence (Benabdelhak *et al.,* 2003).

Combined with the facts that several repeats of the RTX consensus sequence were found in the Cag_1919 sequence which are involved in the model of a typical β-roll structure for the C-terminal end of Cag_1919**,** Cag_1919 could encode a repeat-in-toxin (RTX) exoprotein.

The protein product of Cag_1919 also seems to be tightly interconnected with the membrane of the central bacterium. Thus the protein has a stronger interaction with the central bacterium than with the epibiont or might even be inserted in the outer membrane of the central bacterium.

As the protein product of Cag_1919 was only localized between the epibionts and the central bacterium, the involvement of Cag_1919 in the consortia biofilm formation is not very likely. If such was the case Cag_1919 would have been localized in the cell envelope of the epibionts facing the outer periphery of the consortium.

Since the protein product of Cag_1919 shows the same protein domains as the BpfA protein, a protein which plays a crucial role during the initial attachment phase of biofilm formation in the opportunistic pathogen *Shewanella oneidensi* and since the protein product of Cag_1919 is not involved in the consortia biofilm formation, the Cag_1919 protein product probably interacts with the cell envelope of the central bacterium.

This would make the protein product of Cag_1919 the first protein with a RTX module which is involved in the symbiotic relationship between two different bacteria and not an interaction between a prokaryotic and a eukaryotic cell. It has been suggested that *Chl. chlorochromatii* acquired the RTX module from proteobacteria via a horizontal gene transfer (Liu *et al.,* 2013; Vogl *et al.,* 2008). Thus, the hypothesis that a genetic module from

proteobacterial pathogens is now used in the symbiotic interaction between two prokaryotes of different species (Vogl *et al*., 2008), has gained higher recognition.

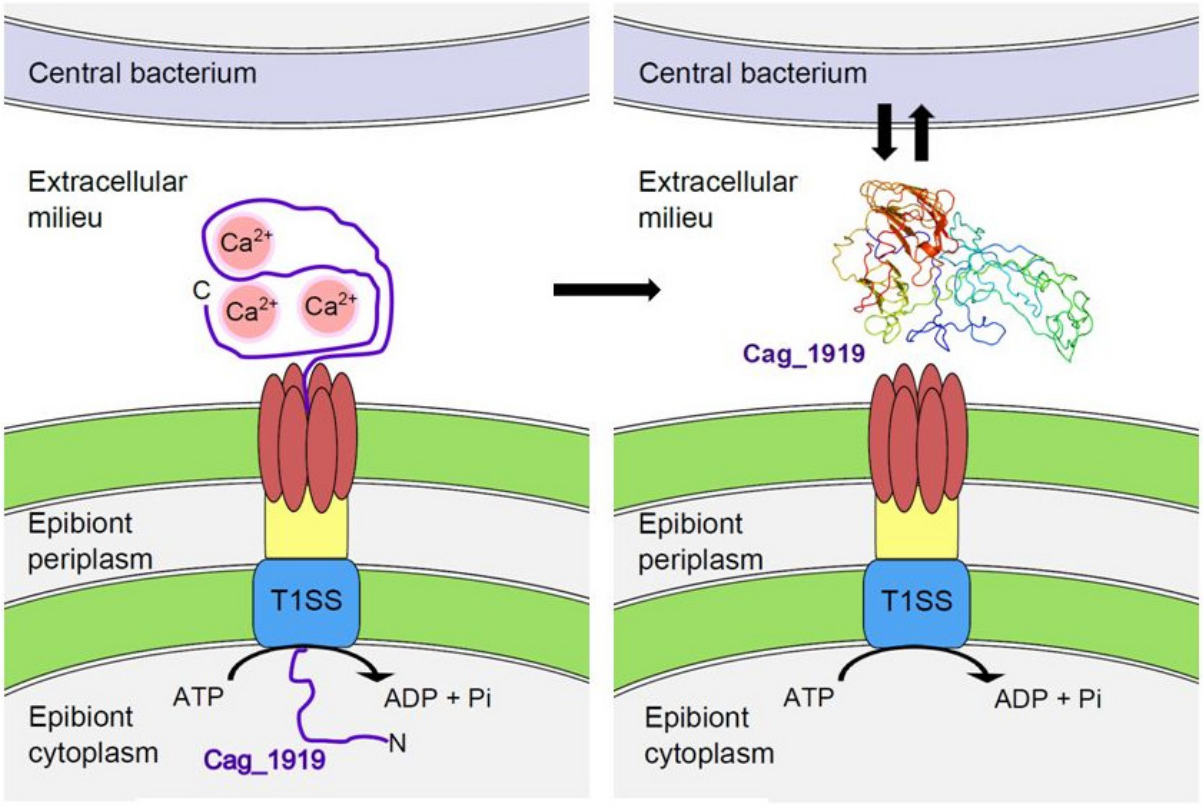

Figure 32: Model displaying a putative transport with T1SS for Cag_1919 across the cell wall of the epibiont.

5.2.1.2 Localization of the protein products of Cag_0614 and Cag_0616

The results of the immunogold labelling of cryosectioned consortia showed a localization of the protein products of Cag_0616 in the cytoplasm of the central bacterium and Cag_0614 in the cytoplasm and the membrane region of the central bacterium. Multiple protein products of Cag_0614 could have been in the process of crossing the membrane of the central bacterium, when the consortium was cryosectioned. Therefore at least the parts of the proteins used for recombinant protein expression had to be transported across the epibionts cell envelope and enter the central bacterium. Interestingly Cag_0614 and Cag_0616 do not harbour any signals for a transport system. The only indications of possible transport are several alignments with autotransport regions and the position of an outer membrane protein TolC. The ORF encoding for TolC is transcribed together with the ORF of Cag_0614.

Transport via an efflux pump was excluded as the periplasmic adaptor of the transport system could not be located in the epibiont's genome. However a single component transporter is present in the genome and shares 27% identity with *E. coli*'s single component transporter *tetA* (Lee *et al.,* 2000), which would enable the proteins to cross the inner

membrane of the epibiont. In regard to the transport across the outer membrane the FhaB domain and the haemagglutinin repeats (Vogl *et al.,* 2008) indicate an autotransporter, similar to TPS system of *Bordetella pertussis*. TPS translocates large, predominately β-helical exoproteins across the outer membrane (Jacob-Dubuisson *et al.,* 2009; Mazar & Cotter, 2007), in which the predicted β-helical character of the TPS proteins are hypothesized to provide the energy for translocation across the membrane (Thanassi *et al.,* 2005). Therefore Cag_0616 could act as an autotransporter for itself and possibly for Cag_0614. Taking into account the presented results a model for the suggested transport was illustrated (Fig. 33).

Cag_0614 and Cag_0616 could be synthesized as preproteins, which are then processed during translocation removing a large C-terminal prodomain (Fig. 33 B), similar to FHA of *Bordetella pertussis* which is synthesized as a preprotein called FhaB and then processed during translocation removing a large C-terminal prodomain (Noël *et al.,* 2012).

It has been reported that the prodomain of FhaB remains intracellular, either in the cytoplasm or the periplasm, affecting the conformation of FHA, likely acting as an intracellular chaperone (Noël *et al.,* 2012). Therefore the FhaB domains of Cag_0614 and Cag_0616 could remain intracellular during transport which would provide sufficient time for the two large proteins to fold correctly in a similar mechanism described by Thanassi *et al*., and subsequently pulling the protein across the outer membrane. Folding of the protein product of Cag_0616 could be facilitated by Ca^{2+} binding sites, located in two Greek key motifs. Epibionts in pure culture analysed with immunofluorescence microscopy were detected outside of the epibiont cell, corroborating an anchoring of the protein during a certain time period.

Since the type IV prepilin peptidase and its homologs play a central role in type IV pilus biogenesis and in toxin and enzyme secretion (Hobbs & Mattick, 1993), the FhaB domain could be cleaved near one of the flagellin or tail fibre domains. A similar system has been described as a fused two partner secretion system (type Vd secretion) for the patatin-like protein from *Pseudomonas aeruginosa*. A lipolytic enzyme is connected to the translocator β-barrel and autocatalytically cleaved after transportation (Salacha *et al.,* 2010). Thus the FhaB domain and the postulated translocator β-barrel of Cag_0616 could remain in the epibiont's membrane, the protein sequence autocatalytically cleaved and the remaining sequence released as a folded protein (Fig. 33 C). The protein product of Cag_0614 might follow through the translocator β-barrel of Cag_0616, applying the same theory for the FhaB domain, cleaved by the type IV prepilin peptidase of Cag_0616 and released as a folded protein (Fig. 33 D). Therefore the complete expression of the ORFs of Cag_0616 and

Cag_0614 and a post-translational modification of the proteins are likely. Considering the energy expended for the production of proteins of their sizes, their role in the symbiosis has to be considerable.

The ORFs of Cag_0616 and Cag_0614 contain RGD motifs, which could mediate adhesion to the central bacterium, as they are known for their adherence properties and have been found in filamentous haemagglutinin (Relman et al. 1989)**.** In prokaryotes these motifs are known for their involvement in attaching proteins of pathogens to mammalian cells (Isberg & Tran Van Nhieu, G, 1994; Kajava *et al.,* 2001). In the consortium this motif is used for the attachment of proteins of a non-pathogenic bacterium to another bacterium. Furthermore these proteins or at least a processed part of these proteins, are being transferred from partner to the other for the mutual benefit of different bacteria in a symbiotic relationship.

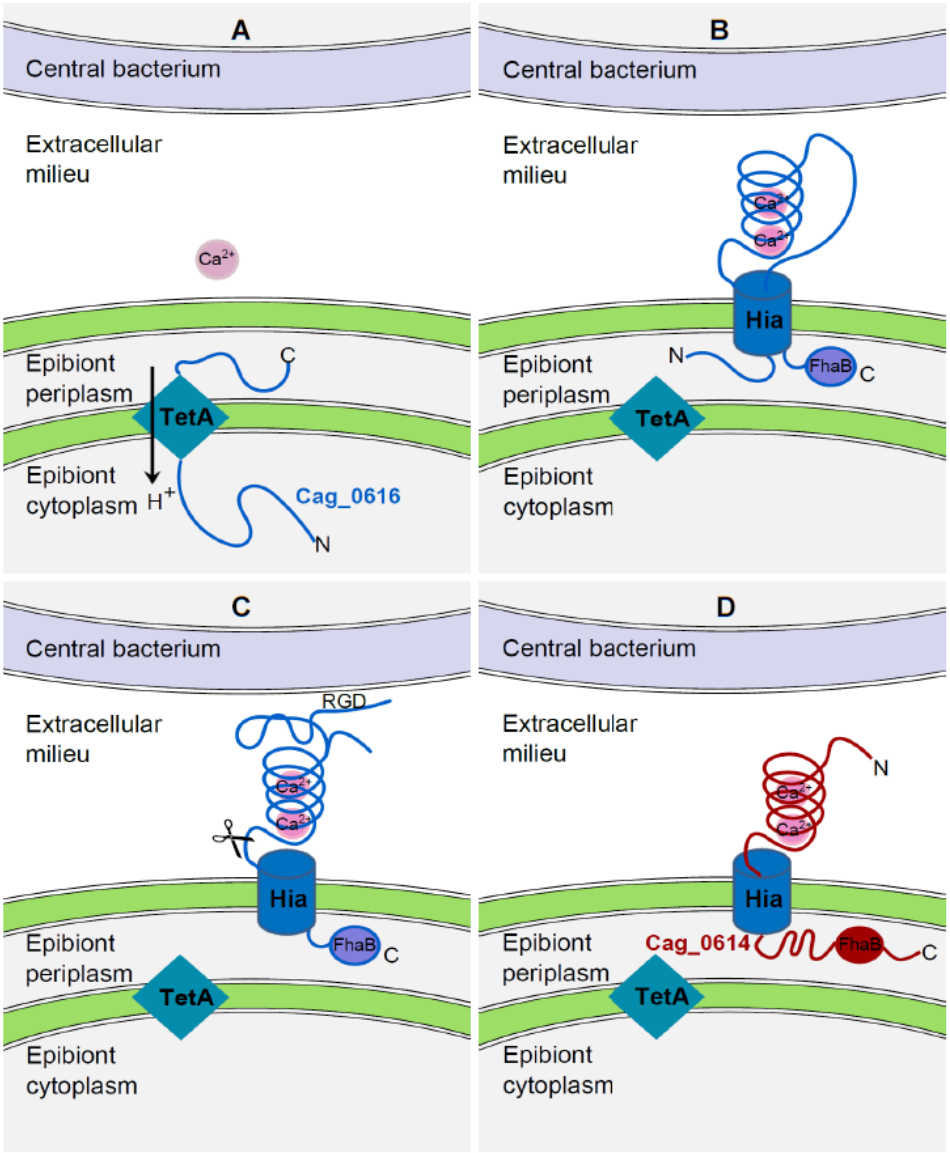

Figure 33: Model for the putative transport of the giant proteins Cag_0614 and Cag_0616 across the cell wall of the epibiont.

The ATP subunit signature of Cag_014 can be connected to the flagellar component FliL, which was studied in *Proteus mirabilis* as an important component in sensing surfaces and regulating virulence gene expression (Belas & Suvanasuthi, 2005). Since it has also been reported that *P. mirabilis* can ascertain its location in the environment or host by assessing the status of its flagellar motors, this part of the protein product of Cag_0614 might be involved in a flagellar monitoring system.

Directed motility is regarded as one of the major advantages that allow phototrophic consortia to outcompete free-living green sulfur bacteria (Müller & Overmann, 2011). However, the central bacterium possesses both the flagellum and the sensory apparatus. Since the epibiont is relying on its non-photosynthetic partner when carried towards more favourable water layers, it is not astonishing that the epibiont might be involved in the motility apparatus of the central bacterium.

5.3 References

Belas, R. & Suvanasuthi, R. (2005). The ability of Proteus mirabilis to sense surfaces and regulate virulence gene expression involves FliL, a flagellar basal body protein. *J. Bacteriol.* **187**, 6789–6803.

Benabdelhak, H., **Kiontke, S.**, **Horn, C.**, **Ernst, R.**, **Blight, M. A.**, **Holland, I. B. & Schmitt, L. (2003).** A specific interaction between the NBD of the ABC-transporter HlyB and a C-terminal fragment of its transport substrate haemolysin A. *J. Mol. Biol.* **327**, 1169–1179.

Boardman, B. K. & Satchell, K. J. (2004). *Vibrio cholerae* Strains with Mutations in an Atypical Type I Secretion System Accumulate RTX Toxin Intracellularly. *Journal of Bacteriology* **186**, 8137–8143.

Dreyfus, G., **Williams, A. W.**, **Kawagishi, I. & Macnab, R. M. (1993).** Genetic and biochemical analysis of *Salmonella typhimurium* FliI, a flagellar protein related to the catalytic subunit of the F0F1 ATPase and to virulence proteins of mammalian and plant pathogens. *J. Bacteriol.* **175**, 3131–3138.

Dyrløv Bendtsen, J., **Nielsen, H.**, **Heijne, G. von & Brunak, S. (2004).** Improved Prediction of Signal Peptides: SignalP 3.0. *Journal of Molecular Biology* **340**, 783–795.

Ghigo, J. M. & Wandersman, C. (1994). A carboxyl-terminal four-amino acid motif is required for secretion of the metalloprotease PrtG through the Erwinia chrysanthemi protease secretion pathway. *J. Biol. Chem.* **269**, 8979–8985.

Hiller, K., **Grote, A.**, **Scheer, M.**, **Munch, R. & Jahn, D. (2004).** PrediSi: prediction of signal peptides and their cleavage positions. *Nucleic Acids Research* **32**, W375.

Hobbs, M. & Mattick, J. S. (1993). Common components in the assembly of type 4 fimbriae, DNA transfer systems, filamentous phage and protein-secretion apparatus: a general system for the formation of surface-associated protein complexes. *Molecular Microbiology* **10**, 233–243.

Isberg, R. R. & Tran Van Nhieu, G **(1994).** Binding and internalization of microorganisms by integrin receptors. *Trends in Microbiology* **2**, 10–14.

Jacob-Dubuisson, F., **Villeret, V.**, **Clantin, B.**, **Delattre, A.-S. & Saint, N. (2009).** First structural insights into the TpsB/Omp85 superfamily. *Biological Chemistry* **390**.

Kajava, A. V., **Cheng, N.**, **Cleaver, R.**, **Kessel, M.**, **Simon, M. N.**, **Willery, E.**, **Jacob-Dubuisson, F.**, **Locht, C. & Steven, A. C. (2001).** Beta-helix model for the filamentous haemagglutinin adhesin of Bordetella pertussis and related bacterial secretory proteins. *Molecular Microbiology* **42**, 279–292.

Kawai, E., **Akatsuka, H.**, **Idei, A.**, **Shibatani, T. & Omori, K. (1998).** *Serratia marcescens* S-layer protein is secreted extracellularly via an ATP-binding cassette exporter, the Lip system. *Mol Microbiol* **27**, 941–952.

Kelley, L. A. & Sternberg, Michael J E **(2009).** Protein structure prediction on the Web: a case study using the Phyre server. *Nat Protoc* **4**, 363–371.

LaPointe, C. F. & Taylor, R. K. (2000). The type 4 prepilin peptidases comprise a novel family of aspartic acid proteases. *J. Biol. Chem.* **275**, 1502–1510.

Lee, A., **Mao, W.**, **Warren, M. S.**, **Mistry, A.**, **Hoshino, K.**, **Okumura, R.**, **Ishida, H. & Lomovskaya, O. (2000).** Interplay between efflux pumps may provide either additive or multiplicative effects on drug resistance. *J. Bacteriol.* **182**, 3142–3150.

Lengeler, J. W., Drews, G. & Schlegel, H. G. (1999). *Biology of the prokaryotes*. Stuttgart, New York, Malden, MA: Thieme; Distributed in the USA by Blackwell Science.

Liu, Z., **Müller, J.**, **Li, T.**, **Alvey, R. M.**, **Vogl, K.**, **Frigaard, N.-U.**, **Rockwell, N. C.**, **Boyd, E. S. & Tomsho, L. P. & other authors (2013).** Genomic analysis reveals key aspects of prokaryotic symbiosis in the phototrophic consortium "*Chlorochromatium aggregatum*". *Genome Biol* **14**, R127.

Mazar, J. & Cotter, P. A. (2007). New insight into the molecular mechanisms of two-partner secretion. *Trends in Microbiology* **15**, 508–515.

Müller, J. & Overmann, J. (2011). Close Interspecies Interactions between Prokaryotes from Sulfureous Environments. *Front. Microbio.* **2**.

Noël, C. R., **Mazar, J.**, **Melvin, J. A.**, **Sexton, J. A. & Cotter, P. A. (2012).** The prodomain of the *Bordetella* two-partner secretion pathway protein FhaB remains intracellular yet affects the conformation of the mature C-terminal domain. *Molecular Microbiology* **86**, 988–1006.

Salacha, R., **Kovačić, F.**, **Brochier-Armanet, C.**, **Wilhelm, S.**, **Tommassen, J.**, **Filloux, A.**, **Voulhoux, R. & Bleves, S. (2010).** The *Pseudomonas aeruginosa* patatin-like protein PlpD is the archetype of a novel Type V secretion system. *Environmental Microbiology*.

Thanassi, D. G., **Stathopoulos, C.**, **Karkal, A. & Li, H. (2005).** Protein secretion in the absence of ATP: the autotransporter, two-partner secretion and chaperone/usher pathways of Gram-negative bacteria (Review). *Mol Membr Biol* **22**, 63–72.

Theunissen, S., **Smet, L. de**, **Dansercoer, A.**, **Motte, B.**, **Coenye, T.**, Van Beeumen, Jozef J., **Devreese, B.**, **Savvides, S. N. & Vergauwen, B. (2010).** The 285 kDa Bap/RTX hybrid cell surface protein (SO4317) of Shewanella oneidensis MR-1 is a key mediator of biofilm formation. *Research in Microbiology* **161**, 144–152.

Thompson, S. A., **Shedd, O. L.**, **Ray, K. C.**, **Beins, M. H.**, **Jorgensen, J. P. & Blaser, M. J. (1998).** Campylobacter fetus surface layer proteins are transported by a type I secretion system. *Journal of Bacteriology* **180**, 6450–6458.

Vogl, K., **Wenter, R.**, **Dressen, M.**, **Schlickenrieder, M.**, **Plöscher, M.**, **Eichacker, L. & Overmann, J. (2008).** Identification and analysis of four candidate symbiosis genes from '*Chlorochromatium aggregatum*', a highly developed bacterial symbiosis. *Environ. Microbiol.* **10**, 2842–2856.

Chapter 6

Metabolic coupling between the two partner bacteria in the phototrophic consortium

6.1 Results

6.1.1 NanoSIMS analysis

Analysis of NanoSIMS generated images were conducted for four consecutive experiments with different conditions regarding the availability of carbon and nitrogen.

The carbon and nitrogen uptake of the consortium's two partner cells was compared by determining changing isotope ratio (Fig. 34 and Tab. 15) of the elements.

Table 15: Summary of four consortia incubations conducted under different conditions.

Experiment	Labelled substrate	Experiment condition
Exp. 1 ($^{13}C/^{12}C$)	$H^{13}CO_3^-$	Standard cultivation with ammonium
Exp. 2a ($^{13}C/^{12}C$)	$H^{13}CO_3^-$	Cultivation depleted of ammonium
Exp. 2b ($^{15}N/^{14}N$)	$^{15}N_2$	Cultivation depleted of ammonium
Exp. 3a ($^{13}C/^{12}C$)	$H^{13}CO_3^-$	Long term ammonium depletion
Exp. 3b ($^{15}N/^{14}N$)	$^{15}N_2$	Long term ammonium depletion
Exp. 4a ($^{13}C/^{12}C$)	$H^{13}CO_3^-$	Long term ammonium depletion
Exp. 4b ($^{15}N/^{14}N$)	$^{15}NH_4^+$	Long term ammonium depletion

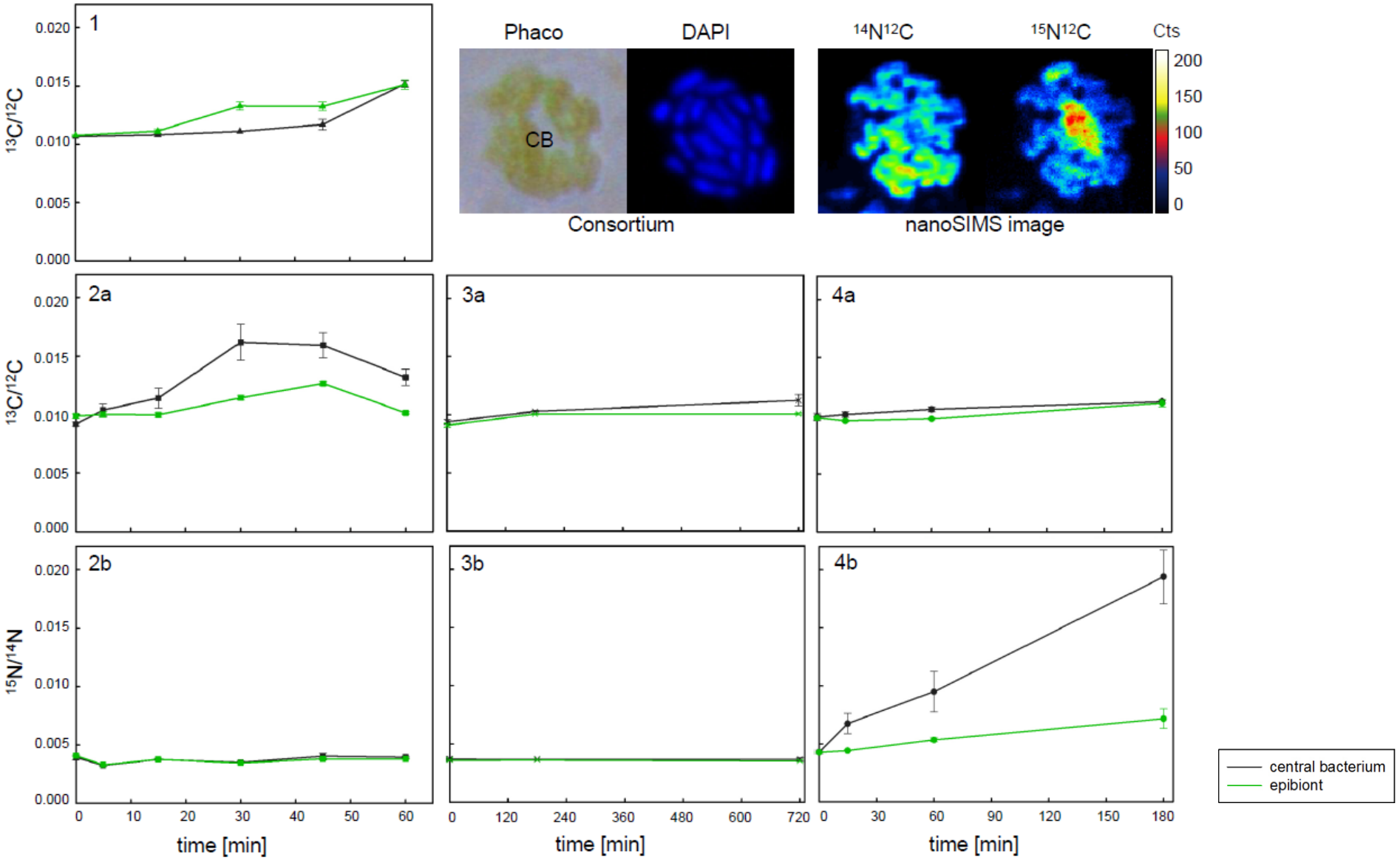

Figure 34: $^{13}C/^{12}C$ and $^{15}N/^{14}N$ ratios determined in consortia with nanoSIMS. (1): $^{13}C/^{12}C$ determined with $H^{13}CO_3^-$; (2): N-limited (a) $^{13}C/^{12}C$ with $H^{13}CO_3^-$ (b): $^{15}N/^{14}N$ with $^{15}N_2$; (3): long term N-limited (a) $^{13}C/^{12}C$ with $H^{13}CO_3^-$and (b) $^{15}N/^{14}N$ with $^{15}N_2$; (4): N-limited (a) $^{13}C/^{12}C$ with $H^{13}CO_3^-$ and (b) $^{15}N/^{14}N$ with $^{15}NH_4^+$. CB = central bacterium.

Labelled $H^{13}CO_3^-$ is autotrophically incorporated by the epibiont cells but not by the central bacterium. An increase of ^{13}C in the central bacterium should therefore be the result of a substrate transfer from the epibiont to the central bacterium. This can be observed when labelled $H^{13}CO_3^-$ was added as the only carbon source to a cultivation of consortia (Fig. 34-1). The $^{13}C/^{12}C$ ratio increases in the epibiont and in the central bacterium, with a 5.8 times higher $^{13}C/^{12}C$ ratio in the epibiont than in the central bacterium. Combined all the epibionts of one consortium thus accumulated 87 times more ^{13}C compared to the central bacterium, considering that each consortium contains an average of 15 epibionts.

This experiment was repeated with consortia which were depleted of ammonium during cultivation under nitrogen gas and used to inoculate fresh medium with labelled sodium carbonate and ^{15}N labelled nitrogen gas. Here the central bacterium contained a 4.5 higher $^{13}C/^{12}C$ ratio and the carbon accumulation in the epibionts dropped to 3.3 compared to the central bacterium (Fig. 34-2a). Surprisingly, an uptake of ^{15}N cannot be shown (Fig. 34-2b), despite the epibiont possessing a complete set of *nif* genes (Liu *et al.,* 2013) which have been shown of being transcribed during a transcriptome experiment conducted light (Müller, 2013). Therefore the cells were probably N-limited from the start and during the second experiment. Figure 35 reflects the difference the cultivation with ammonium or nitrogen gas created in the $^{12}C/^{12}C^{14}N^{15}N$ content of the cells of the consortium.

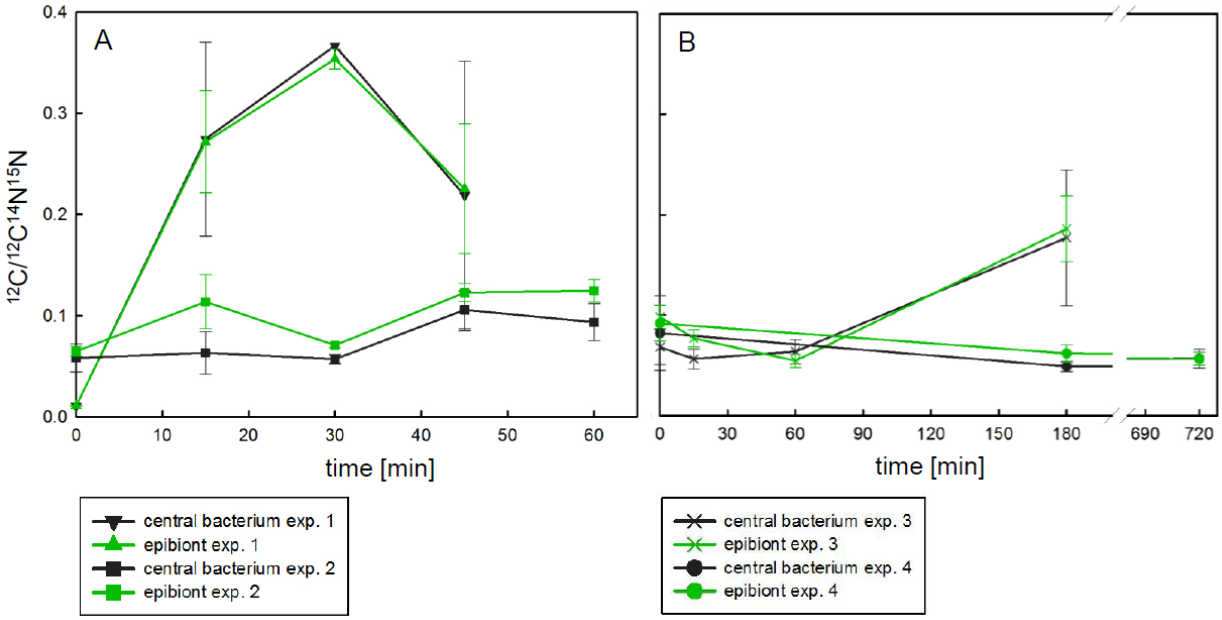

Figure 35: $^{12}C/^{12}C^{14}N^{15}N$ ratios for the four experiments conducted with nanoSIMS. (A), experiment 1 and 2; (B), experiment 3 and 4. The ratio for experiment 1 is $^{12}C/^{12}C^{14}N$. The 60 min time point for experiment 1 could not be calculated, due to an information not available failure in the Look@NanoSIMS program.

Interestingly, figure 35 also shows a decrease of nitrogen in the cells during the first 30 min of cultivation in the first experiment with ammonia, indicating that the cells of the consortium were C-limited at the beginning of the experiment. Consortia medium contained a molar C:N ratio of 5, corresponding to average C:N bacteria cell ratios (Fagerbakke *et al.,* 1996). However, the consortia biofilm was collected after two weeks of cultivation, in which time no further carbon was added. As soon as the consortia were transferred into fresh media during the first experiment where carbon was available again, nitrogen was metabolized together with carbon, lowering the nitrogen content of the cells (Fig. 35) of the consortium.

The experiments 3 and 4 were conducted with long-term ammonium depleted consortium cultures. Consortia used in the experiment 3 were incubated with labelled $H^{13}CO_3^-$ and labelled $^{15}N_2$, while the nitrogen source in experiment 4 was labelled ^{15}N-ammonium. Once the cells were depleted of ammonium in experiment 3 no increase in the $^{13}C/^{12}C$ or $^{15}N/^{14}N$ ratio could be detected even after 12 h of cultivation (Fig. 34-3 a and b). A slight increase in the $^{13}C/^{12}C$ ratio can be seen in the experiment 4 (Fig. 34-4 a), while the $^{15}N/^{14}N$ ratio shows a sudden increase (Fig. 34-4 b). The central bacterium contains a 5.2 times higher ratio compared to the epibiont, but the epibionts in total still accumulated 2.9 times more nitrogen. Transfer between the epibiont and the central bacterium cannot be traced with labelled ammonium as both partners metabolize this substrate. Figure 35 shows the reaction to ammonia with a decrease in nitrogen compared to ^{12}C in the cells, while the incubation under nitrogen gas causes no changes in the $^{12}C/^{12}C^{14}N^{15}N$ ratio.

6.2 Discussion

6.2.1 Analysis of the metabolite transfer in consortia

In a preceding investigation (J. Müller, Suppl. Fig. S 6) using magnetic bead capture a parallel labelling of the rRNA of both the epibionts and the central bacterium of consortia incubated in light could be shown. When the experiment was repeated in the dark, the epibiont and the central bacterium did not incorporate $H^{14}CO_3^-$ into their rRNA.

Epibionts seem to be able to fix $H^{13}CO_3^-$ autotrophically and transfer ^{13}C to the central bacterium almost simultaneously when the consortia are incubated in the light. A transfer of small organic molecules from the epibiont to the central bacterium with emphasis on amino acids was postulated (Müller, 2013). Using nanoSIMS the incorporation of ^{13}C into the epibionts and subsequent transfer to the central bacterium was not only confirmed, but also allowed the calculation of the fraction each epibiont has to contribute to the total amount of transferred ^{13}C. If an average of 15 epibionts contribute to the transferred ^{13}C in the central bacterium, only 1.15 % of the incorporated ^{13}C in each epibiont is transferred. The central bacterium is therefore benefiting from the enrichment of ^{13}C by all its epibionts. The parallel incorporation of ^{13}C into both partners of the consortium supports the hypothesis that small organic molecules are transferred from the epibiont to the central bacterium rather than macromolecules.

Since amino acids are used as carbon and ammonium shuttles in legume-root nodules (Lodwig *et al.,* 2003) and an amino acids transfer has also been demonstrated in the archaea-archaea association of *Ignicoccus hospitalis* and *Nanoarchaeum equitans* (Jahn *et al.,* 2008), the small organic molecules could be amino acids.

The property of amino acids to provide both a carbon and nitrogen source is interesting with respect to the symbiosis of phototrophic consortia, as it has been postulated that epibonts might be experiencing nitrogen limitation in the symbiotic state. Being associated with a green sulfur bacterium able to perform nitrogen fixation and transferring the fixed nitrogen via amino acids theoretically should therefore provide the central bacteria with a competitive advantage over their heterotrophic competitors. N_2-fixation by the epibiont is conducted by the enzymes coded in the *nif* regulon. The main enzymes of this complex, the dinitrogenase reductase and one part of the dinitrogenase are active with RPKMs of 5.6 and 8.8, even in epibionts provided with ammonium.

Therefore, experiment 2 employed N-limited cells which were incubated with ^{15}N labelled nitrogen gas. The uptake of ^{15}N was not observed via nanoSIMS measurements, but a

clear effect on the ^{13}C distribution in the consortium was seen. The accumulated ^{13}C in the epibionts compared to the central bacterium decreased from 87-fold to 3.3-fold. Each epibiont in the consortium had to have transferred 30.3 % of its incorporated ^{13}C to the central bacterium. Green sulfur bacteria are able to synthesize glycogen, usually in the presence of excess carbon substrates and light energy but limiting amounts of inorganic nutrients like ammonium and phosphate (Sirevåg, Ormerod 1977). Considering that there was no uptake of ^{15}N during this time period, the epibionts might be transferring carbohydrates to the central bacterium when the cells are N-limited. Still an advantage for the symbiotic central bacterium, as it relies on exogenous carbon (Liu et al. 2013). In addition, transcriptome analysis revealed that although the central bacterium should be active in the dark, its activity is highly reduced compared to its activity in the light, where the epibiont is able to perform photosynthesis.

The culture used for the experiment 2 was thought to be depleted of ammonium beforehand, but cells may have been in a resting phase. Therefore the cultures used for the experiments 3 and 4 were more severely depleted of ammonium and the time periods for sampling were extended. No ^{13}C or ^{15}N uptake was observed during experiment 3. As ammonium uptake cannot be contributed to one of the partners of the consortia, the transfer rate between the partners cannot be determined. But as soon as the culture was supplemented with ammonium a ^{15}N uptake was observed and consortia started with a slow ^{13}C uptake. Thus consortia growth does not solely rely on nitrogen gas, even if the epibionts are fixing N_2 during cultivation in the light.

Since the transfer of incorporated ^{13}C to the central bacterium increased from 1.15 % to 30.3 % depending on nitrogen availability, the symbiotic epibionts might be changing their preferred transferred organic molecule from substances with nitrogen, like amino acids, to substances without nitrogen, like carbohydrates.

It is interesting to note that when the soluble proteome of free-living epibionts was compared with the proteome of symbiotic epibionts, a P-II protein (Cag_1245) was identified in the proteome of the symbiotic epibiont. P-II proteins are involved in the regulation of the nitrogen metabolism (Forchhammer, 2008; Leigh & Dodsworth, 2007) and are often transcriptionally linked to an ammonium transporter gene or glutamine synthetase. Cag_1245 however is localized between the nitrogenase structural genes *nifH* and *nifD* and would therefore belong to the Nifl subgroup of P-II (Sant'Anna *et al.,* 2009). The inhibitory effect of Nifl on nitrogenase occurs via direct interaction of a $Nifl_1/Nifl_2$ heteromer with the nitrogenase NifDK component reacting to increasing ammonium levels (Leigh & Dodsworth, 2007). The deletion of *nif* genes in *Methanococcus maripaludis* abolished the reversible

inactivation of nitrogenase by ammonium (Kessler *et al.,* 2001). Cag_1245 is also highly expressed (189-fold) compared to free-living epibionts (Wenter *et al.,* 2010), indicating a high regulation of the nitrogenase activity in the symbiotic lifestyle. At this point it can only be speculated that as the consortium needs ammonium for growth, the nitrogenase in the epibionts is under higher regulation than in the free-living epibionts.

In summary these experiments show that, (i) a change of transferred substrate between the partners depended on the nitrogen availability in the epibiont cell, (ii) the consortium does not possess the ability to grow solely on nitrogen gas (iii) the central bacterium benefits from the enrichment effect by its surrounding epibionts.

6.3 References

Fagerbakke, K. M., **Heldal, M. & Norland, S. (1996).** Content of carbon, nitrogen, oxygen, sulfur and phosphorus in native aquatic and cultured bacteria. *Aquat. Microb. Ecol.* **10**, 15–27.

Forchhammer, K. (2008). P(II) signal transducers: novel functional and structural insights. *Trends in Microbiology* **16**, 65–72.

Jahn, U., **Gallenberger, M.**, **Paper, W.**, **Junglas, B.**, **Eisenreich, W.**, **Stetter, K. O.**, **Rachel, R. & Huber, H. (2008).** *Nanoarchaeum equitans* and *Ignicoccus hospitalis*: new insights into a unique, intimate association of two archaea. *Journal of Bacteriology* **190**, 1743–1750.

Kessler, P. S., **Daniel, C. & Leigh, J. A. (2001).** Ammonia switch-off of nitrogen fixation in the methanogenic archaeon Methanococcus maripaludis: mechanistic features and requirement for the novel GlnB homologues, NifI(1) and NifI(2). *Journal of Bacteriology* **183**, 882–889.

Leigh, J. A. & Dodsworth, J. A. (2007). Nitrogen regulation in bacteria and archaea. *Annual review of microbiology* **61**, 349–377.

Liu, Z., **Müller, J.**, **Li, T.**, **Alvey, R. M.**, **Vogl, K.**, **Frigaard, N.-U.**, **Rockwell, N. C.**, **Boyd, E. S. & Tomsho, L. P. & other authors (2013).** Genomic analysis reveals key aspects of prokaryotic symbiosis in the phototrophic consortium "*Chlorochromatium aggregatum*". *Genome Biol* **14**, R127.

Lodwig, E. M., Hosie, A H F, **Bourdès, A.**, **Findlay, K.**, **Allaway, D.**, **Karunakaran, R.**, **Downie, J. A. & Poole, P. S. (2003).** Amino-acid cycling drives nitrogen fixation in the legume-*Rhizobium* symbiosis. *Nature* **422**, 722–726.

Müller, J. (2013). Interspecies interaction and diversity of green sulfur bacteria. Ph.D thesis München: LMU, Department of Biology.

Sant'Anna, F. H., **Trentini, D. B.**, de Souto Weber, Shana, **Cecagno, R.**, da Silva, Sérgio Ceroni **& Schrank, I. S. (2009).** The PII superfamily revised: a novel group and evolutionary insights. *Journal of molecular evolution* **68**, 322–336.

Wenter, R., **Hütz, K.**, **Dibbern, D.**, **Li, T.**, **Reisinger, V.**, **Plöscher, M.**, **Eichacker, L.**, **Eddie, B. & Hanson, T. & other authors (2010).** Expression-based identification of genetic determinants of the bacterial symbiosis "*Chlorochromatium aggregatum*". *Environmental Microbiology*.

Chapter 7

Effect of zaragozic acid on the stability of consortia

7.1 Results

The effect of zaragozic acid on the stability of consortia was tested with the addition of 30 µmol and 60 µmol to a standard cultivation of consortia. The numbers of intact consortia, single epibionts detached from consortia and visible disaggregating consortia were determined and compared (Fig. 36 A - C). The numbers of intact consortia under standard growth conditions without the addition of zaragozic acid, show a lag phase in the first 8 h of (Fig. 36 A) cultivation. In contrast the numbers of consortia in cultures treated with zaragozic acid did not increase after 24 h.

The zaragozic acid treatment showed a pronounced difference in the number of single epibionts detected (Fig. 36 B). After 52 h, the numbers of single epibionts for both zaragozic acid concentrations had doubled compared to the controls. Samples containing the higher zaragozic acid concentration also showed the highest count of single epibionts. But the number of single epibionts in the experiment with 30 µmol zaragozic acid reached a similar value.

Figure 36 C clearly shows a distinct increase of disaggregated consortia compared to the control in the first 24 h, with a slight decrease between 24 h and 52 h. The maximum of disaggregated consortia was reached in the 30 µmol zaragozic acid experiment at 24 h with 18 disaggregated consortia μl^{-1}.

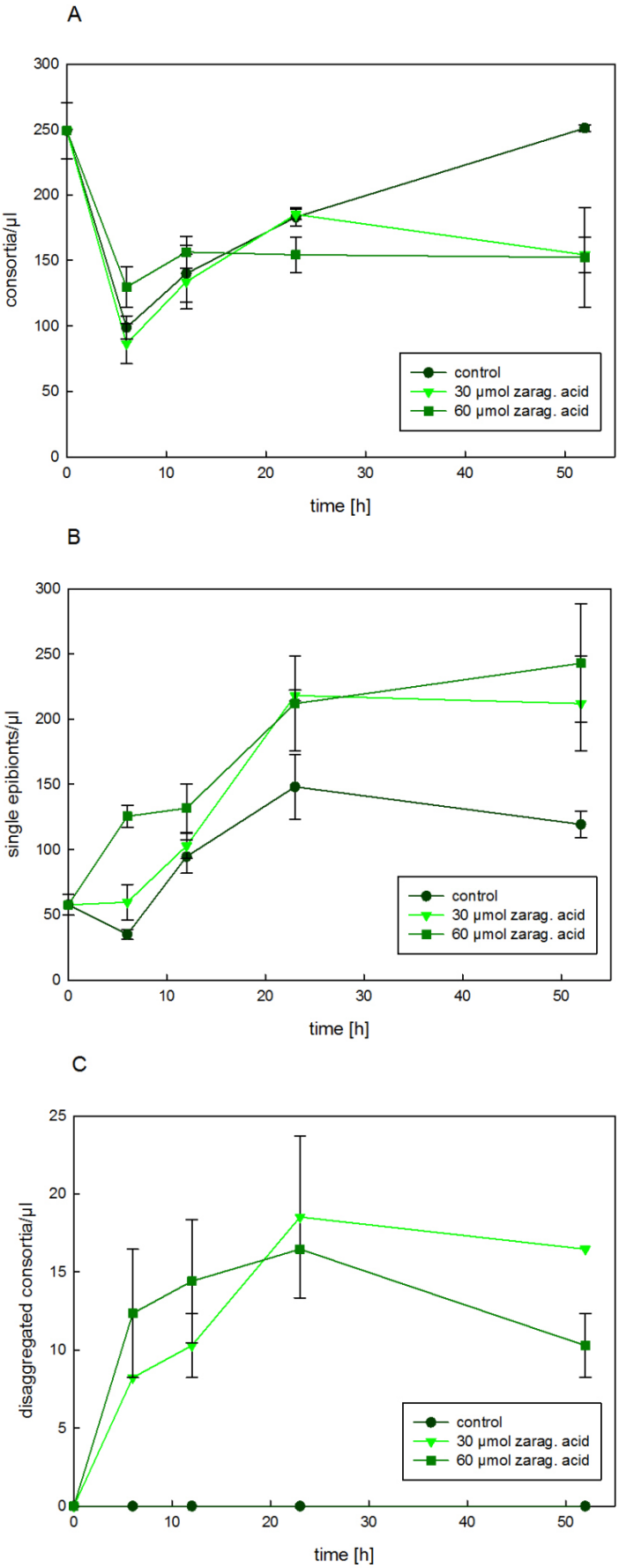

Figure 36: Cell count per µl plotted over time showing the effects of 30 and 60 µmol zaragozic acid on the stability of consortia. P.c. = positive control, consortia culture with no added zaragozic acid. (A) Number of intact consortia per µl. (B) Number of epibionts not attached to a consortium per µl. (C) Number of disaggregated consortia per µl.

7.2 Discussion

7.2.1 Is Cyclic β-1,2-glucan involved in cell-cell interaction?

Since the addition of zaragozic acid showed an effect on the stability of consortia and has been reported to affect the ability of *Bacillus subtilis* and *Staphylococcus aureus* to form biofilms (López & Kolter, 2010), zaragozic acid was considered as a competitive inhibitor of the enzyme squalene synthase. López *et al.* postulated that the inhibition of biofilm formation could be the result of a disrupted production of functional microdomains lipids (López & Kolter, 2010).

Similar to eukaryotic "lipid rafts", functional mircodomains are bacterial membrane regions rich on polyisoprenoid lipids. In eukaryotes the cellular functions can be attributed in major parts to the recruitment and concentration of molecules involved in cellular signaling thereby enhancing signaling efficiency (Triantafilou *et al.,* 2002).

The isoprenoid biosynthesis in bacteria follows the mevalonate or glyceraldehyde-3-pyruvate route before the condensation of several isoprenoid molecules forms polyisoprenoid molecules, such as squalene (Balibar *et al.,* 2009; Takahashi *et al.,* 1998; Wilding *et al.,* 2000). Both pathways can be targeted by zaragozic acid (Bergstrom *et al.,* 1993). A possible polyisoprenoid in *Chl. chlorochromatii* is carotenoid, a noncyclic polyisprenoid lipid abundant in bacteria (Taylor, 1984). The epibiont contains 12 different carotenoids of which six are unidentified compounds and two so far have only been detected in the epibiont (Vogl *et al.,* 2006). These so far unidentified carotenoids could be important for the formation of lipid microdomains.

Since eukaryotic membranes harbor raft-associated proteins like Flotellin-1, which recruits proteins to lipid rafts (Babuke & Tikkanen, 2007; Langhorst *et al.,* 2005; Otto & Nichols, 2011) and bacterial flotillins have also been reported (Tavernarakis *et al.,* 1999), the epibionts genome was analysed with the SMART software (Letunic *et al.,* 2012) to identify proteins with a PHB domain characteristic for flotillins. The search yielded exactly one gene, Cag_1233. This protein also harbors a coiled-coiled region downstream of the SPFH domain matching the description of bacterial flotillins (Solis *et al.,* 2007).

Pathogenic bacteria are known to use eukaryotic lipid rafts as concentration devices or as cluster of receptors for their toxins (Lafont *et al.,* 2004) in order to infect cells. Interestingly, López *et al.* also postulated that in the pathogenic *Brucella abortus* cyclic β-1,2-glucan (CβG) acts on the eukaryotic host cell membranes via their lipid rafts (Arellano-Reynoso *et al.,* 2005).

The CβG synthetases are present in a number of symbiotic or pathogenic bacteria, in which it is required for successful host interactions (Arellano-Reynoso *et al.,* 2005; Dylan *et al.,* 1986; Puvanesarajah *et al.,* 1985). Cenrod_1441 in the genome of the central bacterium was identified as a cyclic β-1,2-glucan synthetase gene. Once synthesized in the cytoplasm of *B. abortus*, CβG has to be transported to the periplasm in order for it to function as a virulence factor (Roset *et al.,* 2004). In the genome of central bacterium, Cenrod_1179 is a possible cyclic beta-1,2-glucan ABC transporter for its similarity to PRK13657 (88% query coverage and 31% identity) (Marchler-Bauer *et al.,* 2015).

A theoretical model which summarizes a possible mode of action of zaragozic acid on the consortium was developed (Fig. 37).

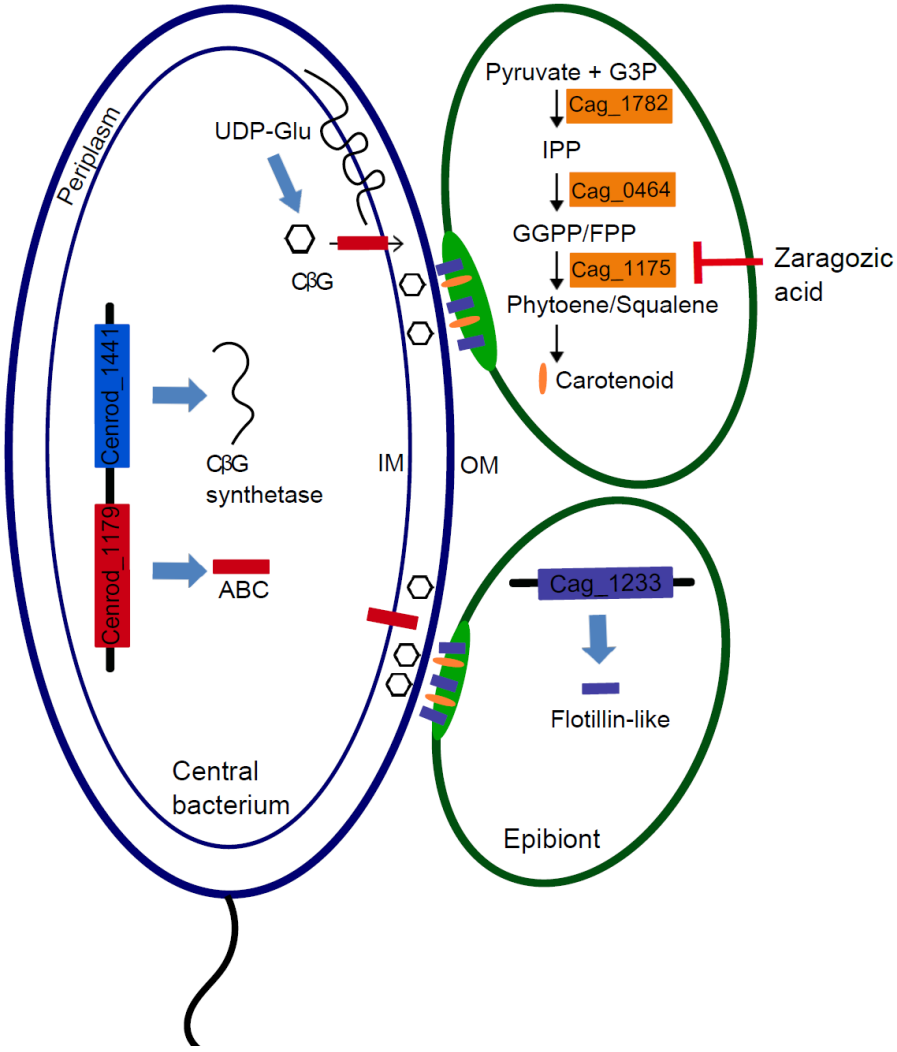

Figure 37: Proposed model for the interaction between the central bacterium and epibionts via cyclic β-1,2-glucan and lipid rafts. The model depicts the genes (colored squares) and proteins involved in the interaction and the possible target for zaragozic acid in the polyisoprenoid synthesis pathway. Abbreviations: IM = inner membrane; OM = outer membrane; UDP-Glu = Uridine diphosphate glucose; CβG = cyclic β-1,2-glucose; G3P = Glyceraldehyde 3-phosphate; IPP = isopentenyl pyrophosphate; GGPP = geranyl-geranyl pyrophosphate; FPP = farnesyl pyrophosphate.

7.3 References

Arellano-Reynoso, B., **Lapaque, N.**, **Salcedo, S.**, **Briones, G.**, **Ciocchini, A. E.**, **Ugalde, R.**, **Moreno, E.**, **Moriyón, I. & Gorvel, J.-P. (2005).** Cyclic beta-1,2-glucan is a Brucella virulence factor required for intracellular survival. *Nature immunology* **6**, 618–625.

Babuke, T. & Tikkanen, R. (2007). Dissecting the molecular function of reggie/flotillin proteins. *European journal of cell biology* **86**, 525–532.

Balibar, C. J., **Shen, X. & Tao, J. (2009).** The mevalonate pathway of Staphylococcus aureus. *Journal of Bacteriology* **191**, 851–861.

Bergstrom, J. D., **Kurtz, M. M.**, **Rew, D. J.**, **Amend, A. M.**, **Karkas, J. D.**, **Bostedor, R. G.**, **Bansal, V. S.**, **Dufresne, C.**, **VanMiddlesworth, F. L. & Hensens, O. D. (1993).** Zaragozic acids: a family of fungal metabolites that are picomolar competitive inhibitors of squalene synthase. *Proceedings of the National Academy of Sciences of the United States of America* **90**, 80–84.

Dylan, T., **Ielpi, L.**, **Stanfield, S.**, **Kashyap, L.**, **Douglas, C.**, **Yanofsky, M.**, **Nester, E.**, **Helinski, D. R. & Ditta, G. (1986).** *Rhizobium meliloti* genes required for nodule development are related to chromosomal virulence genes in Agrobacterium tumefaciens. *Proceedings of the National Academy of Sciences of the United States of America* **83**, 4403–4407.

Lafont, F., **Abrami, L. &** van der Goot, F Gisou **(2004).** Bacterial subversion of lipid rafts. *Current opinion in microbiology* **7**, 4–10.

Langhorst, M. F., **Reuter, A. &** Stuermer, C A O **(2005).** Scaffolding microdomains and beyond: the function of reggie/flotillin proteins. *Cellular and molecular life sciences : CMLS* **62**, 2228–2240.

Letunic, I., **Doerks, T. & Bork, P. (2012).** SMART 7: recent updates to the protein domain annotation resource. *Nucleic Acids Research* **40**, D302-5.

López, D. & Kolter, R. (2010). Functional microdomains in bacterial membranes. *Genes & development* **24**, 1893–1902.

Marchler-Bauer, A., **Derbyshire, M. K.**, **Gonzales, N. R.**, **Lu, S.**, **Chitsaz, F.**, **Geer, L. Y.**, **Geer, R. C.**, **He, J. & Gwadz, M. & other authors (2015).** CDD: NCBI's conserved domain database. *Nucleic Acids Research* **43**, D222-6.

Otto, G. P. & Nichols, B. J. (2011). The roles of flotillin microdomains--endocytosis and beyond. *Journal of cell science* **124**, 3933–3940.

Puvanesarajah, V., **Schell, F. M.**, **Stacey, G.**, **Douglas, C. J. & Nester, E. W. (1985).** Role for 2-linked-beta-D-glucan in the virulence of *Agrobacterium tumefaciens*. *Journal of Bacteriology* **164**, 102–106.

Roset, M. S., **Ciocchini, A. E.**, **Ugalde, R. A. &** Iñón de Iannino, Nora **(2004).** Molecular cloning and characterization of cgt, the *Brucella abortus* cyclic beta-1,2-glucan transporter gene, and its role in virulence. *Infection and immunity* **72**, 2263–2271.

Solis, G. P., **Hoegg, M.**, **Munderloh, C.**, **Schrock, Y.**, **Malaga-Trillo, E.**, **Rivera-Milla, E. &** Stuermer, Claudia A O **(2007).** Reggie/flotillin proteins are organized into stable tetramers in membrane microdomains. *The Biochemical journal* **403**, 313–322.

Takahashi, S., **Kuzuyama, T.**, **Watanabe, H. & Seto, H. (1998).** A 1-deoxy-D-xylulose 5-phosphate reductoisomerase catalyzing the formation of 2-C-methyl-D-erythritol 4-phosphate in an alternative nonmevalonate pathway for terpenoid biosynthesis. *Proceedings of the National Academy of Sciences* **95**, 9879–9884.

Tavernarakis, N., **Driscoll, M. & Kyrpides, N. C. (1999).** The SPFH domain: implicated in regulating targeted protein turnover in stomatins and other membrane-associated proteins. *Trends in biochemical sciences* **24**, 425–427.

Taylor, R. F. (1984). Bacterial triterpenoids. *Microbiological reviews* **48**, 181–198.

Triantafilou, M., **Miyake, K.**, **Golenbock, D. T. & Triantafilou, K. (2002).** Mediators of innate immune recognition of bacteria concentrate in lipid rafts and facilitate lipopolysaccharide-induced cell activation. *Journal of cell science* **115**, 2603–2611.

Vogl, K., **Glaeser, J.**, **Pfannes, K. R.**, **Wanner, G. & Overmann, J. (2006).** *Chlorobium chlorochromatii* sp. nov., a symbiotic green sulfur bacterium isolated from the phototrophic consortium "Chlorochromatium aggregatum". *Archives of Microbiology* **185**, 363–372.

Wilding, E. I., **Brown, J. R.**, **Bryant, A. P.**, **Chalker, A. F.**, **Holmes, D. J.**, **Ingraham, K. A.**, **Iordanescu, S.**, **So, C. Y.**, **Rosenberg, M. & Gwynn, M. N. (2000).** Identification, Evolution, and Essentiality of the Mevalonate Pathway for Isopentenyl Diphosphate Biosynthesis in Gram-Positive Cocci. *Journal of Bacteriology* **182**, 4319–4327.

Chapter 8

Conclusion

The phototrophic consortium "*Chlorochromaticum aggregatum*" gives a unique opportunity to study two different bacteria in a close and structured interaction. Few bacterial associations have reached this complex organization level and can be kept in a laboratory culture. This study significantly contributes to further understand the interaction between the two partners of "*C. aggregatum*", analyzing symbiotic proteins of the epibiont and the carbon and nitrogen flux between the partners.

Symbiotic proteins were proven to be transferred from the epibiont to the central bacterium. It could be shown in this study that RTX and RGD motifs, known from pathogenic interactions, are being used in the symbiotic interaction between two prokaryotes, and further research in this field should focus on these symbiotic proteins more closely.

It has long been postulated that a signal exchange exists between the two partners, due to the scotophobic response of the consortium and the chemotaxis towards substrates, both benefiting the epibiont, where the central bacterium is the motor for this response. In return the central bacterium receives fixed CO_2 in the form of small organic matter. Although, the transfer of proteins is not conclusive evidence of signal exchange, the proven protein transfer into the cytoplasm of the central bacterium indicates the involvement of these transported proteins in the partner organism. Further studies in this area should focus on the central bacterium, determining if the central bacterium also transports proteins to and into the epibiont. The first indication of an interaction initiated by the central bacterium, excluding prominent structures like the periplasmic tubules, was devised with the proposed theoretical model of CβG and lipid raft interaction in the consortium. While this model is purely theoretical at the moment, CβG synthetases have been found in a number of symbiotic or pathogenic bacteria, in which they are required for successful host interactions (Arellano-Reynoso *et al.,* 2005; Dylan *et al.,* 1986; Puvanesarajah *et al.,* 1985).

A future and challenging assignment in consortia research could therefore be the development of a system which is able to genetically manipulate one or both partners. Could this be achieved, it would open a complete new field of symbiotic interaction research.

It could be shown that the flux of carbon changes depending on the nitrogen availability of the epibiont cell, indicating a complex picture of substrate utilization within the phototrophic consortium. Further nanoSIMS analysis using 2-oxoglutarate as an alternative substrate might give insight into the complex coupling within the consortium. A surprising result in this study was the finding that the consortium does not solely grow on nitrogen gas,

as previously assumed. The association with a green sulfur bacterium, capable of nitrogen fixation, was considered a competitive advantage. Thus the combined nitrogen metabolism and/or regulation of those in both partners harbours unresolved questions, more complex than the exchange of amino acids in legume-root nodules (Lodwig *et al.,* 2003) or transfer of amino acids archaea-archaea association of *Ignicoccus hospitalis* and *Nanoarchaeum equitans* (Jahn *et al.,* 2008).

8.1 References

Arellano-Reynoso, B., **Lapaque, N.**, **Salcedo, S.**, **Briones, G.**, **Ciocchini, A. E.**, **Ugalde, R.**, **Moreno, E.**, **Moriyón, I. & Gorvel, J.-P. (2005).** Cyclic beta-1,2-glucan is a Brucella virulence factor required for intracellular survival. *Nature immunology* **6**, 618–625.

Dylan, T., **Ielpi, L.**, **Stanfield, S.**, **Kashyap, L.**, **Douglas, C.**, **Yanofsky, M.**, **Nester, E.**, **Helinski, D. R. & Ditta, G. (1986).** *Rhizobium meliloti* genes required for nodule development are related to chromosomal virulence genes in Agrobacterium tumefaciens. *Proceedings of the National Academy of Sciences of the United States of America* **83**, 4403–4407.

Jahn, U., **Gallenberger, M.**, **Paper, W.**, **Junglas, B.**, **Eisenreich, W.**, **Stetter, K. O.**, **Rachel, R. & Huber, H. (2008).** *Nanoarchaeum equitans* and *Ignicoccus hospitalis*: new insights into a unique, intimate association of two archaea. *Journal of Bacteriology* **190**, 1743–1750.

Lodwig, E. M., Hosie, A H F, **Bourdès, A.**, **Findlay, K.**, **Allaway, D.**, **Karunakaran, R.**, **Downie, J. A. & Poole, P. S. (2003).** Amino-acid cycling drives nitrogen fixation in the legume-*Rhizobium* symbiosis. *Nature* **422**, 722–726.

Puvanesarajah, V., **Schell, F. M.**, **Stacey, G.**, **Douglas, C. J. & Nester, E. W. (1985).** Role for 2-linked-beta-D-glucan in the virulence of *Agrobacterium tumefaciens*. *Journal of Bacteriology* **164**, 102–106.

I. Supplementary Figures

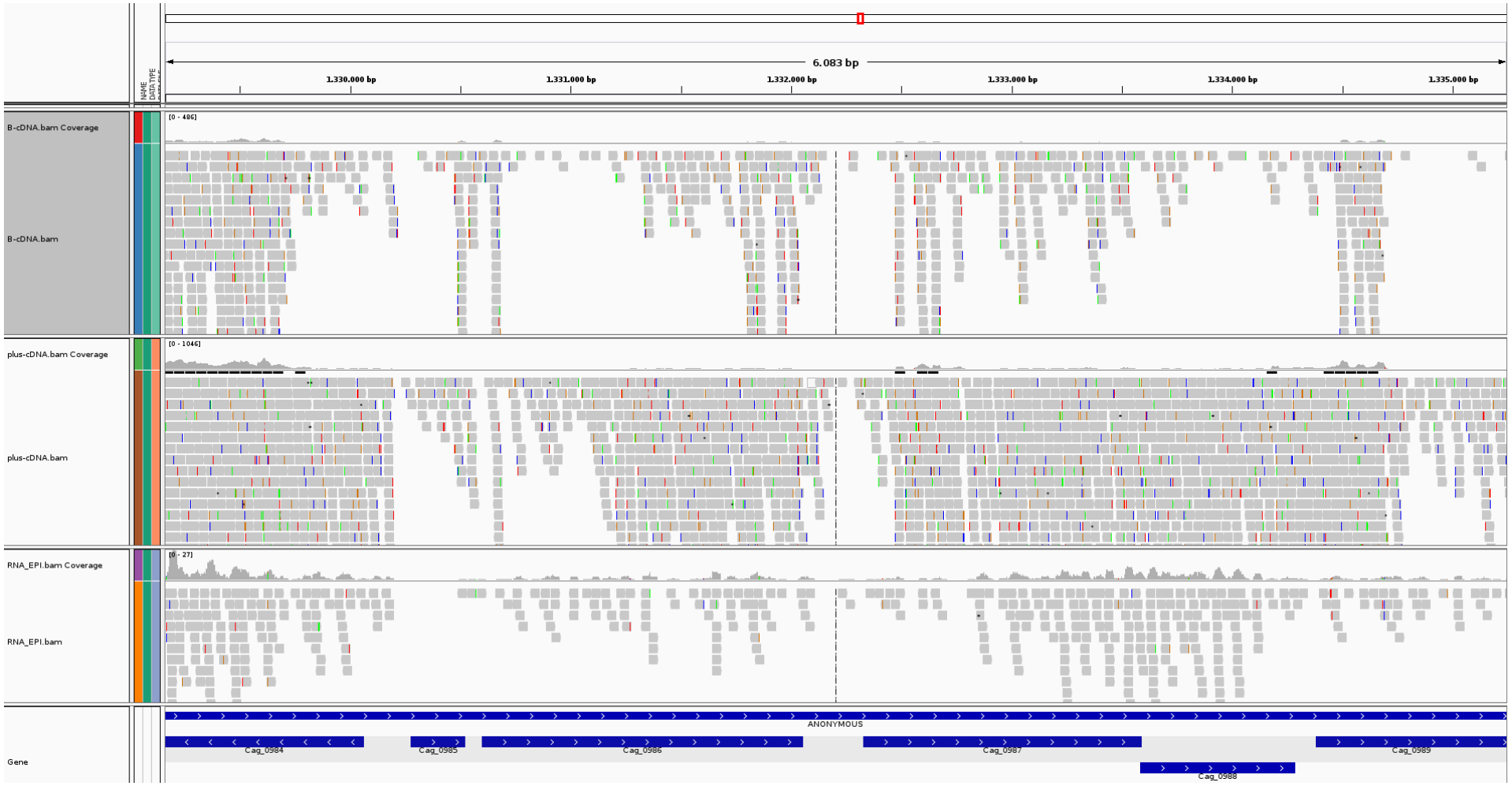

Suppl. Fig. S1: Transcriptome analysis Cag_0985-Cag_0989**.**

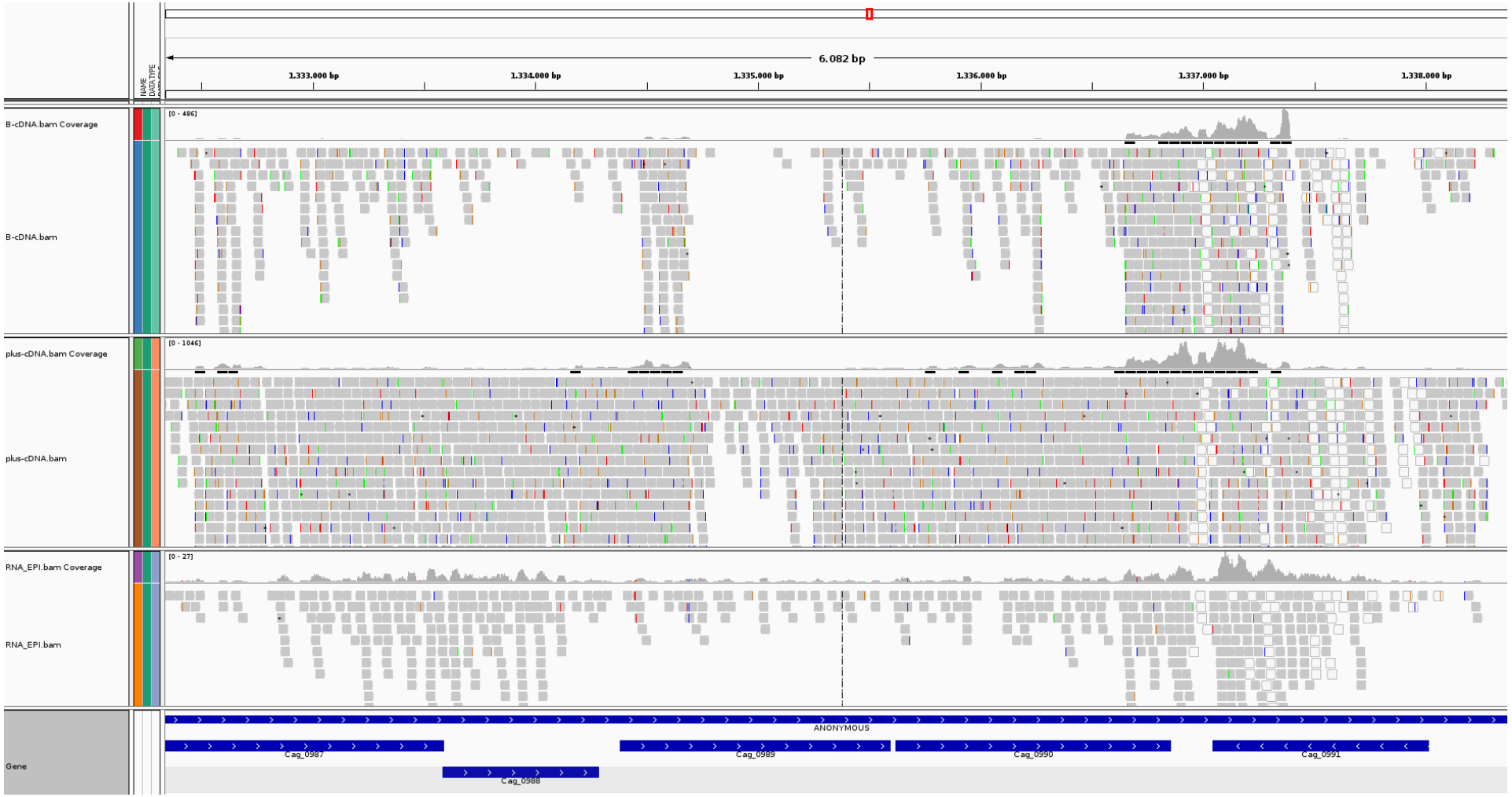

Suppl. Fig. S 2: Transcriptome analysis of Cag_0987-Cag_0991.

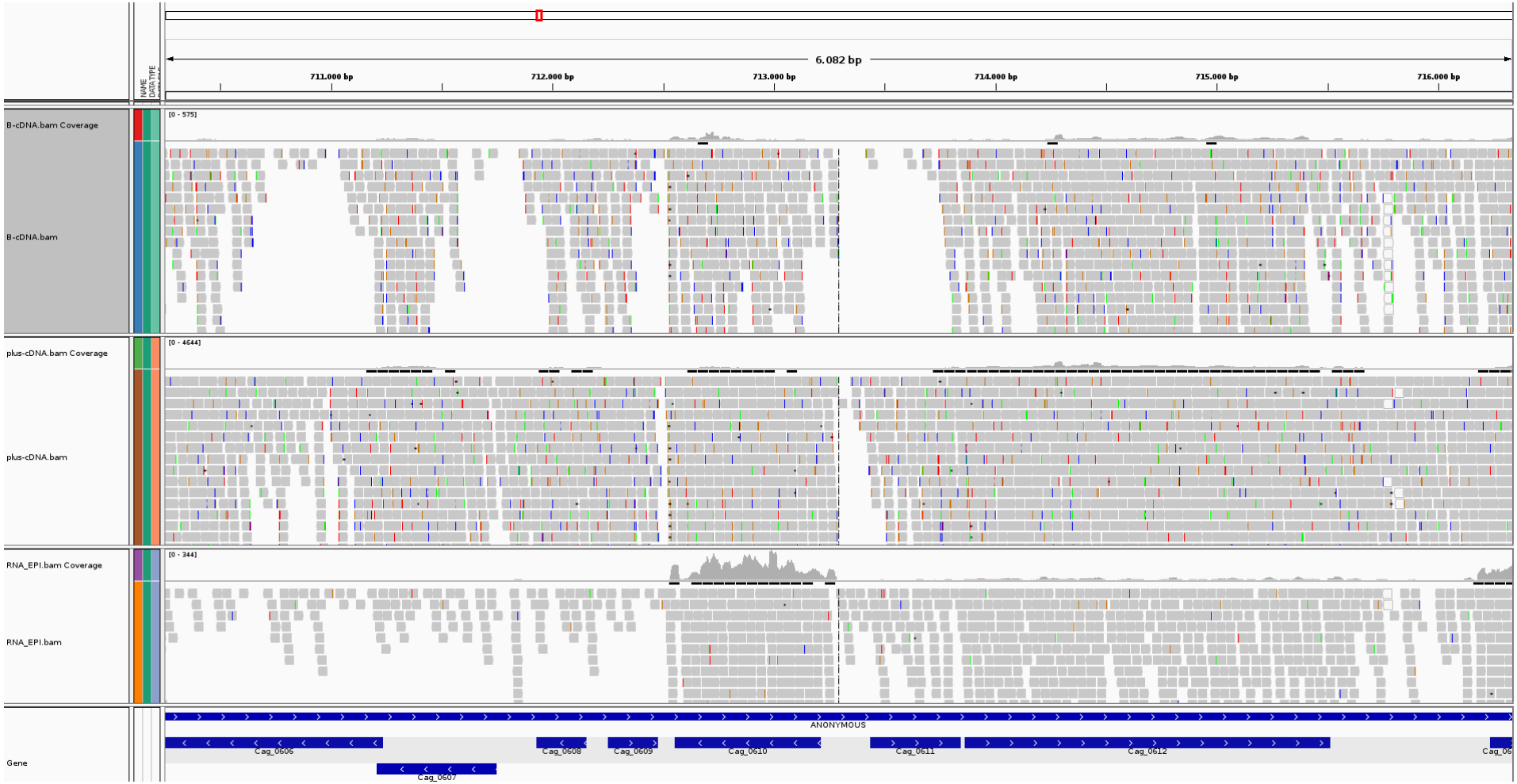

Suppl. Fig. S 3: Transcriptome analysis Cag_0606-Cag_0612**.**

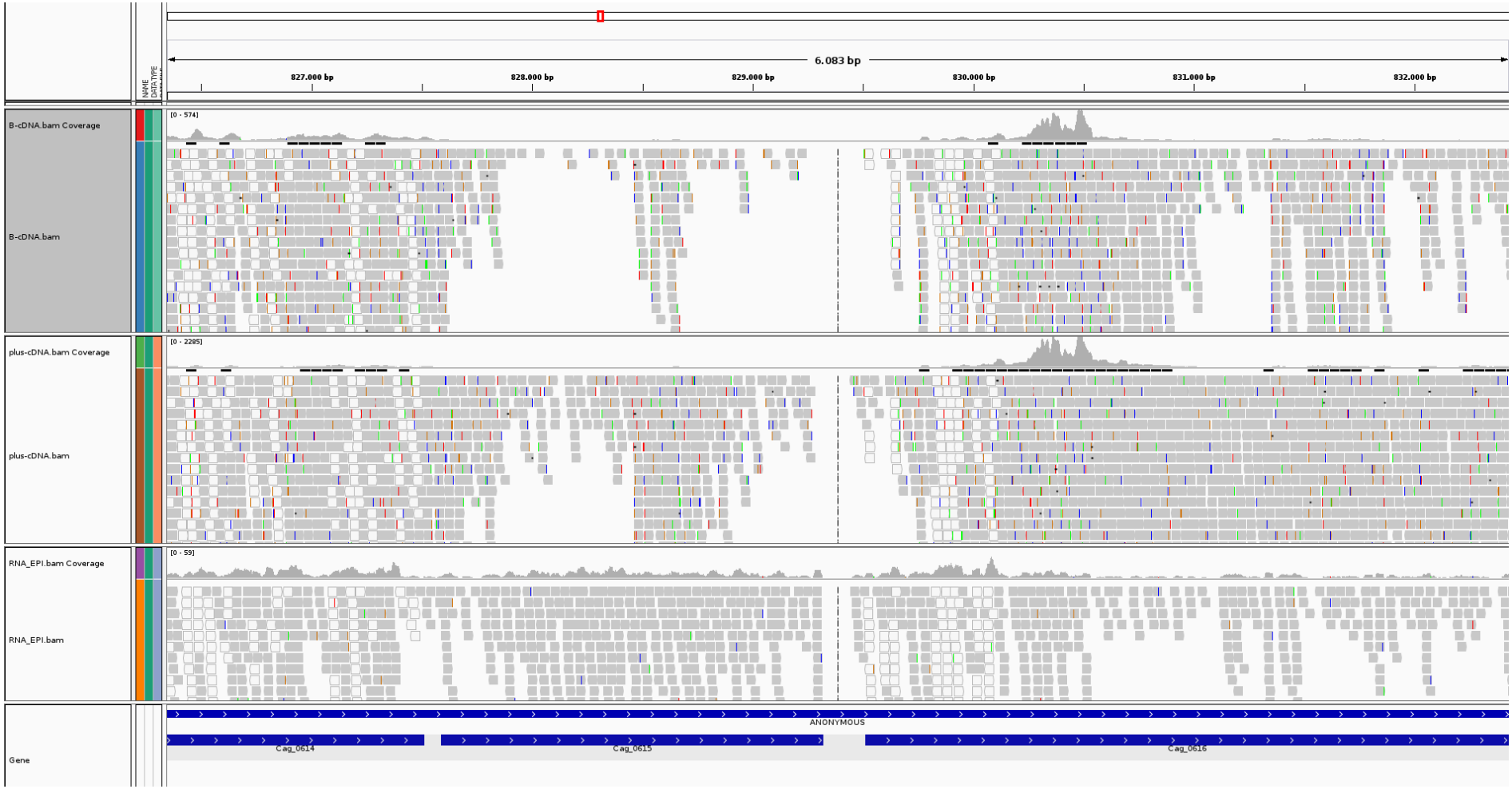

Suppl. Fig. S 4: Transcriptome analysis Cag_0614-Cag_0616**.**

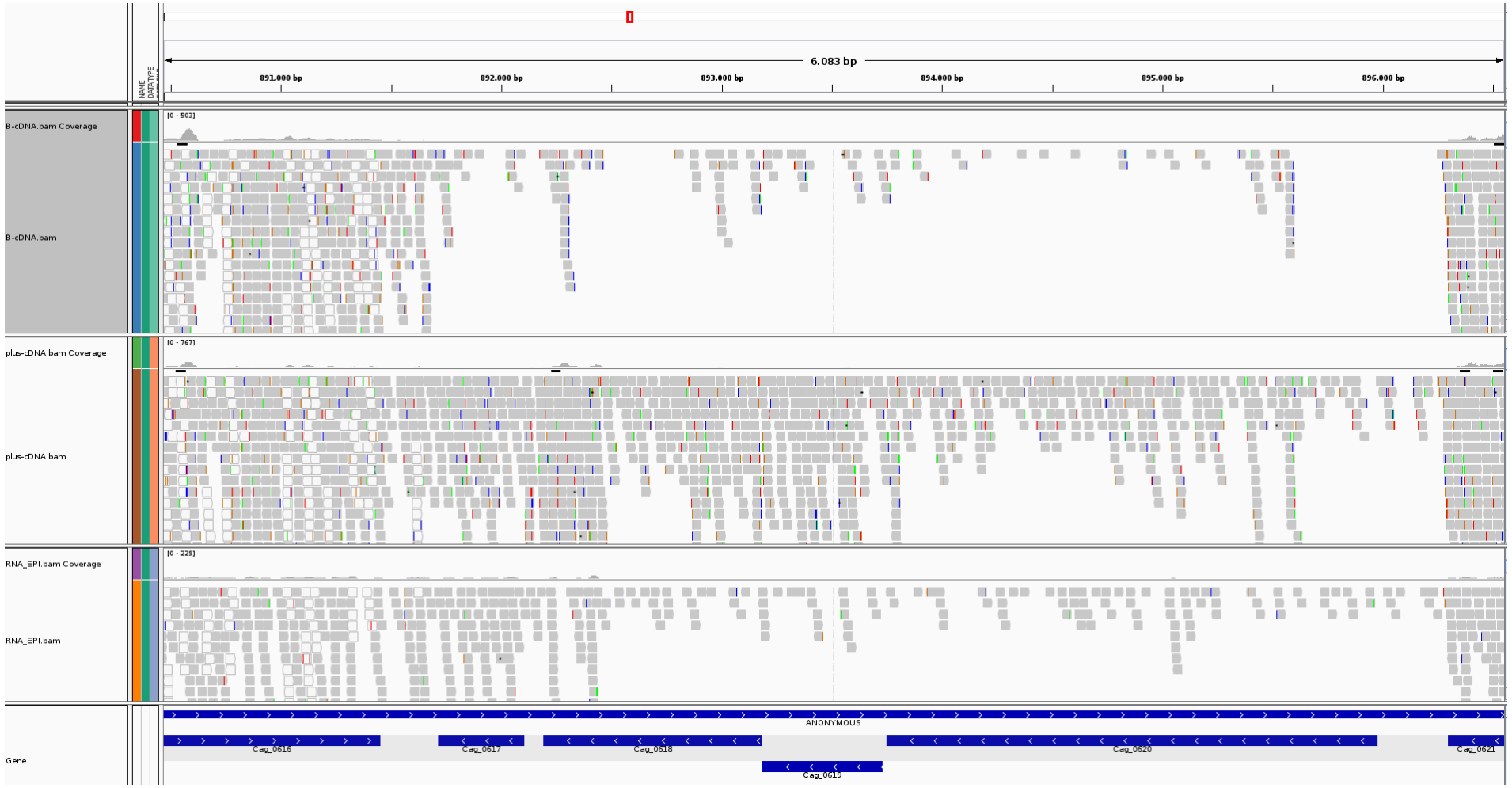

Suppl. Fig. S 5: transcriptome analysis Cag_0616-Cag_0620.

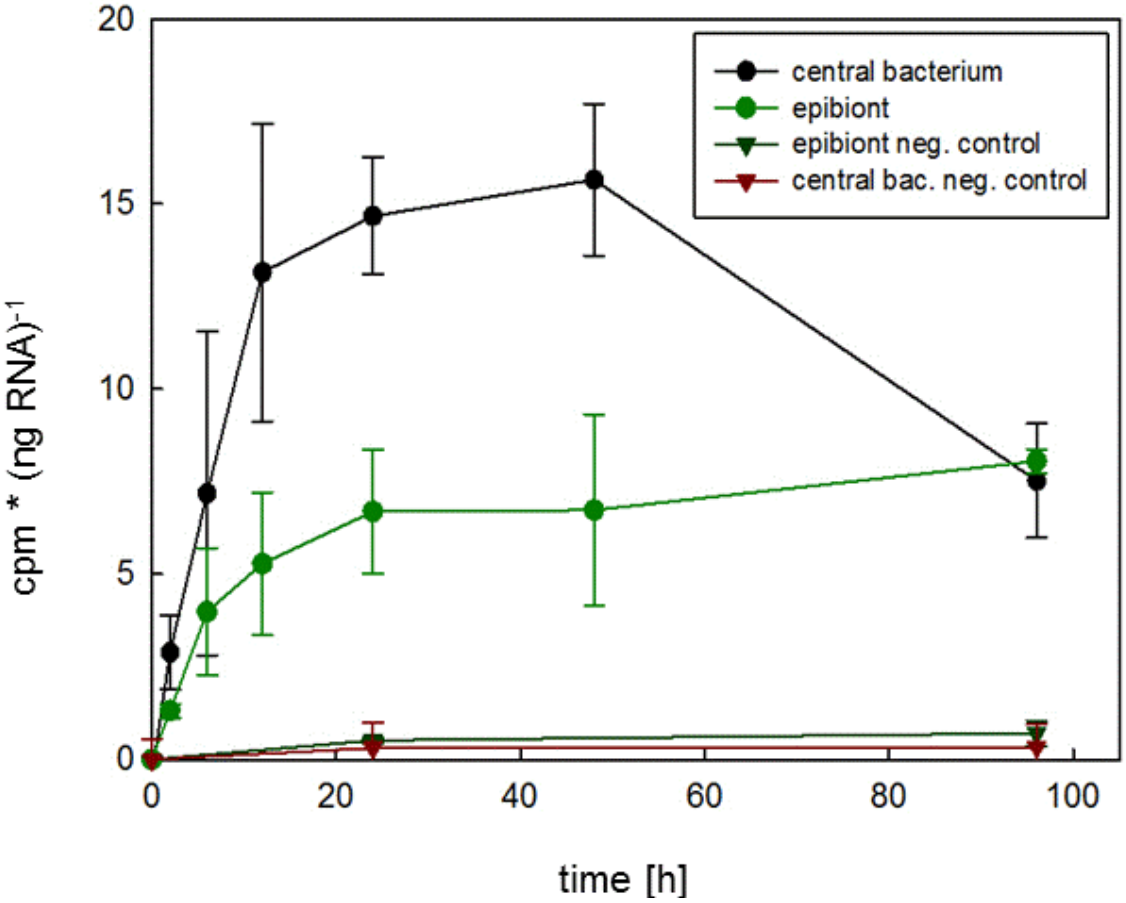

Suppl. Fig. S 6: Measurement of the ^{14}C content of 16S rRNA collected from the central bacterium and the epibiont (Müller, 2013).

II. Abbreviations

BCAAs	Dissolved combined amino acids
BChl	Bacteriochlorophyll
bp	base pairs
C.	*Chlorochromatium*
CB	Central bacterium
Chl.	*Chlorobium*
CβG	cyclic β-1,2-glucose
Epi	Epibiont
IMF	Immunofluorescence
IMG	Immunogold
MARTX	Multifunctional-autoprocessing RTX
nanoSIMS	nanoscale secondary ion mass spectrometry
PCR	Polymerase chain reaction
PT	Periplasmic tubules
RGD	Arg-Gly-Asp tripeptide
RTX	Repeat-in-toxin
T1SS	Type I secretion system
v/v	volume/volume
w/v	weight/volume

Chemical Substances

APS	Ammonium persulfate
BChl	Bacteriochchlorophyll
BSA	Bovine serum albumin
DAPI	4',6-diamidino-2-phenylindole
DTT	Dithiothreitol
EDTA	Ethylenediamine tetraacetic acid
FM4-64FX	Fixable analogue of the FM4-64 membrane stain
HEPES	(4-(2-hydroxyethyl)-1-piperazineethanesulfonic acid
HRP	Horseradish peroxidase
IMF	Immunofluorescence
IPTG	Isopropyl-β-D-1-thiogalactopyranoside
Ni-NTA	Ni-nitrilotriacetic acid
PBS	Phosphate-buffered saline

PVDF	Polyvinylidene difluoride
SDS	Sodium dodecyl sulfate
TEMED	Tetramethylethylenediamine

Acknowledgements

I would like to thank many people who have helped me complete this dissertation. Firstly, I would like to express my sincere gratitude to my mentor Prof. Jörg Overmann for his continuous support of my research and Ph.D thesis studies, for the great opportunity to work with fascinating organisms, for signing all the order slips for yet another new protein purification column and for the experience of procuring the FACS machine.

Johannes Müller, who worked with the consortia before me, I would like to thank for the introduction to the fascinating consortia project and the very interesting discussions regarding them.

For the set-up of the Nikon microscope at the DSMZ, just at the right time, I would like to thank Christian Jogler and for the help operating it, I would also like to thank Christian Boedecker.

For all their work on the electron microscopes, I would like to thank Manfred Rohde at the HZI in Braunschweig and Gerhard Wanner at the LMU in Munich. I would also like to thank Silvia Dobler for preparing all the consortia samples for the immunogold analysis.

I would like to express my gratitude and appreciation towards Hilmar Quentmeier and Margarete Zaborski for their commiseration in dealing with the FACS machine in the first month of set-up, and figuring out single cell sorting.

I would like to thank Wulf Menzel and the project team plant virus for generously sharing their Äkta machine with me and in the case of antibody purification how to employ it.

For the help with very stubborn recombinant proteins, I would like to thank Tom Hanson from the Delaware University who chose to spend his sabbatical leave at the DSMZ. I think I would not have expressed Cag_1919 without him.

All my former and current office mates I would like to thank for such a good time and all the discussions concerning scientific and not so scientific questions. I would especially like to thank Felizitas, Kathi and Thomas for helping me to weather the last weeks of my Ph.D thesis.

I would also like to express my appreciation towards Elke Melenk and the shipping team for dealing with numerous dry ice packages going to many parts of the world, Sabine Kammin

and Andreas Stoll for all the small things concerning every day lab life and all the other lab technicians for their generous help.

Last but certainly not least I would like to thank Sabrina Willems for helping me with multiple repeats of blots, purifications and cultivations and Michaela Blank for helping me with all the SDS PAGEs checking for protein expression. I would also like to thank my fellow lab and office mates for the stimulating discussions and for all the fun we had in the last five years.

My final and special thanks go to my parents, without their love and support I would not be where I am today.

Curriculum vitae

Personal Data

Name	Petra Marion Henke
Day of birth	03.08.1984
Place of birth	Braunschweig, Germany

University education

June 2010-August 2015	Ph.D thesis at the DSMZ (German Collection of Microorganisms and Cell Cultures), Braunschweig, Germany
February 2010	Diploma of Biotechnology at the Carolo-Wilhelmina University Braunschweig, Germany
July 2009-February 2010	Diploma thesis at the University of Dundee, Scotland; "Regulation of the minor channel component *tatE* of the Tat system"
October 2004-February 2010	Studies of biotechnology at the Carolo-Wilhelmina University Braunschweig, Germany

School education

1997-2004	A level at Gymnasium Martino-Katharineum, Braunschweig, Germany
1995-1997	Orientierungsstufe Rothenburg, Braunschweig, Germany
1991-1995	Elementary school Timmerlah, Braunschweig, Germany